UNIVERSITEIT VAN PRETORIA
UNIVERSITY OF PRETORIA
YUNIBESITHI YA PRETORIA

Unravelling the role of Aurora kinases in cell cycle regulation of malaria parasites

---

Clarissa Abrie

Submitted in partial fulfilment of the requirements of the degree
Magister Scientiae
(Specialisation in Biochemistry)

Faculty of Natural and Agricultural Sciences
Department of Biochemistry, Genetics and Microbiology
Division of Biochemistry
University of Pretoria
South Africa

November 2018

UNIVERSITEIT VAN PRETORIA
UNIVERSITY OF PRETORIA
YUNIBESITHI YA PRETORIA

SUBMISSION DECLARATION

I, Clarissa Abrie, declare that the dissertation, which I hereby submit for the degree *Magister Scientiae* in the Department of Biochemistry, Genetics and Microbiology at the University of Pretoria, is my own work and has not previously been submitted by me for a degree at this or any other tertiary institution.

SIGNATURE: 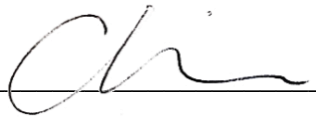

DATE: 04/02/2019

UNIVERSITEIT VAN PRETORIA
UNIVERSITY OF PRETORIA
YUNIBESITHI YA PRETORIA

DECLARATION OF ORIGINALITY

UNIVERSITY OF PRETORIA

FACULTY OF NATURAL AND AGRICULTURAL SCIENCES

DEPARTMENT OF BIOCHEMISTRY, GENETICS AND MICROBIOLOGY

DIVISION OF BIOCHEMISTRY

Full names of student: Clarissa Abrie

Student number: 11228271

Declaration:

1. I understand what plagiarism is and am aware of the University's policy in this regard.
2. I declare that this dissertation is my own original work. Where other people's work has been used (either from a printed source, Internet or any other source), this has been properly acknowledged and referenced in accordance with departmental requirements.
3. I have not used work previously produced by another student or any other person to hand in as my own.
4. I have not allowed, and will not allow, anyone to copy my work with the intention of passing it off as his or her own work.

SIGNATURE: 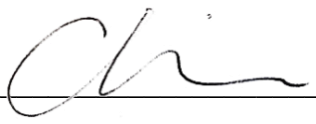

DATE: 04/02/2019

Acknowledgements

Today, after months of intense preparation to finish this dissertation, I would like to express my profound gratitude to everyone who made it possible.

I am truly appreciative of my supervisor, Prof. Lyn-Marie Birkholtz (DST/NRF SARChI Chair in Sustainable Malaria Control; Biochemistry Division, University of Pretoria), for her continuous support and guidance in completing my *Magister Scientiae* degree. Her vast knowledge allowed me to fully and meaningfully participate in academic research. Without her endless patience, motivation and contagious excitement about the field of biochemistry and research, this dissertation would not have been successfully completed. I am grateful for the opportunities she provided me to further my career as an independent scientist, even though I still my lack the full context of the overwhelming number of challenges any scientist may face, I would like to use it as the charge and motivation to move in such a worthy direction.

I am grateful for my co-supervisor, Dr. Jandelie Niemand (Biochemistry Division, University of Pretoria). She has enthusiastically offered me much advice, insight and meaningful guidance throughout my research. I would also like to express my sincere appreciation for the opportunity given to collaborate with Prof. Christian Doerig (Monash Biomedicine Discovery Institute, Monash University, AUS) and Prof. Jose Garcia-Bustos (Microbiology, Monas University, AUS). Their immense knowledge, insight, and expertise in the field has made me ever grateful for their involvement in this project. To the members of the M^{2}PL Laboratory, especially Christiaan Breedt, Hilde von Grüning, Dr. Janette Reader and Dr. Bianca Verlinden who generously provided the necessary support, you have been extremely kind to me and I am richer for it.

I am grateful for the financial support given by the National Research Foundation and the University of Pretoria by funding this degree through the NRF Grantholder-linked bursary and the University of Pretoria Postgraduate bursary, respectively.

Finally, I must express my very profound gratitude to my parents, Jean and Louisa Abrie, for their unfailing support throughout my years of study and their continuous encouragement in the time of researching and writing this dissertation. This accomplishment would not have been possible without them.

"The price of success is hard work, dedication to the job at hand, and the determination that whether we win or lose, we have applied the best of ourselves to the task at hand."

-Vince Lombardi

Summary

The *P. falciparum* parasite's life cycle, and implied cell cycle, is strictly controlled allowing the parasite to rapidly develop during the intraerythrocytic stages alternating DNA synthesis and mitosis during endocyclic schizogony. This results in asynchronous nuclear divisions to form multinucleated schizonts during mitosis. However, mitotic nuclear division in *P. falciparum* parasites remain poorly understood. Several mitotic kinases of the *P. falciparum* kinome, such as aurora related kinases (ARKs), have been suggested to be cell cycle regulators. The PfARKs are essential for intraerythrocytic stages of the *Plasmodium* parasite of which PfARK-1 are highly conserved and associated with spindle pole bodies (SPB) during schizogony. The role of PfARK associated with SPB in cell cycle regulation of *P. falciparum* parasites has been understudied, despite the close link to centrosome and bipolar microtubule dynamics, chromosome segregation and cytokinesis of Aurora kinases in various other organisms. Knowledge gaps regarding the parasite's cell cycle regulatory mechanisms is mostly due to the complexity associated with cell cycle compartment synchronisation of the parasite under *in vitro* conditions. In this dissertation, an innovative approach is used for cell cycle compartmentalisation of parasites as a tool to interrogate the importance of PfARK in cell cycle regulation during the intraerythrocytic stages of the parasite through hesperadin-induced PfARK inhibition. Collectively, this dissertation provides extensive insight to PfARK cell cycle regulation during parasite asynchronous nuclear division associated with M-phase progression, chromosomal segregation and spindle formation. The data demonstrate that novel cell cycle regulatory mechanisms of mitotic kinases, such as PfARKs and their involved pathways, serve as attractive future drug targets in *Plasmodium* parasites.

Table of Contents

List of Figures

List of abbreviations:

ACT	Artemisinin-based combination therapies
AdoMetDC	*S*-adenosyl methionine decarboxylase
AGC	cAMP-dependent, cGMP-dependent and protein kinase C
ARK	Aurora-related kinase
CaMK	Calcium-mediated kinase
CDK	Cyclin-dependent kinases
CDPK	Calcium-dependant protein kinase
CK	Casein kinase
CLK	Cyclin-dependent-like kinases
DDT	dichlorodiphenyltrichloroethane
DFMO	α-Difluoromethylornithine
ePK	Eukaryotic protein kinase
FI	Fluorescence intensity
FIKK	Phenylalinine-Isoleucine-Lysine-Lysine motif
GAP	Glideosome-associated protein
GSK	Glycogen synthase kinase
HEPES	4-(2-hydroxyethyl)-1-piperazineethanesulfonic acid
hpi	Hours post invasion
IDC	Intraerythrocytic developmental cycle
IF	Immunofluorescence
MAPKKs	Mitogen-activated protein kinase kinases
MAPKs	Mitogen-activated protein kinases
NIMA/NEK	Never-in-mitosis A
PBS	Phosphate buffered saline
PKG	cGMP-dependent protein kinase
R-point	Restriction point
SPB	Spindle pole body
TK	Tyrosine kinase
TKL	Tyrosine kinase-like
WHO	World Health Organisation

1 Chapter 1: Literature review

1.1 Malaria Epidemiology

Nearly half of the world's population, 3.2 billion people, is at risk of being infected with the malaria parasite, a parasitic protozoan from the genus *Plasmodium,* transmitted by adult female *Anopheles* mosquitoes [1]. In 2016, the malaria parasite was responsible for 216 million clinical cases and resulted in 445 000 deaths [1]. The transmission intensity of malaria is influenced by the mosquito vector's behavioural and physiological characteristics such as their biting habits, longevity, density and their efficiency of transfection [2, 3]. Malaria remains one of the greatest global challenges due to the long-lived nature and robustness of the anopheline vector species to environmental changes, which mainly occurs in high densities in tropical climates allowing them to breed readily. Even though malaria is a global disease, sub-Saharan Africa disproportionally accounts for more than 90% of malaria deaths [1, 4], mainly in children under the age of 5 [1]. However, Latin America, Southeast Asia and the Middle East are not risk free and are also prone to the socio-economic burden of malaria [5]. Besides the high risk to infants and young children, *Plasmodium* parasite infection can lead to chronic anaemia and placental malaria infection in pregnant women [1].

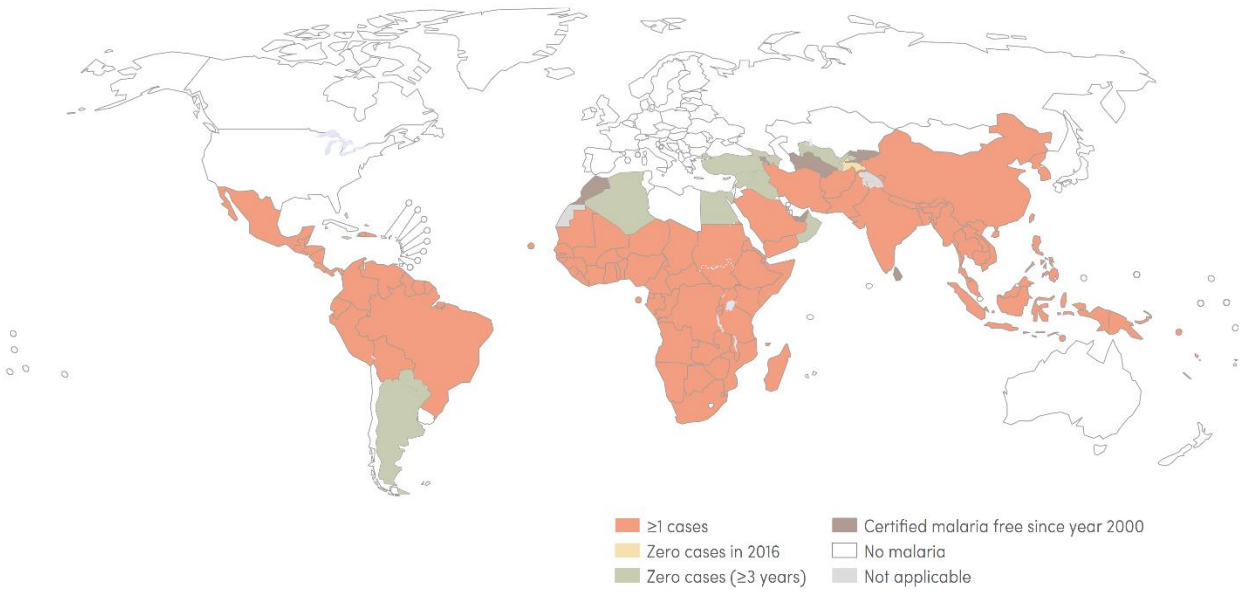

Figure 1.1: Comparison of the global distribution of indigenous malaria cases in 2000 and their status by 2016. Countries who reported zero cases in three or more consecutive years up to 2016 are eligible to be certified malaria free by the WHO (green), while, countries with zero cases reported in 2016 (yellow) and with ≥1 cases (red) remain at high risk. Countries certified malaria free since 2000 (purple), no malaria (white) and not applicable (grey) countries, are free of risk [1]. Image adapted from freely accessible WHO malaria report 2017 (URL link: https://www.who.int/malaria/publications/world_malaria_report/en/) [1].

The World Health Organisation (WHO) reported that, from 2000 to 2016, Latin America, Southeast Asia and sub-Saharan Africa had the highest *Plasmodium* parasite infection rate and with ≥1 cases in 2016 (Fig. 1.1) [1]. Countries recently certifed as malaria free regions (zero locally transmitted cases for ≥3 years) include southern parts of South America, Algeria and Egypt in Africa and several countries in Asia including Iraq, Syria, Turkey and Ozbekistan. Morocco (Africa), Turkmenistan and Kyrgyzstan (Asia) were certified malaria free since 2000 (Fig. 1.1) [1]. Tajikistan (Asia) had zero cases in 2016 (Fig. 1.1) [1].

In 2012, the SADC Ministers of Health finally affirmed regional elimination strategies, and the Elimination 8 (E8) was launched. The E8 is a regional attempt to eliminate malaria by 2020-2030 in eight southern Africa countries. South Africa, Botswana, Namibia and Swaziland are frontline countries reoriented to begin malaria elimination and are considered as the frontline countries. Collaboration with Zimbabwe, Angola, Mozambique and Zambia as second line countries, due to higher malaria transmission rates, are required for successful malaria elimination in southern Africa. Additionally, the Global Technical Strategy for malaria (2016-2030) was developed and authorised by the WHO in 2015 [1]. With this, global targets were set for 2030, aiming at malaria elimination in at least 35 countries with a 90% decrease in global malaria cases and mortality rates [1]. The E-2020 initiative was established in 2016 by the WHO where 21 countries were identified to have the potential for zero indigenous cases and eliminate malaria by 2020 [1]. However, spreading of resistance to antimalarial drugs and insecticide resistance, land-use and –cover changes, contributes to the difficulty of malaria control. Several countries, including South Africa, have been reported to be off-track with the E-2020 initiative's common goal [1].

Malaria intervention strategies aimed at inhibiting contact between human and *Plasmodium*-infected mosquitoes as it is essential to disrupt malaria transmission (reviewed in [6]). In 1960, the WHO Pesticide Evaluation Scheme was launched and were collaborating with other WHO institutions such as the International Programme on Chemical Safety to evaluate and test pesticides for public health (www.who.int) [1]. Insecticides such as dichlorodiphenyltrichloroethane (DDT) [1] and more recently, pyrethroids [1, 7], were commonly used as an effective indoor residual spray as a mosquito vector control. Nonetheless, a significant number of insecticide classes, like DDT, have lost their efficiency against continuously evolving mosquito species [1, 3, 8-10]. Vector control using insecticides-treated nets resulted in a significant improvement in the control of mosquitoes and malaria transmission [1]. However, mosquitoes continue to adapt their feeding regimes [11]. Therefore, emphasis shifted from adult

mosquito control to larvae control [12] and larvae control strategies included biological control[13].

Despite extensive research on vaccine development, no vaccine against the *Plasmodium* parasite to prevent malaria have been successfully developed yet [14, 15]. Malaria vaccine development is mainly focussed on the pre-erythrocytic and intraerythrocytic stages as well as transmission blocking of the *Plasmodium* parasite [16]. Pre-erythrocytic vaccine development is aimed at disrupting the establishment of the parasite exoerythrocytic cycle (reviewed in [17]). Intraerythrocytic developmental cycle (IDC) vaccines aims at parasitaemia reduction, while transmission blocking vaccines aims at gametocytogenesis disruption [16, 18]. The leading vaccine candidate RTS,S/AS01 [19], reached phase III of clinical trials [20] and has shown protective efficacy against clinical and severe malaria at 31% and 56% in infants (6 – 12 weeks) and children (5-17 months), respectively [21, 22].

The most successful strategy to target the parasite remains the use of chemoprophylactic and chemotherapeutic compounds [1]. However, the spread of drug-resistant *Plasmodium* parasites, due to the misuse of clinically available antimalarials, has undermined their efficacy [1]. The leading parasite control strategy, endorsed by the WHO as first-line gold standard, is artemisinin-based combination therapies (ACT) for all malaria infections [23]. Parasite resistance against artemisinin and some of its partner drugs have developed in some countries; however, in Africa, the leading continent in malaria fatalities, fortunately, parasites remain susceptible to ACTs [24]. However, as a result of continuous drug resistance development in the parasite, the Medicine for Malaria Venture was established in 1999 as a public-private partnership and non-profit organisation, which supports the efforts of the WHO through the development of affordable antimalarial drugs (www.mmv.org). This has resulted in the development of synthetic drugs aimed towards multiple stages of the parasite's development and therefore useful in the context of malaria elimination strategies [25, 26].

1.2 Plasmodium parasite

The *Plasmodium* genus consists of more than 170 species and cause infection in different vertebrates [27], however only six *Plasmodium* species are known to infect humans [1]. Even though *P. falciparum* and *P. vivax* predominates malarial infections, *P. ovale, P. malariae*, *P. knowlesi* and *P. cynomolgi* (zoonotic species) are also responsible for malarial infections in humans [1]. *P falciparum* is the major contributor of all malarial deaths [1].

The life cycle of *P. falciparum* parasites in humans are initiated after parasites are transmitted from an adult female *Anopheles* mosquito taking a blood feed on a human host [1], thereby inoculating sporozoites from her parasite-infected salivary glands (Fig. 1.2) [28]. The microscopic motile sporozoites enter the asexual, exoerythrocytic cycle in the human liver within 30 min by invading hepatocytes [28, 29]. Here, a sporozoite undergoes multiple nuclear divisions during hepatic schizogony within 5-10 days to produce more than 30 000 daughter merozoites per infected hepatocyte. These daughter merozoites are released into the bloodstream to initiate the asexual, IDC [30].

The sequence of events during the IDC of *Plasmodium* parasites is well characterised. Erythrocyte entry is associated with deformation of the targeted erythrocyte when the anterior end of the merozoite makes initial contact and during erythrocyte penetration [31] as the merozoite apical organelles (rhoptries, micronemes and dense granules) discharge their content [32]. Once inside the erythrocyte, the *Plasmodium* parasite subsequently develops from a morphologically characterised 'ring' stage to a metabolically active trophozoite-stage parasite, characterised by irregular bulges and deep tubular invaginations formed on the surface of the parasite (Fig. 1.2) [33]. Schizogony ensues when the parasite undergoes multiple, asynchronous nuclear divisions, releasing up to 32 daughter merozoites per infected erythrocyte [34, 35], depending on the *Plasmodium* species. These merozoites can re-infect new erythrocytes and thereby perpetuate unlimited rounds of subsequent IDCs in an untreated or nonimmune individual. The IDC of *P. falciparum, P. vivax* and *P. ovale* parasites each takes approximately 48 h [36].

A minor proportion of asexual parasites are stochastically converted to form intraerythrocytic sexual forms of the parasite [37], able to support transmission to mosquitoes. Sexually committed merozoites leave the IDC to develop into intraerythrocytic micro- (male) and macrogametocytes (female) over a period of 10-14 days through differential gene expression [38] in a process known as gametocytogenesis (Fig. 1.2). Gametocyte gender is predetermined [39] and is already established in the schizont committed to gametocytogenesis [40]. A female-biased (>5-fold) gender ratio is typically found [41]. For *P. falciparum* infections, clinical gametocytaemia can be detected 7-15 days after asexual parasitaemia [42]. Five distinct morphological stages (I – V) occur during *P. falciparum* gametocytogenesis, of which stage I to IV sequester in the bone marrow and spleen (reviewed in [43]. Mature stage V gametocytes are released in the peripheral blood system [44, 45] where they circulate for another two to three

days while they become infectious to female anopheline mosquitoes taking blood meals [46]. During gametocyte maturation, molecular alterations, such as an increase in mRNA transcripts stored in the cytoplasm, prepare the *Plasmodium* parasite for the rapid adaption to the mosquito midgut [42].

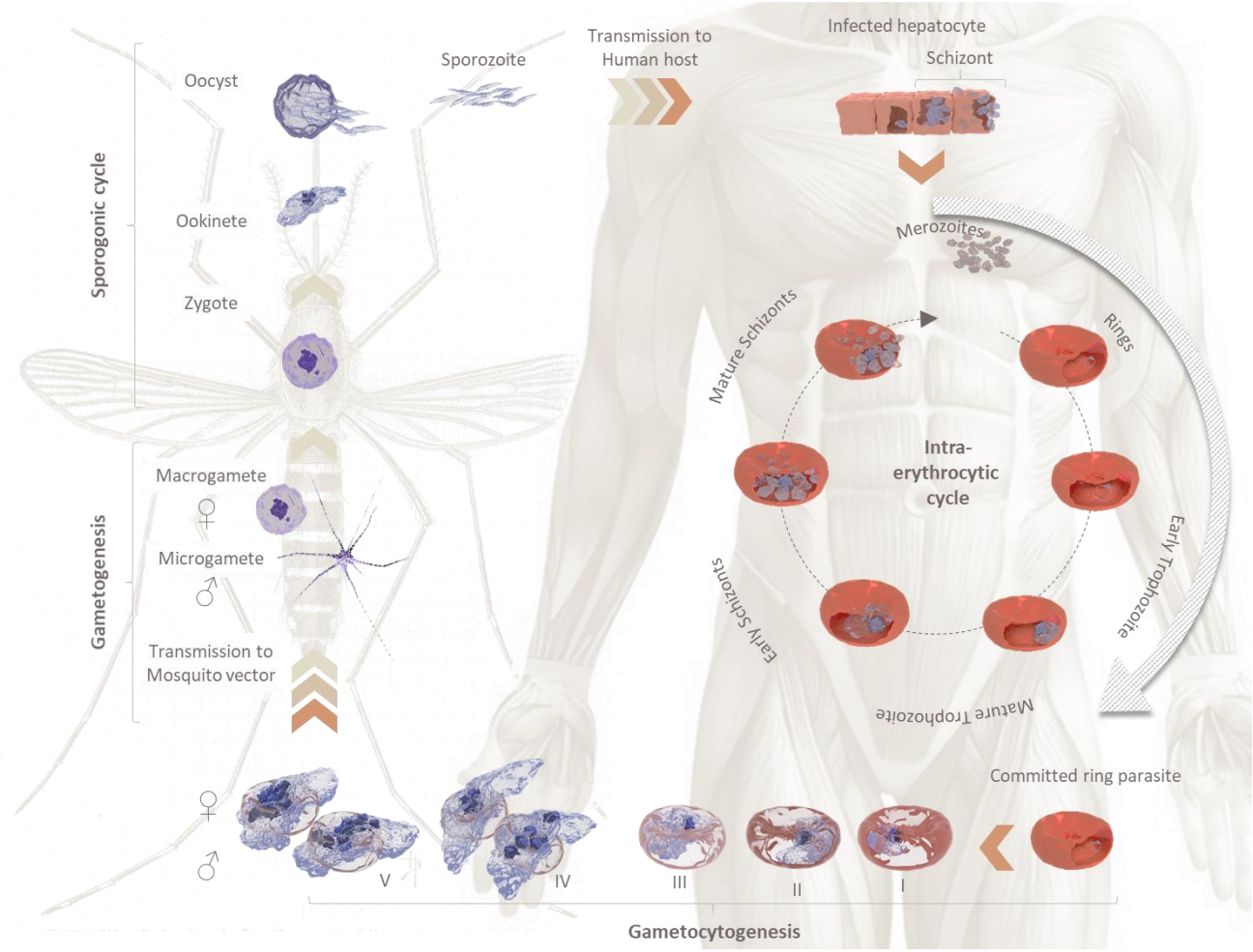

Figure 1.2: The life cycle of *P. falciparum* parasites.
During a blood meal the *Anopheles* mosquito transmit sporozoites to the human host where they develop into exo-erythrocytic and intraerythrocytic parasites. Within the erythrocyte the *Plasmodium* parasite develops from a ring to a mature trophozoite, which undergoes multiple nuclear divisions to form a schizont. Committed merozoites leave the IDC to develop into intraerythrocytic micro- (male) and macrogametocytes (female) during gametocytogenesis before mature gametocytes enter the sporogonic stages in the mosquito midgut after a blood meal. Images were designed using Blender software (www.blender.org) and others were adapted from freely available images.

The microgametocyte will mature into eight microgametes through exflagellation in the female anopheline mosquito midgut [47]. The macrogametocyte, however, matures to one large macrogamete [48]. The sporogonic cycle subsequently ensues in the mosquito midgut, where the environment from the human host's blood compartment to the mosquito vector midgut, is responsible for the induction of gamete development [49]. Fertilization of the mature macrogamete and flagellated microgametes occur through fusion of the gamete plasma

membranes followed by nuclear fusion and meiotic division to form a tetraploid zygote (Fig. 1.2) [50]. The end of the malaria sexual phase is reached when the zygotes develop into motile ookinetes [51, 52]. Ookinetes penetrates the midgut epithelium through their apical complex and position themselves between the epithelium and basal lamina [50] where they develop into oocysts. A haploid state is restored when sporozoite budding occurs in the oocysts [50]. The growing oocysts rupture and release sporozoites which migrate to the salivary glands of the mosquito ready to infect a human host upon a blood meal [53].

1.3 *P. falciparum* parasites have an unusual cell cycle

Eukaryotes rely on precise cell progression and cell cycle regulation for genomic DNA duplication and subsequent cell division into daughter cells [54]. Only a few eukaryotic organisms, especially those with short embryonic stages or fast cell cycles [55], have developed and formed our molecular understanding of the classic eukaryotic cell cycle. However, the cell cycle of unicellular protozoans, such as *P. falciparum*, is also under severe control to facilitate development. This has to occur through cell growth regulation and genome replication for subsequent division, as in metazoans, but the molecular mechanisms of these processes in protozoa is comparably less well understood [56]. The multistage *P. falciparum* parasite life cycle, and implied cell cycle, is strictly controlled and the cell cycle is rather unique compared to the classic eukaryotic cell cycle model allowing the parasite to rapidly develop during the IDC [57, 58].

1.3.1 Phases of the cell cycle

Different cell cycle phases can be associated with *P. falciparum* parasite life cycle stages (Fig. 1.3). The cell cycle commences in the interphase, which accounts for more than 90% of cell cycle duration. The interphase is divided into sub-phases: initial gap (G_1) phase, synthesis (S) phase the second gap (G_2) phase and the quiescent period (G_0) [59]. Invading merozoites are generally accepted to be in a non-replicative state with condensed chromatin and therefore, are in a G_0-like quiescent state [60]. In a classic eukaryotic cell cycle, non-dividing cells enters a quiescent phase (G_0) whereby the cell temporarily exits the cell cycle [61]. Upon cell cycle re-entry of these G_0 cells, cell proliferation is under strict control and regulation [61]. Deficiencies and abnormalities in cell cycle control, often associated with pathologies such as cancer, could result in uncontrolled proliferation [62, 63].

Throughout the G_1-phase, the cell increases in size, RNA and protein content together with chromatin decondensation; preparing the cell for DNA replication in the subsequent S-phase, in

both the classic eukaryotic cell cycle [64] and the *Plasmodium* parasites' cell cycle (Fig. 1.3) [65]. During the *Plasmodium* parasite's G_1-phase, uncondensed chromatin is associated with the development of ring to early trophozoites stage parasites, remaining at 1N DNA copy number [60]. In early trophozoites, an increase in RNA and protein content [66] is seen up to 24 h post-invasion (hpi) [67].

Upon completion of the G_1-phase, the cells enter the S-phase where the classic eukaryotic cell cycle conventionally undergoes a single round of genomic DNA replication, resulting in duplicated chromosomes (reviewed in [68]). During the S-phase and throughout the subsequent G_2-phase the chromatin remains uncondensed [64]. In *Plasmodium*, the S-phase is initiated in mature trophozoites (2N) and the parasite is classified as a schizonts (>2N) following 3-4 rounds of DNA replication from 24-28 hpi [57, 66, 67]. In a classic eukaryotic cell cycle, the G_2-phase prepares the cell for mitosis through additional cell growth and protein synthesis (Fig. 1.3). However, in *Plasmodium* an unusual occurrence is seen of alternating DNA synthesis and mitosis during endocyclic schizogony [57]. This results in asynchronous nuclear divisions with no discernible G_2-phase, to form multinucleated schizonts (Fig. 1.3) [57].

The mitotic (M) phase consists of four major sub-phases during which the cell will divide into two daughter cells in the classic eukaryotic cell cycle and up to 32 daughter merozoites in the *P. falciparum* cell cycle [34, 35]. In the classic eukaryotic cell cycle the initial sub-phase of mitosis, prophase, the chromatin starts to condense into discrete chromosomes, which appear as two sister chromatids joined at their centromere [69]. In contrast, *Plasmodium* parasite chromosomes remain uncondensed during the M-phase as it alternates between the S-phase and M-phase [57]. Microtubule organizing centers (MTOCs), are responsible for nucleation. The formation of the mitotic spindle from MTOCs is initiated during the prophase [66]. In the classic eukaryotic cell cycle, the nuclear envelope fragments, partially or completely [70], allowing the mitotic spindle microtubules to invade the nuclear area for chromosome attachment at kinetochores during the metaphase [71]. This aligns chromosomes on the metaphase plate equidistant from opposing spindle poles at MTOCs [66]. However, *Plasmodium* parasites have intact nuclear envelopes during schizogony and forms multinucleated parasites through repeated mitosis in the absence of cell division, a concept known as closed mitosis [57]. The metaphase is the longest phase of the mitotic phases [66]. Upon completion of the metaphase, the shortest mitotic phase, anaphase, commences. During the anaphase, the sister chromatids part from each other and are subsequently pulled to opposite spindle poles through microtubule

shortening; while non-kinetochore microtubules lengthen and elongate the cell [66]. During final mitotic phase, telophase, the cell divides into two identical daughter cells with uncondensed daughter nuclei followed by nucleus envelope reconstruction together with cytokinesis. Cytokinesis is a process whereby cell division occurs through mechanical separation as a cleavage furrow is formed [72]. The cleavage furrow consists of contractile actin microfilaments associated with myosin, which further deepens the cleavage furrow to pinch off the parental cell into two daughter cells [72, 73]. Despite asynchronous nuclear division in *Plasmodium* parasites, synchronous nuclear division occurs in the final round of mitosis followed by subsequent segmentation and a single cytokinesis event, to release multiple daughter merozoites (Fig. 1.3) [57].

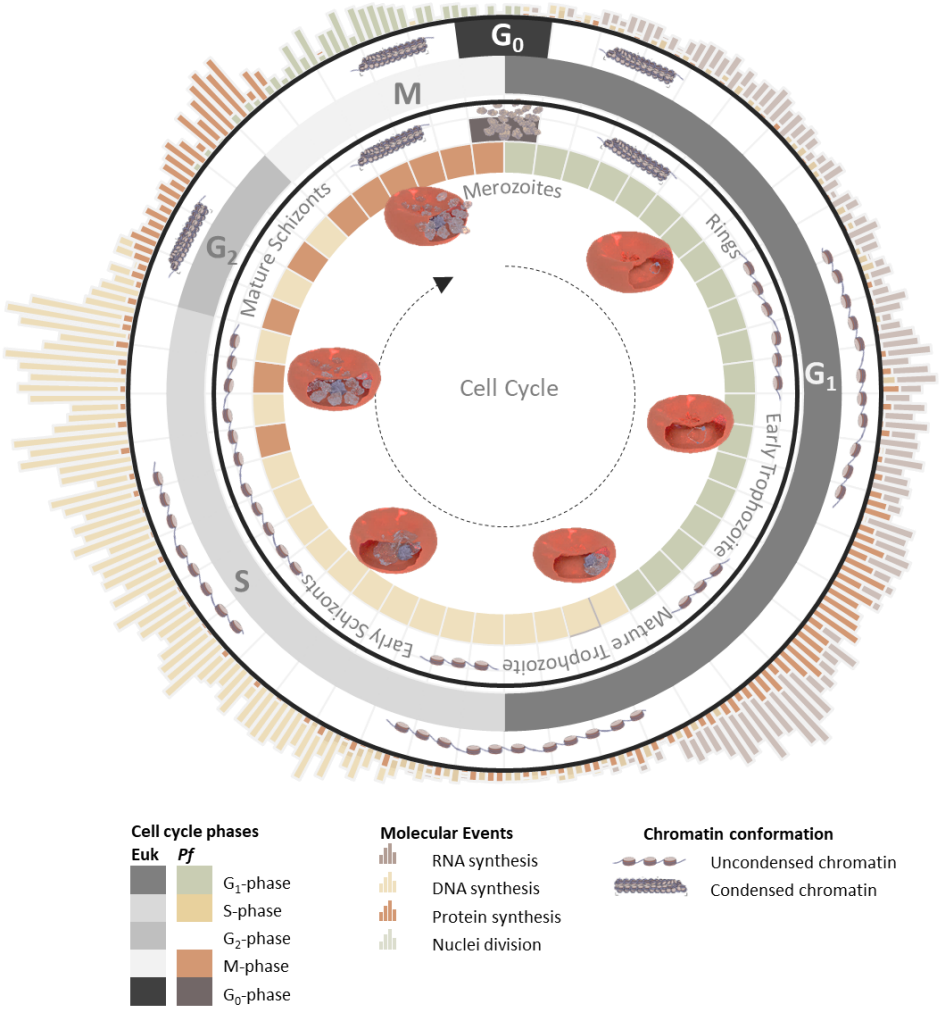

Figure 1.3: Classic eukaryotic and *P. falciparum* cell cycle summary.
The eukaryotic cell cycle consists of four major phases; the first gap phase (G_1) phase, the DNA synthesis phase (S), the second gap phase (G_2) and the mitotic phase (M). Classic eukaryotic cell cycle enters a G_0 phase, a quiescent, non-replicative phase, after a cell exits the cell cycle (outer cell cycle ring, shades of grey). In *P. falciparum* parasites (inner cell cycle ring), merozoites are in a G_0 phase (dark purple), a quiescent, non-replicative phase. Ring-stage parasites during the G_1-phase (green blocks) develop in to trophozoite-stage parasites in the S-phase (yellow blocks). Parasites alternate S- and M-phases (red blocks) during schizont development. In parasites, the second gap phase (G_2) is non-apparent. Individual cell cycle phase blocks are associated with the 48 h life cycle of *P. falciparum* parasite. Specific molecular events (histograms) and chromatin conformations are associated with

particular cell cycle phases. Images were designed using Blender software (www.blender.org) and Microsoft Excel and Powerpoint Office 365.

1.3.2 Cell cycle checkpoints

The cell cycle control system, responsible for the dynamic regulation of sequential events, is typically regulated by internal and external cellular signals at certain checkpoints. Governed by decision-making signals, cell cycle checkpoints ensure that cells either commence the next cell cycle phase upon completion of the current phase or enters a quiescent state by leaving the cell cycle until the cell cycle can recommence [74]. If the cell cycle cannot recommence, cell death ensues. Three major checkpoints are present in classic eukaryotic cell cycle for quality control of 1) cell growth (G_1/S), 2) replicated DNA fidelity (G_2/M) and 3) the assembly of a bipolar spindle and chromosome attachment (M-checkpoint) [66, 75, 76]. In *Plasmodium,* little is known about the existence of cell cycle checkpoints. However, induced parasite cell cycle dormancy through drug treatment [24, 77, 78] or nutrient starvation [79] have suggested a G_1-checkpoint in pre-replicative ring-stage parasites, that may resemble a growth-factor dependent restriction point (R-point) in metazoa. With no discernible G_2-phase in the parasite cell cycle (Fig. 1.3), the parasite is deprived of the opportunity of a G_2-checkpoint [57, 80, 81]. Nonetheless, the highly conserved parasite DNA repair machinery is upregulated in response to DNA damage [82]. The ability of *Plasmodium* parasites to have a S- or M-checkpoint is challenged by the high rate of genomic DNA replication during schizogony [57]. There is some evidence of chromosome separation control: chromosomes align with the hemi-spindle in an uncondensed conformation while remaining anchored to the MTOCs [83]. However, the ability of parasites to be multinucleated within a shared cytoplasm remains poorly understood [80] and schizogony is consistently completed around 48 hpi, despite the number of merozoites formed [84]; suggestive of some level of intra-S or M-checkpoints in parasites. Despite unclear understanding of the molecular process controlling checkpoints in *Plasmodium* parasite's cell cycle, it seems unlikely that the parasite will proceed through its cell cycle unchecked with timely precision and intricacy.

1.3.3 Cell cycle clock: cyclins and cyclin-dependent kinases

In the classic eukaryotic cell cycle, cell cycle control proteins, the abundance of cyclins and cyclin-dependent kinases, regulate the sequential cell cycle events [66]. Cyclins associate with the G_1-phase (Cyclin D), the S-phase (cyclin A and E) and the M-phase (cyclin A and B) (reviewed in [85]). Cyclins activate cyclin-dependent kinases (CDK) as effectors of cell cycle regulation, through phosphorylating additional proteins important for the cell cycle to progress

[85]. In contrast to the classic eukaryotic cell cycle, *Plasmodium* parasites have an unusual cyclin, cyclin-dependant kinase (CDK) and CDK-related kinase (CRK) repertoire. Three cyclins have been identified (CYC1, -3 and -4) [86], together with seven CDKs or CRKs: protein kinase (PK) 5 and -6, MRK-1, CRK-1,-3,-4 and -5 [87, 88]. None of the *Plasmodium* parasite cyclins are homologues to classic eukaryotic cell cycle cyclins and their expression are not confined to cell cycle phases, rather these are expressed at many life cycle stages [86, 89]. However, CDKs are not the only kinases associated with the cell cycle, as kinases of never-in-mitosis A (NIMA/NEK) and Aurora-related kinase (ARK) groups have been reported to be involved in the parasite's cell cycle [90-95].

1.3.4 Protein phosphorylation in cell cycle regulation

Eukaryotic cells rely on intracellular signalling for 1) cell division, differentiation and progression throughout the life cycle, and 2) responding to extracellular signalling [96]. Besides the release of secondary messenger molecules and site-specific recruitment of required elements downstream, protein modifications play a major role in signalling pathways. Undeniably, the most prominent protein modifications in eukaryotic cells are reversible protein phosphorylation performed by protein kinases and phosphatases [97] and *Plasmodium* is no exception [98]. However, the essential roles of protein phosphorylation in *Plasmodium* cell cycle regulation have been understudied, despite protein phosphorylation being a universal regulatory mechanism in other eukaryotic organisms [97, 99].

The majority of the *Plasmodium* kinome, consisting of approximately 90 kinase members [100-102], fall within the familiar mammalian kinome groups: cAMP-dependent, cGMP-dependent and protein kinase C (AGC), CMGC, casein kinase 1 (CK1), tyrosine kinase-like (TKL) and calcium-mediated kinase (CaMK) [103], and the biochemical regulation correlates with their homologues. However, not all *Plasmodium* kinases, such as the Phe-Ile-Lys-Lys kinases (FIKKs) and a family of Calcium-dependant protein kinase (CDPKs), fall within the traditional eukaryotic protein kinase (ePK) groups and are thus considered to be orphan families with no orthologues in other higher eukaryotes [100, 102, 104]. The FIKKs constitute novel, atypical protein kinase-like enzymes consisting of 21 members all with a conserved Phe-Ile-Lys-Lys motif [103]. In *P. falciparum,* the expanding FIKK family consists of 19 kinase genes and 2 pseudogenes [105].The FIKK family accounts for the majority of the kinome diversity between *P. falciparum* and other *Plasmodium* species, in the sub-telomeric regions [101], a chromosomal region prone to evolve

rapidly [106]. Therefore, the FIKK proteins are postulated to be involved in specific host-parasite interactions located in distinct infected erythrocytic cellular compartments [106].

The pivotal role of CDPKs in metabolism, transcription, ion pumps and channels, and cytoskeleton control has marked its importance in the *Plasmodium* kinome in the early 1990's [107]. CDPKs, conventionally found in plants and not in metazoans, contain a kinase domain directly fused to calmodulin-like EF-hands commonly found at the C-terminal [108]. An auto-inhibitory domain acts as a pseudo substrate and inhibits the kinase domain which is released upon calcium binding to the fused EF-hands [108]. In *P. falciparum,* 5 CDPKs have been identified, PfCDPK-1 -5 with EF-hand-containing, amino-terminal tails [107]. Conversely, the *Plasmodium* kinome notably lacks the tyrosine kinases (TKs) and members of mitogen-activated protein kinase kinases (MAPKKs) that are present in the human kinome [102].

The remainder of the *Plasmodium* kinome are members of the AGC, CaMK, CK1, CMGC, TKL, orphan, NIMA/NEK and ARK groups [102]. Characteristically, three conserved regulatory phosphorylation sites are present on the AGC protein kinases [109]. Three essential intraerythrocytic *P. falciparum* kinases, PfPKA, PfPKB and PfPKG, belong to the AGC group [98]. To date, the only known cAMP-dependant protein kinase in *P. falciparum* is PfPKA which acts on PfAMA1 protein essential for merozoite invasion [110, 111]. An essential role during intraerythrocytic schizogony and gametogenesis has been assigned to the cGMP-dependent protein kinase, PfPKG [112, 113]. PKGs are major cGMP signal transduction mediators, which are expressed during the ring-stages of *P. falciparum* parasites [112, 113]. Phosphorylation of the glideosome-associated protein GAP45 through PfPKB is essential for motor function and erythrocyte invasion upon calcium-bound calmodulin activation associated with its N-terminus calmodulin-binding domain [114]. A further 13 *P. falciparum* kinases belong to the CaMK group involved in essential parasitic functions including cell invasion, protein secretion, cell motility and egress [98]. Within the CaMK group, 7 kinases belong to the CDPK family discussed earlier. A single member CK1 group, PfCK1, is essential during the intraerythrocytic stages of the *Plasmodium* parasite development [98].

The CMGC group is the largest kinase group in *Plasmodium* and consists of 4 kinase families; CDK, MAPK, GSK3 and CLK, hence the name. The pivotal role of the CMGC kinases in intraerythrocytic proliferation is emphasised through 26 kinases present in the *P. falciparum* kinome [98].

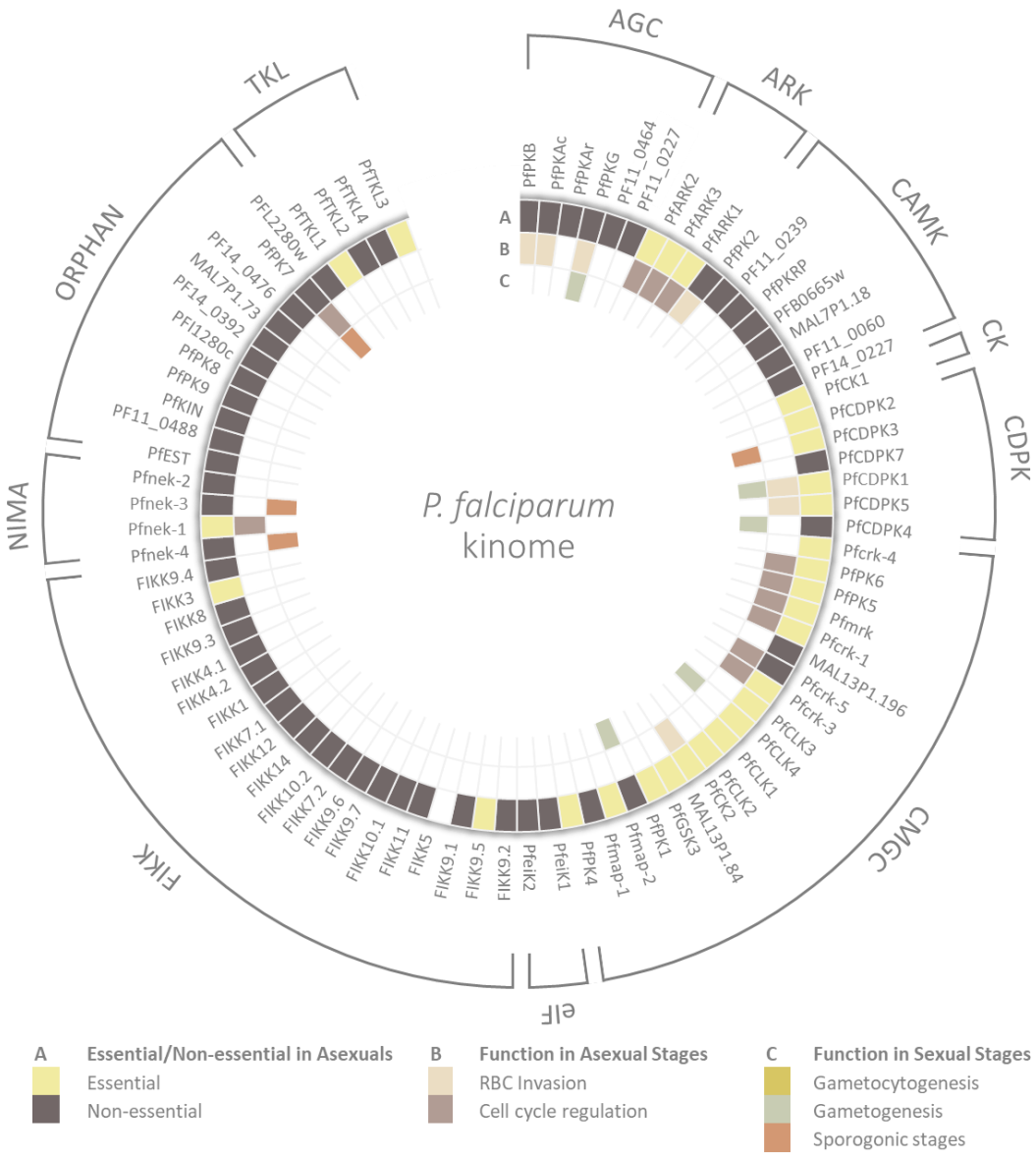

Figure 1.4: Summary of all identified kinases of the *P. falciparum* kinome.
The *Plasmodium* kinome, consisting of 90 kinase members and cluster within 11 kinome groups/families; AGC, ARK, CaMK, CK1, CDPK, CMGC, eIF, FIKKs, NIMA, Orphans and TKL (group/family- and gene names; far outer layer). (Layer-A) identified essential end non-essential kinases for intraerythrocytic parasites stages. (Layer-B) Characterised kinase functions in IDC and (Layer-C) gametocytogenesis, gametogenesis or sporogonic cycle. Data compiled from [87, 90-95, 98, 115-119].

Classic eukaryotic cell cycles are regulated by CDKs, among other regulators. Here, 5 CDKs are present in the *P. falciparum* kinome; however, their involvement in *P. falciparum* cell cycle control is still unclear [102, 120]. Merckx *et al*. have recently identified 3 novel CRKs of which PfMRK and PfPK5 associates with and are subsequently regulated by cyclins Pfcyc1,-3 and -4 [89]. PfMRK may be associated with nuclear DNA replication machinery; however, very little is known about the distinct roles of these kinases [121]. Furthermore, 2 mitogen-activated protein kinases (MAPKs) are represented in the *P. falciparum* kinome, MAP-1 and MAP-2, of which the latter is essential for IDC completion [117]. However, due to the lack of MAPKK in the *Plasmodium*

kinome, both Dorin *et al*. and Lye *et al*. argued in favour of atypical MAPK regulation by members of NIMA/NEK kinases [91, 118]. Three enzymes encoded in the *P. falciparum* kinome belong to the glycogen synthase kinase family (GSK) of which PfGSK3 have been reported to associate with erythrocytic Golgi-like apparatus, co-localise with Maurer's clefts and aids in protein export to erythrocytic membranes [122]. Finally, 4 cyclin-dependent-like kinases (CLKs) of the CMGC group, PfCLK1-4, are present in the *P. falciparum* kinome and are essential for IDC completion [123]. Four TKL members are present in the *P. falciparum* kinome despite the absence of tyrosine kinases in *Plasmodium* [102]. Notably, only 2 TKLs, PfTKL1 and PfTKL3, are essential for IDC completion [98]. Both of these kinases, similar to mammalian TKLS, share MORN and SAM motifs found at the N-terminal [115].

In a study performed on the *P. falciparum* parasite's global kinomic and phosphoproteomic, several essential cell cycle associated kinases have been functionally assessed through reverse genetic approaches [98]. Several of these essential kinases are involved in cell cycle regulation and progression such as the NIMA/NEK and ARK kinases [90, 92].

1.3.5 *P. falciparum* kinases involved in the cell cycle

NIMA/NEK kinases, a kinase family mainly involved in eukaryotic mitosis and meiosis, are represented by 4 members in the *P. falciparum* kinome [98, 102]. The majority of the NEK kinases are predominantly expressed in the gametocyte stages of the parasite life cycle [92, 117], with the only exception of PfNEK-1 expressed in the intraerythrocytic stages as well [98]. Interestingly, PfNEK-1 is male gametocyte specific in *Plasmodium* while, both PfNEK-2 and PfNEK-4 are expressed irrespective of the parasite sex [92]. The latter is essential for meiotic zygote-ookinete transitioning of the parasite in the mosquito midgut [94, 95]. Mitotic kinases, such as NEKs and ARKs among others, have been described as centrosomal cycle regulators in higher eukaryotes [124].

The *P. falciparum* kinome has three conserved Ser/Thr protein kinases distantly related to AGC kinases, belonging to the Aurora family PfARK-1-3 [119]. All the ARKs are essential for intraerythrocytic stages of the *Plasmodium* parasite due to previous unsuccessful gene disruption attempts. Uniquely, PfARK-2 is only present in *Plasmodium* species while PfARK-3 is found in only a subset of apicomplexans, *Plasmodium, Neospora* and *Toxoplasma.* By contrast, PfARK-1 is highly conserved across all apicomplexans. Previous studies indicated co-localisation of PfARK-1 with a subset of nuclei during schizogony, with no more than one PfARK-1 pair per

nucleus in a maximum of 4 nuclei per schizont at any given time, in favour of the asynchronous model of nuclear division in *Plasmodium* parasites [57, 119]. This strongly suggested an essential role of PfARK-1 in parasite cell cycle events. Furthermore, co-localisation studies indicated PfARK-1 pairs flank intra-nuclear microtubule spindles during the onset of mitosis [119]. However, as mitosis progresses to developed full bipolar mitotic spindles, PfARK-1 pairs are undetected; suggesting altogether, PfARK-1 associates with spindle pole bodies (SPB), a distinctive feature of mitosis [98, 119]. SPB, often referred to as centriolar plaques, are the functional equivalent of the centrosomes (MTOCs) found in higher eukaryotes. These SPB are embedded in intact nuclear membrane pores and anchors spindle microtubules inside the nucleus [65, 125]. Duplication of SPB, together with microtubule assembly, is an early hallmark of mitosis in *Plasmodium* [65].

1.4 Work leading up to this dissertation

1.4.1 Aurora kinase and ARK interrogation

As attractive anti-neoplastic drug targets, Aurora kinases have been exploited extensively in cancer [126] and Aurora kinase-specific inhibitors are continuously developed and assessed for their potential as Aurora-based targeted anti-cancer therapy [127]. Hesperadin, among other commercially available Aurora kinase inhibitors (reviewed in [128, 129]), is an Aurora kinase specific indolinone and has been successfully used in previous studies as a tool for functional kinase analysis [130]. Inhibition of mammalian AUR-B through hesperadin treatment revealed its function in correcting kinetochore-microtubule attachment and subsequent maintenance of the spindle assembly checkpoint, reminiscent of AUR-B RNAi phenotype [130]. Furthermore, hesperadin has shown to have nanomolar range activity (250 nM) against mammalian cells and significantly reduce cancer cell proliferation as a result of mitotic defects through AUR-B inhibition [131]. Hesperadin was recently reported as a repurposed inhibitor of the human Aurora kinase family with nanomolar activity against protozoans such as *Trypanosoma brucei* [132] and *Plasmodium* parasites [133]. In other protozoans, such as *T. brucei*, TbAUK-1 inhibition resulted in blocked nuclear division with S-phase re-initation and impaired spindle formation during mitosis [132, 134].

Aurora kinases have been described in various organisms with a close association with centrosome and bipolar microtubule dynamics, as well as chromosome segregation and cytokinesis [90, 135]. The role of PfARK associated with SPB in cell cycle regulation of *P.*

falciparum parasites has not been completely elucidated. This is mostly due to the complexity associated with tight synchronisation of the parasite to a particular cell cycle compartment under *in vitro* conditions. Therefore, to aid in cell cycle studies, tight compartmentalisation of the parasites within a minimal age range within parasites is required [58].

1.4.2 A system to allow parasite synchronisation for cell cycle analysis

In erythrocytes, polyamines are present in low levels as they lack ornithine decarboxylase (ODC) and *S*-adenosyl methionine decarboxylase (AdoMetDC) [136] and absorb polyamines from the environment [137, 138]. Naturally occurring polyamines (including putrescine, spermidine and spermine) [139] are essential mitogens of normal cell cycle progression. The polyamine pathway is essential for cell growth and proliferation of all proliferating cells including *P. falciparum* parasites and inhibition thereof leads to decreased cell growth and apoptosis [140, 141]. Mitogen (polyamine) depletion leads to R-point induction in cells and cells cannot progress through the G_1/S transition [142, 143].

P. falciparum infected erythrocytes have significant increased polyamine levels due to polyamine synthesis by the parasite as the parasite matures during the IDC (Fig. 1.5) in preparation of increased macromolecular biosynthesis required for DNA replication and nuclear division during the schizont stages [54, 55]. This characteristic was exploited in an innovative study on *P. falciparum* parasites by Van Biljon *et al*., 2018 [142] where a developmental block was induced in early trophozoite-stages through polyamine biosynthesis disruption using α-difluoromethylornithine (DFMO) (Fig. 1.5), an ODC inhibitor [142]. As polyamine biosynthesis is essential for parasite proliferation, DFMO treatment arrested parasites synchronicity (93.3 ± 1.0%) in the early trophozoite-stage of development with essentially no parasites able to escape the block (Fig. 1.5) [142].

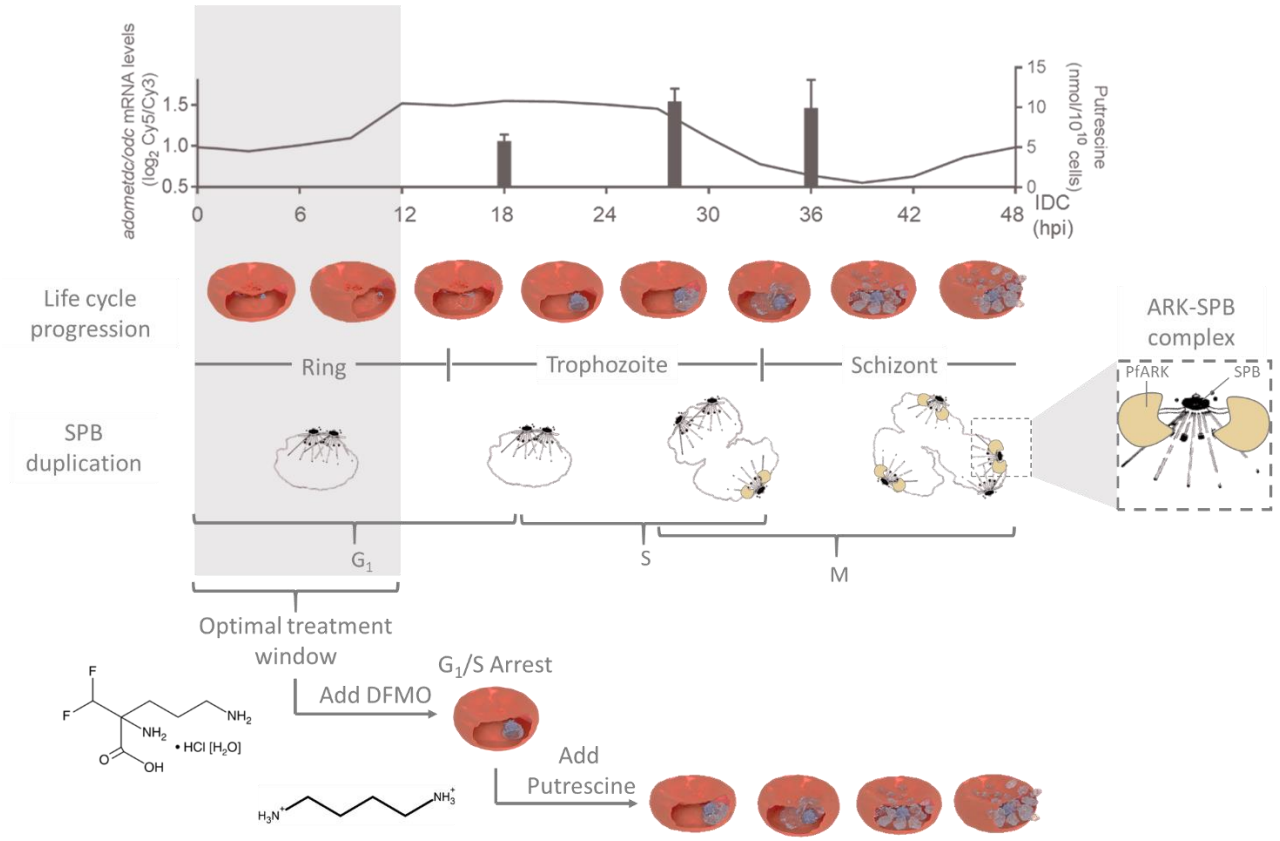

Figure 1.5: *P. falciparum* parasite cell cycle events correlated to inducing controlled cell cycle arrest and re-entry. Expression of PfAdoMetDC/ODC (top panel line graph) from 12 hpi correlates with detectable putrescine levels (top panel bar graph) at early and late trophozoite (S) and schizont (M) parasite stages. An optimal window for DFMO treatment (grey block) is therefore 0-12 hpi, ring-stage (G_1) parasites, resulting in 18-22 hpi synchronised early trophozoite-stage parasites (G_1/S). Parasite arrest can be reversed upon putrescine addition after 24 h of DFMO treatment, with normal life cycle progression as a result. Correlated with life cycle progression, duplication of SPB (middle panel), together with microtubule assembly, is an early hallmark of the M-phase. PfARK-1 pairs (yellow shapes) flank intra-nuclear microtubule spindles during the onset of M-phase. Images were created using Blender software (www.blender.org) and others were adapted from previous publications [65, 90, 94, 119, 142].

The morphologically observed tight synchronisation was used to evaluate if these parasites are indeed also regulated in their cell cycle development. For arrest to be a true reflection of a cell cycle arrest event (e.g. parasites enter a quiescent G_0 state and re-initiate the cell cycle once conditions are favourable), the arrest should be fully reversible and parasites remain viable and free of obvious negative perturbation effects [58, 144]. The presence of polyamine uptake mechanisms in *P. falciparum* parasites was established [145] and it was used to prove the DFMO-induced arrested parasites could re-initiate their cell cycle after mitogen (polyamine) stimulation [142]. Additionally, DFMO-treated parasites comply with a quiescent, arrested phenotype as they remain morphologically unaffected, metabolically viable and they still actively synthesise ATP [146]. DFMO-treated parasites can re-enter the cell cycle upon putrescine supplementation without observable stress and increased gametocytogenesis rate[142].

The system was used to interrogate regulation of the parasite during its G_1-phase, since these parasites were unable to initiate DNA synthesis and remained at a 1N DNA copy number associated with the G_1-phase [142]. Polyamine supplementation resulted in subsequent DNA replication during schizogony and nuclear division in mitosis [142]. This phenomenon is indicative of cell cycle arrest at a mitogen-dependent R-point prior to the G_1/S transition (Fig. 1.5) [142]. The system therefore provides a useful tool by which parasites can be compartmentalised in their cell cycle, and this is a much-needed resource for cell cycle studies of malaria parasites.

This dissertation focused on the involvement of PfARK regulatory mechanisms in cell cycle phase progression and life cycle development of the parasite through chemical interrogation. The novelty of the dissertation is embedded in the use of an innovative approach, established by Van Biljon *et al*. [142] for cell cycle phase-specific synchronisation of parasites as a tool to provide extensive insights to the importance of PfARK cell cycle regulation during the intraerythrocytic stages of the parasite. Ultimately, the dissertation provides a better understanding of PfARK cell cycle regulation during parasite asynchronous nuclear division associated with M-phase progression.

1.5 Hypothesis

DFMO synchronisation of intraerythrocytic *P. falciparum* parasites allow investigation of the involvement of Aurora-related kinases in M-phase regulation of intraerythrocytic *P. falciparum* parasites.

1.6 Aim

The main research aim of this study was to define the role of PfARK during M-phase cell cycle regulation in intraerythrocytic *P. falciparum* parasites.

1.7 Specific objectives

1.7.1 To validate DFMO-induced *P. falciparum* parasite cell cycle arrest at the G_1/S transition and subsequent parasite recovery as a valuable synchronisation tool.

Here, the antiproliferative properties of DFMO-treated parasites were validated quantitatively. This was extrapolated to validate the developmental stage of DFMO-arrested parasites and assessment of life cycle progression of DFMO-arrested parasite reversal through putrescine supplementation.

1.7.2 Assess the potential of DFMO synchronisation as an applicable system to study the M-phase of *P. falciparum* parasite cell cycle.

Life cycle progression to M-phase of putrescine-rescued parasites was assessed and validated to the developmental stage of putrescine-rescued parasites. Furthermore, nuclei formation during M-phase development of putrescine-rescued parasites was described.

1.7.3 Characterise of the role of *P. falciparum* ARK in M-phase cell cycle regulation.

Here, the antiproliferative properties of hesperadin was validated as an PfARK inhibitor. DFMO synchronisation was used as a tool to evaluate the effect on M-phase cell cycle regulation of PfARK inhibition on life cycle progression and proliferation, the ability of parasite proliferation recovery after hesperadin treatment, DNA replication during schizogony, nuclei development during schizogony, parasite viability and spindle formation during mitosis.

1.8 Research outputs

1.8.1 Peer reviewed publications

Van Biljon, R., Niemand, J., van Wyk, R., Clark, K., Verlinden, B., Abrie, C., von Grüning, H., Smidt, W., Smit, A., Reader, J., Painter, H., Llinás, M., Doerig, C., and Birkholtz, L.-M., Inducing controlled cell cycle arrest and re-entry during asexual proliferation of *Plasmodium falciparum* malaria parasites. Scientific Reports, 2018. 8(1): p. 16581.

Results of aim 2 and 3 are being prepared as part of a manuscript for submission to Nature Chemical Biology (impact factor of 15.066).

1.8.2 Conference proceedings:

Abrie C., van Biljon R., Doerig C., Niemand J., Birkholtz L. Functional investigation of essential kinase regulatory elements of cell cycle regulation in *Plasmodium falciparum.* MRC Office of Malaria Research Conference. Poster presentation. Pretoria, South Africa, 2017.

2 Chapter 2: Materials and Methods

2.1 Ethics statement

All experiments of this study were carried out at the Malaria Parasite Molecular Laboratory (M2PL) with certified Biosafety level P2 facilities for *P. falciparum* parasite cultivation. The University of Pretoria Research Ethics Committee, Health Sciences Faculty has granted ethical clearance (506/2018) for the cultivation of parasites and the use of human erythrocytes.

2.2 *In vitro* culturing of intraerythrocytic *P. falciparum* parasites

Blood was donated from consenting A+, B+ or O+ human donors. Serum and buffy coat was removed from whole blood by washing with phosphate buffered saline (PBS) containing 137 mM NaCl (Sigma Aldrich, USA), 2.7 mM KCl (Merck, Germany), 4.3 mM Na_2HPO_4 (Merck, Germany), and 1.47 mM KH_2PO_4 (Merck, Germany) at pH 7.4 followed by centrifugation at 3500*g* for 10 min. Erythrocytes were stored at 4°C in culture medium (RPMI–1640 (Sigma Aldrich, USA) supplemented with 23.81 mM $NaHCO_3$ (Sigma Aldrich, USA) [147], 25 mM HEPES (Sigma Aldrich, USA), 0.024 mg/mL gentamycin (HyClone, USA), 0.2 mM hypoxanthine (Sigma Aldrich, USA), 0.2% glucose (Merck, Germany), and 5 g/L Albumax II (ThermoFischer, New Zealand)) for no longer than 2 weeks at 50% haematocrit. Cryopreserved *P. falciparum* NF54, NF54$^{PfS16\text{-}GFP\text{-}Luc}$, 3D7 and W2 parasites were thawed at 37˚C followed by adding 200 µl of 12% NaCl and 1800 µl of 16% NaCl in a stepwise manner with 5 min incubation periods after each addition. Thawed parasites were suspended in human erythrocytes and complete RPMI–1640 culture medium at a 5% haematocrit. In preparation for *in vitro,* studies cultures with a ring-stage parasitaemia of >2% were consecutively synchronised to ~80% ring-stage parasites by 5% (w/v) D-sorbitol (Sigma Aldrich, USA) treatment at 37˚C for 15 min to allow iso-osmotic lysis of trophozoite and schizont infected erythrocytes [148]. Synchronized cultures were maintained in complete culture medium at a 5% haematocrit. Routine culture maintenance included daily media changes and cultures were gassed with 5% CO_2, 5% O_2, and 90% N_2 (Afrox, South Africa) for approximately 50 s prior to incubation at 37°C in a rotatory incubator at 60 rpm. Parasitaemia was monitored daily using light microscopy of Giemsa stained parasites.

2.3 SYBR Green I-based fluorescence assay to validate antiproliferative effects against intraerythrocytic *P. falciparum* parasite stages

Malaria SYBR Green I-based fluorescence assay was used as screening method to determine compound *in vitro* antiproliferative efficacy against *P. falciparum* parasites. The assay is based on the detection of nucleic acid content. SYBR Green I is known to have a high affinity for double stranded DNA [149]. Human erythrocytes are known to lack nucleic acids. However, parasitic cells contain both DNA and RNA and are thus prone to SYBR Green I fluorophore staining. An >80% synchronised ring-stage intraerythrocytic *P. falciparum* parasite culture (1% parasitaemia, 1% haematocrit) was used. Chloroquine disulphate (0.5 µM), a well-known potent antimalarial, was used as a positive control for inhibition and an untreated control was used as a positive control for parasite growth. Compounds were dissolved in non-lethal dimethyl sulfoxide (final concentration lower than 0.1%) for full dose response evaluation in a 96-well plate serially diluted two-fold in complete culture medium. The parasites were placed in a modular gas chamber, gassed (5% CO_2, 5% O_2, and 90% N_2) for 1 min and incubated at 37°C in a stationary incubator for 96 h. Equal volumes of thawed parasites were resuspended in SYBR Green lysis buffer containing 0.002% (v/v) SYBR Green I dye (Invitrogen, USA), 20 mM Tris, 0.008% (w/v) saponin (Sigma Aldrich, USA), 5 mM EDTA (ethylene dinitrotetraacetic acid) (Merck, Germany), 0.08% (v/v) Triton X-100 (Sigma Aldrich, USA) and incubated for 1 h in the dark at room temperature. SYBR Green I fluorescence was measured using a multimode reader GloMax®-Multi Detection System (Promega, USA) at excitation wavelength of 485 nm and emission wavelength of 538 nm. Normalisation to the untreated parasite growth control was performed after subtracting background fluorescence of the positive control for parasite growth inhibition and parasite proliferation was expressed as a percentage. Data were analysed and non-linear regression curves were generated using GraphPad 6.01 software to determine the half-maximal inhibitory concentrations (IC_{50}) [150] for all compounds.

2.4 Measurement of *P. falciparum* parasite nucleic content

Parasite DNA content as a measurement of DFMO-induced cell cycle arrest was investigated with flow cytometry as described [142]. Synchronised ring-stage *P. falciparum* 3D7 parasites (5% parasitaemia, 5% haematocrit) 6-10 hpi, were treated with 2xIC_{50} DFMO (Sigma Aldrich, USA). After 24 h DFMO treatment, DFMO-arrested intraerythrocytic parasites was reversed with 2 mM putrescine dihydrochloride (Sigma Aldrich, USA) and parasite recovery was monitored hourly up to 72 h after DFMO treatment. Aliquots (50 µl) were removed at every time point and

fixed in a 1:10 ratio with 0.025% (v/v) glutaraldehyde (Sigma Aldrich, USA) in PBS for 30 min at room temperature and stored at 4ºC. In preparation for flow cytometry, cell pellets were washed twice with 500 µl PBS followed by centrifugation at 500*g* for 5 min to remove the glutaraldehyde. For cell cycle compartmental analysis, cell pellets were stained for with 10 µl of 1:1000 SYBR Green I (Invitrogen, USA) together with 10 µl of 1:1000 Pyronin Y (Sigma Aldrich, USA) and incubated in the dark for 30 min at room temperature. The dye was removed through two consecutive washing steps with 500 µl PBS followed by centrifugation at 500*g* for 5 min. Cell pellets were resuspended in PBS to a final volume of 750 µl.

Flow cytometric analysis was performed on a Becton Dickinson Accuri™ C6 Plus (Becton Dickinson, USA) with voltage settings set to FSC: 50 V, SSC: 200 V and FITC: 380 V. For each sample, 100 000 events were counted, and fluorescence was measured for SYBR Green I (DNA) with a 515-545 nm filter (FL-1 channel, FITC signal) and for Pyronin Y (RNA) with a 564-606 nm filter (FL-2 channel, PE signal). A single stained SYBR Green I and Pyronin Y sample was used to calculate compensation.

2.5 Flow cytometry gating strategy

Flow cytometry datasets were analysed using FlowJo version 10 software (FlowJo LLC, USA). Dataset cleansing was done by removing instrument induced fluorescence anomalies, doublets and/or cell clumps, cell debris and any unwanted events. Primary gating was performed manually based on control samples; an unstained uninfected erythrocyte sample and a stained uninfected erythrocyte sample. Background DNA-free erythrocyte fluorescence signal was deducted using the latter control sample. Primary gating was performed to separate parasite infected erythrocytes from the uninfected erythrocytes, as a measure of parasitaemia. The parasite infected erythrocyte population was used to perform secondary gating; segregate parasite infected erythrocytes according to their DNA copy number. Ring and early trophozoite parasites with a single nucleus corresponded to 1N DNA copy number [57], while mature trophozoite and schizont parasites contained multiple nuclei, 2N [57] and >2N [57, 151], respectively.

2.6 Morphological evaluation of *P. falciparum* parasites

2.6.1 *P. falciparum* parasite sample preparation for immunofluorescence assay (IFA)

Samples of 2 ml synchronised intraerythrocytic *P. falciparum* parasites (5% haematocrit, 5-10% parasitaemia) were aliquoted and centrifuged at 1200*g* for 3 min. Supernatant was discarded

and samples were resuspended in 1 ml PBS at 4ºC. Parasites were released from erythrocytes through 0.15% (w/v) saponin in PBS lysis on ice for 2 min (trophozoite and schizont parasite stages) and 10 min (ring-stages) thereby releasing the parasite from the erythrocytic plasma membrane and haemoglobin responsible for background fluorescence. After saponin incubation, parasites were centrifuged at 1500*g* for 5 min at 10ºC. Parasite pellets were resuspended in 1 ml cold PBS and washed through centrifugation at 5300*g* for 2 min, twice. Preservation of parasite sub-cellular molecular arrangements at a given time is required for accurate parasite morphology assessment. *P. falciparum* parasites were fixed with 4% (w/v) paraformaldehyde (PFA) with 0.025% (v/v) glutaraldehyde in PBS for 30 min on ice to create cross-linkages between amine groups on proteins and nucleic acids. Unreacted aldehyde groups were blocked through 0.1% (w/v) glycine treatment for additional 5 min on ice. Fixatives were removed from the parasite suspension through centrifugation at 5300*g* for 5 min. The fixed parasite pellet was washed in cold PBS followed by centrifugation at 5300*g* for 5 min, resuspended in 100 µl cold PBS and stored at 4ºC.

2.6.2 Coverslip cleaning and preparation for IFA

To remove any chemical residue present on the coverslips, a series of 100% acetone, 100% methanol and triple distilled water (dddH_2O) was used to rinse coverslips, repeated twice. Coverslips were then incubated in 1 M KOH for 45 min using a Branson Sonifier cell disruptor B-30 (Branson, USA) to clear the surface of the coverslips from small debris, which may result in autofluorescence or non-specific binding. Coverslips were sonicated an additional two times in dddH_2O for 15 min and subsequently rinsed twice in dddH_2O prior to storage in 40% (v/v) ethanol in dddH_2O at room temperature.

To ensure parasites adhere to the surface of the coverslips through ionic attraction to negative charges in cell membranes, cationic surface charge was created by incubating coverslips in 0.01% (w/v) poly-L-lysine (PPL) (Sigma Aldrich, USA) in PBS for 30 min in a moist chamber. Following incubation, coverslips were rinsed twice with PBS. Fresh coverslips were prepared on the day of immunofluorescence (IF) imaging.

2.6.3 Direct IFA

IF allows for molecular antigen detection and visualisation through specific binding of antibodies. Direct IF labelling is based on a primary antibody conjugated to a fluorophore specific for a target molecule. For direct IF, 50-100 µl fixed parasites (as prepared above) were aliquoted onto clean

PPL-coated coverslips (as prepared above). Parasites were left to settle for 1 h to adhere and form a monolayer on the coverslip surface. Unattached parasites were carefully rinsed off without disturbing the monolayer using PBS. Parasites were permeabilised with 0.1% (v/v) Triton X-100 in PBS incubated for 5 min at room temperature. After permeabilisation, the parasites were washed with PBS. Non-specific antibody binding was blocked by incubating coverslip adhered parasites for 20 min with 1% (w/v) bovine serum antigen (BSA) in PBS at room temperature. AlexaFluor 647 conjugated rabbit anti-α-tubulin (Biocom Biotech, RSA) was used at 1:500 dilution in 1% (w/v) BSA in PBS incubated 45 min in a humid chamber in the dark. To remove unbound primary antibodies, the parasites were washed three times with PBS. Coverslips with antibody-labelled parasites with suitable fluorophore counterstaining (Table 2.1 below) were mounted on glass slides in Fluoroshield (Sigma Aldrich, USA) mounting medium.

2.6.4 Fluorophore staining

Fluorophore staining is based on light absorption and emission through a fluorescent chemical compound. Parasite morphology was correlated to parasite maturity through confocal fluorescence microscopy using fluorophores (Invitrogen. USA) with applicable binding specificity. Thin smears of intraerythrocytic *P. falciparum* parasites were made and air-dried parasites were fixed by rinsing slides in 100% methanol. Applicable fluorophores were selected, and fixed parasites were incubated with fluorophores at specified dilution (as indicated in Table 2.1) for 15 min in the dark at room temperature. In the case of dual staining, fluorophores were selected based on their excitation and emission wavelengths to ensure spectrally distinct fluorophores were used. Excess fluorophores were removed by rinsing the slide twice in PBS. Parasites were freshly stained on the day of visualisation.

Table 2.1: Fluorophores used in fluorescent labelling assays.

Fluorophore	Probe type	Em[1] (nm)	Ex[2] (nm)	UV-*vis* spectrum colour	Dil.[3] used
Hoechst 33258	Nucleic acids; AT-selective	478	345	Blue	1:1000
SYBR Green I	Nucleic acids; AT-selective	520	497	Green	1:1000
Propidium Iodide (PI)	Nucleic acids; membrane impermeant	617	536	Orange/Red	1:1000

1) Em: Peak emission wavelength (nm).
2) Ex: Peak excitation wavelength (nm).
3) Dil. Used: dilution used.

2.6.5 Confocal fluorescence microscopy and image processing

For parasite morphology analysis, imaging was performed on a Zeiss LSM 880 Inverted Confocal Laser Scanning Microscope (LSM) - Airyscan detector (Zeiss, Germany) for super-resolution imaging with appropriate channels, based on fluorophore emission and excitation wavelengths. A 100x oil immersion objective with 1.4 numerical aperture was used for imaging parasites. Photomultiplier gain was set to 600 V and laser scanning times were kept at 45 s. Zeiss ZEN lite blue edition software (Zeiss, Germany) was used for initial digital image processing and ImageJ version 1.52d open source software (NIH, USA) was used for fluorescence intensity analysis as grey values in pixels.

3 Chapter 3: Results

3.1 DFMO-induced parasite G_1/S transition cell cycle arrest and subsequent parasite recovery as a synchronisation tool

3.1.1 Antiproliferative properties of DFMO

The antiproliferative effects of DFMO, an AdoMetDC/ODC inhibitor (Fig. 3.1A), was evaluated across different *P. falciparum* parasite strain, drug sensitive NF54 (or NF54$^{PfS16\text{-}GFP\text{-}Luc}$) and 3D7 parasite strains, as well as drug resistant (chloroquine, cycloguanil, quinine, sulfadoxine and pyrimethamine) W2 parasite strain. The IC_{50} of DFMO against intraerythrocytic *P. falciparum* parasites was confirmed through *in vitro* SYBR Green I fluorescence assay (Fig. 3.1B).

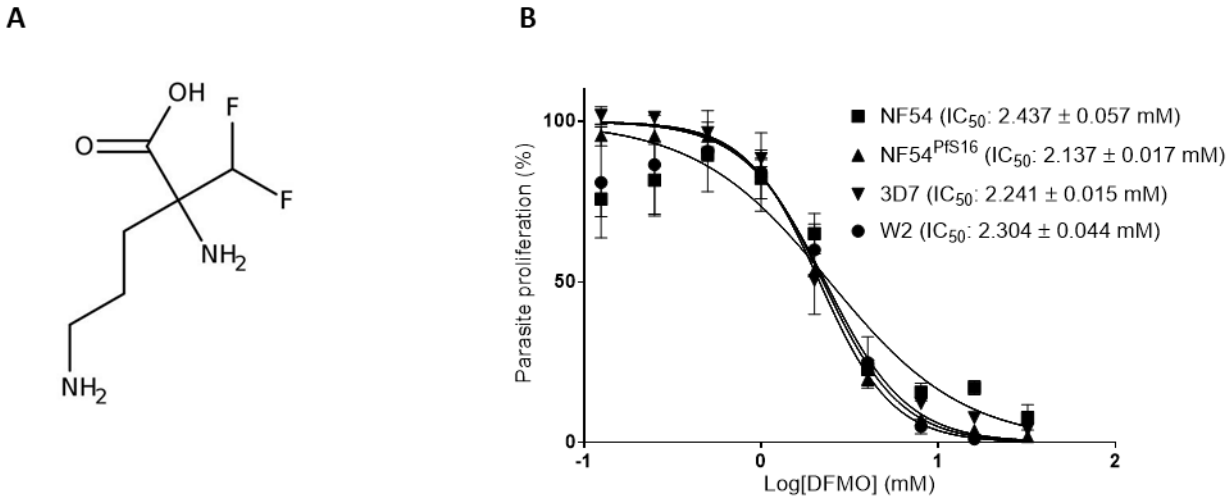

Figure 3.1: Dose-response evaluation of DFMO inhibition of intraerythrocytic *P. falciparum* parasite strains. **(A)** The structure of DFMO **(B)** DFMO dose-response against NF54 (drug sensitive, ■), NF54$^{PfS16\text{-}GFP\text{-}Luc}$ (drug sensitive, ▲) 3D7 (drug sensitive, ▼) and W2 (drug resistant, ●) parasite strains were determined using SYBR Green I-based assay for 96 h drug pressure, initiated on ring-stage *P. falciparum* parasite cultures (1% parasitaemia, 1% haematocrit). Results are representative of one biological replicate (n=1± SD), performed in technical triplicate. Non-linear regression curves were generated using GraphPad Prism version 6.01 software. Error bars represent standard deviation. For some points, error bars fall within the symbols.

Collectively, the IC_{50} values of DFMO treatment across different *P. falciparum* parasite strains (W2, NF54 and 3D7) were determined as 2 mM and corresponds to previous reports of IC_{50} 1.25± 0.42 mM for the 3D7 strain [152]. No cross-resistance or loss of efficacy was observed between the strains. For DFMO-induced cell cycle arrest studies, parasites were treated with DFMO at 2xIC_{50} concentrations.

3.1.2 Flow cytometry evaluation of DFMO-arrested parasites

3.1.2.1 Quality control evaluation and gating strategy of infected erythrocytes stained with SYBR Green I

Flow cytometry was used to evaluate DNA synthesis (SYBR Green I staining) as a proxy for cell cycle arrest and to determine the phase of arrest. To ensure the sensitivity of flow cytometry measurements, strict quality control parameters were applied to eliminate fluorescent anomalies (Fig. 3.2). Flow run stability was used to determine the population of cells present in even flow and eliminate cells affected through uneven flow caused by instrument clogging and back pressure from the dataset. Fig. 3.2A indicates a forward scatter (FSC-A) parameter against time to evaluate the quality of the flow over the time of acquisition, which was consistent through the experiment. Secondly, pulse geometry gating was performed to acquire only single cells from the dataset. A forward scatter height (FSC-H) against area (FSC-A) density plot (Fig. 3.2B) was used to select for single cells along the diagonal, thereby removing doublets and cell clumps from the dataset and increasing the accuracy of flow cytometry measurements. Uninfected and *P. falciparum* infected erythrocytes were identified based on relative cell size (FSC-A) and cell complexity (SSC-A) represented by a density plot (Fig. 3.2C). The forward and side scatter gating eliminate cell debris, free merozoites and events not of interest from the dataset.

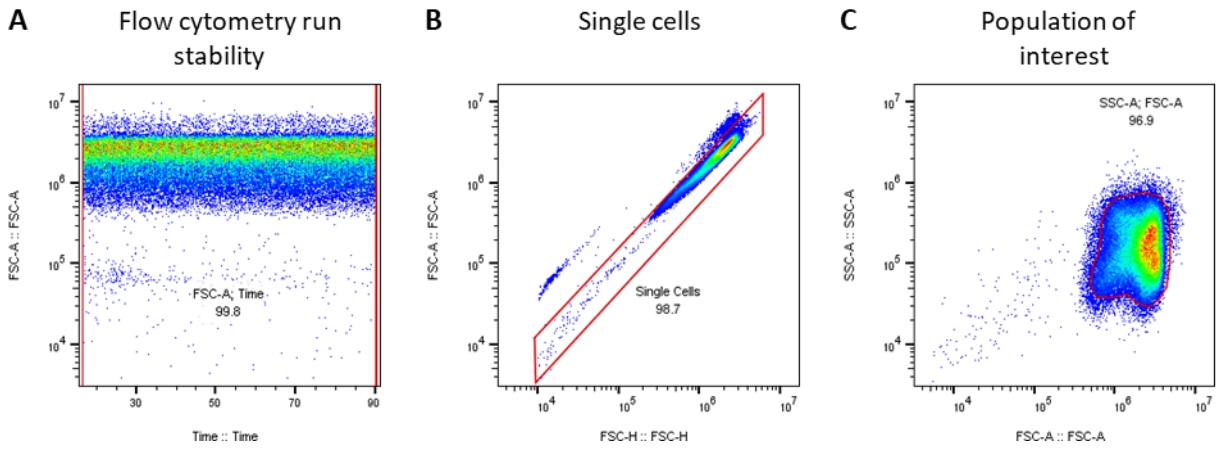

Figure 3.2: Flow cytometry quality control parameters evaluation.
(A) Flow stability gating. A forward scatter (FSC) parameter against time represents the quality of the flow over the time of acquisition. The stability gate (red) represents the population of cells with an even flow. **(B)** Pulse geometry gating. Forward scatter height (FSC-H) against area (FSC-A) density plot allows for differentiation between single cells and cell clumps. **(C)** Forward and side scatter gate. Density plot represents cell size (FSC) correlated with its complexity (SSC) to select for wanted cells. All density plots were generated using FlowJo version 10.1 software.

Subsequently, the *P. falciparum* infected erythrocyte population was identified by evaluating differences between SYBR Green I nuclear stained uninfected and infected populations (Fig. 3.3), respectively, using flow cytometry as described previously [151, 153]. *P. falciparum*

infected erythrocytes can be clearly distinguished from the uninfected erythrocytes with complexity SSC-A analysis associated with fluorescent output (Fig. 3.3). Quadrant gates identified Q4 as a population with erythrocyte-generated fluorescence whilst Q3 represent the *P. falciparum*-infected erythrocyte population. Quantification of Q3 populations indicated a large difference between uninfected (0.29%) (Fig. 3.3A) and parasite infected (9.31%) erythrocyte samples (Fig. 3.3B), the latter corresponding to parasitaemia (9%) morphologically quantified using Giemsa-stained thin smears. This gating strategy was subsequently applied to all samples to identify the *P. falciparum*-infected erythrocyte population of interest.

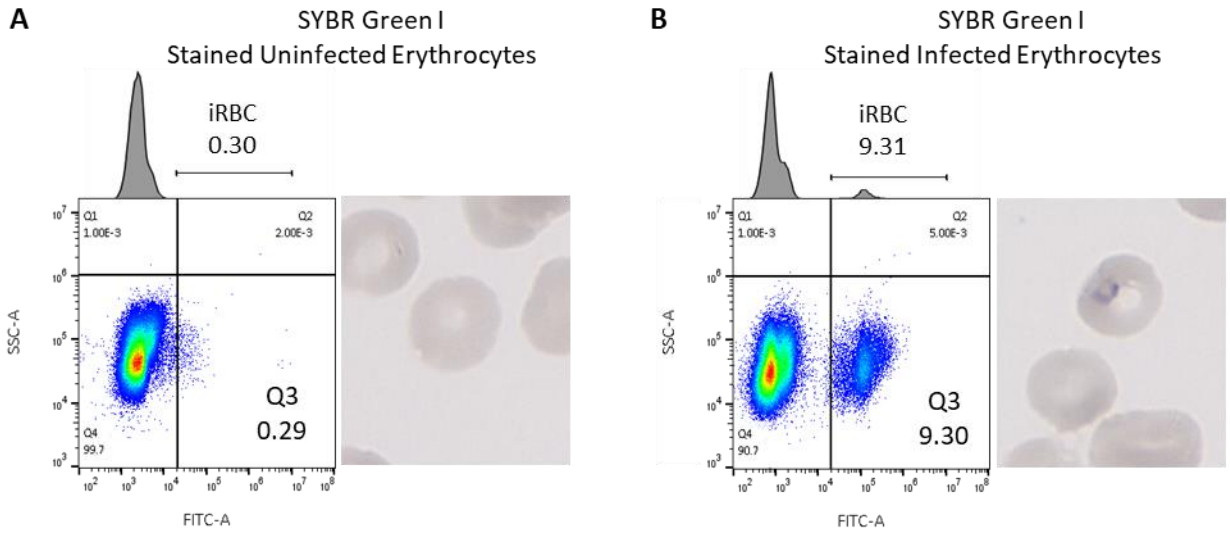

Figure 3.3: Flow cytometry gating strategy used for intraerythrocytic *P. falciparum* parasite life cycle progression. **(A)** Density plot represents the side scatter (SSC) of the SYBR Green I stained uninfected erythrocytes. The bar indicated on the corresponding histograms (iRBC) corresponds to the gate set to differentiate between SYBR Green I stained uninfected erythrocytes and infected erythrocytes fluorescence. **(B)** Gating conditions (as in fig. 3.3A) were applied to SYBR Green I stained intraerythrocytic *P. falciparum* 3D7 parasites. Density plots and histograms were generated using FlowJo version 10.1 software. Parasitaemia was confirmed through Giemsa stained light microscopy at 1000x magnification.

3.1.2.2 Using flow cytometry to evaluate parasite cell cycle compartments

Once the parasite-infected erythrocyte population was separated from uninfected erythrocytes, the population could be evaluated for cell cycle progression. Here, SYBR Green I nuclear stain was used to monitor cell cycle progression based on an increase fluorescence associated with increased nucleic acid content (Fig. 3.4). In all cases, the flow cytometric populations were associated morphologically with life cycle stages and independent nuclear counts through fluorescent imaging (SYBR Green I stained nuclei). Ring-stage parasites were haploid (1N), trophozoite-stages were considered to contain 2N nuclear content (two distinct nuclei observed). Schizonts were classified as containing any number of nuclei >2N [57, 151]. Therefore, flow cytometry can be used to assess cell cycle progression in *P. falciparum* parasites.

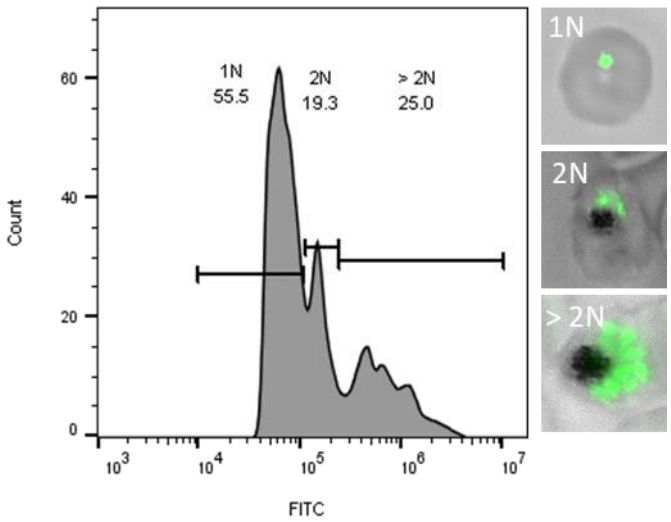

Figure 3.4: Flow cytometry gating strategy used for intraerythrocytic *P. falciparum* parasite DNA copy number progression.
Intraerythrocytic *P. falciparum* parasite culture (3% parasitaemia, 5% haematocrit) was stained with SYBR Green I before analysis. Fluorescence collected in the FL-1 channel (FITC signal) on a Becton Dickenson AccuriTM C6 Plus cytometer. Histogram represents parasite DNA copy number (N) with corresponding parasite morphology; ring-stage parasites (1N), trophozoite-stage parasites (2N), schizont-stage parasites (> 2N) as described [57, 151]. In all cases, a total of 100 000 events were captured. Histograms were generated using FlowJo version 10.1 software. Morphology was confirmed through SYBR Green I confocal fluorescence microscopy using a Zeiss LSM 880 Confocal Laser Scanning Microscope (LSM).

Additionally, SYBR Green I, in conjunction with Pyronin Y, staining was used for cell cycle compartmentalisation into G_1 and S-phase parasites (Fig. 3.5). DNA and RNA synthesis are associated with different cell cycle phases. Early G_1-phase are associated with ring-stage (1N) parasites and contains mainly DNA [151] and will therefore stain with SYBR Green I. During late G_1-phase RNA synthesis occurs as the parasite develops into early trophozoites [151]. Pyronin Y fluorescence is directly related to RNA content levels and will therefore increase during late G_1-phase. As the parasites develop to mature trophozoite (2N) and schizont (>2N) stages during the S-phase, both DNA and RNA content increases [151] and are associated with SYBR Green I and Pyronin Y fluorescence, respectively.

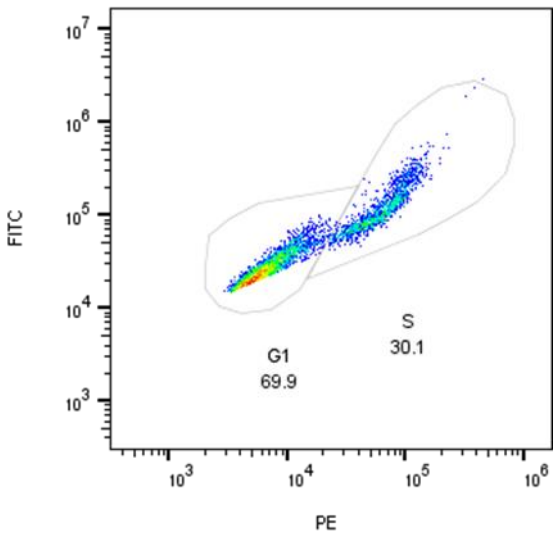

Figure 3.5: *P. falciparum* parasite cell cycle compartmentalisation.
P. falciparum parasite cultures (3% parasitaemia, 5% haematocrit) was stained with SYBR Green I and Pyronin Y before analysis. SYBR Green I fluorescence was collected in the FL-1 channel (FITC signal) and Pyronin Y fluorescence was collected in the FL-2 channel (PE signal) on a Becton Dickenson Accuri™ C6 Plus cytometer. Parasites were compartmentalised into G_1 and S-phase based on RNA fluorescence and DNA fluorescence as described [151]. In all cases, total of 100 000 events were captured. Density plots were generated using FlowJo version 10.1 software.

In all cases, the parasites' DNA and RNA content were monitored as the parasites progressed through its cell cycle (Fig. 3.5). The flow cytometric G_1-compartment gate associated with ring-stage parasites, and the S-compartment gate with increased DNA and RNA content in trophozoite and schizont stages of the parasite. Parasite life cycle progression was confirmed with SYBR Green I fluorescence microscopy. Thus, flow cytometry was found to be accurate for correlating life cycle stage to cell cycle phase and progression through DNA and RNA content quantifying. Therefore, flow cytometry can be used to investigate cell cycle phases in *P. falciparum* parasites.

3.1.2.3 Flow cytometry correlation of DFMO-treated parasites

Once the flow cytometry gating strategy was established and untreated parasites were accurately classified into cell cycle phases, this strategy could be applied to evaluate DFMO-arrested parasites for 1) parasite synchronicity and 2) the cell cycle phase. SYBR Green I fluorescence was used to evaluate cell cycle progression over two life cycles (72 h) in untreated parasites compared to DFMO-treated parasites (Fig. 3.6).

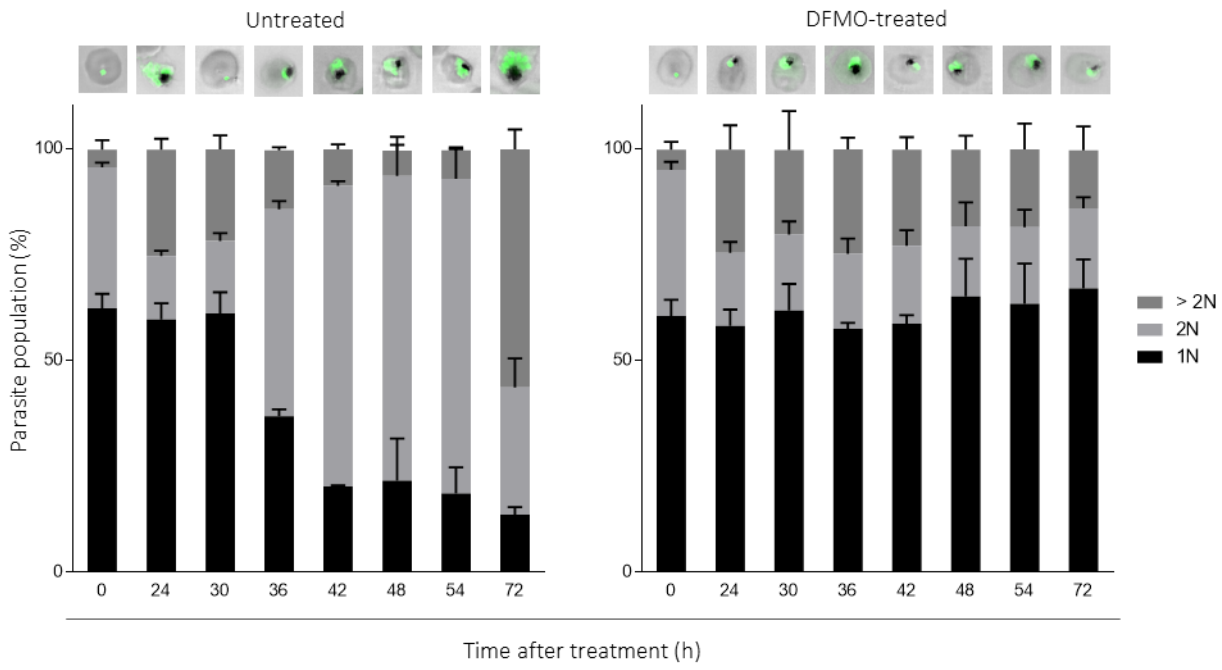

Figure 3.6: *P. falciparum* parasite synchronization through DFMO treatment.
Intraerythrocytic *P. falciparum* 3D7 ring-stage (~10 hpi) parasites (3% parasitaemia, 5% haematocrit) were synchronised by 2xIC_{50} DFMO treatment. Parasites sampled after 24 h DFMO treatment then every 6 h onwards up to re-initiation of the following IDC (72 h). SYBR Green I fluorescence indicative of parasite DNA copy number (N) was measured by flow cytometry: ring-stage parasites (1N), trophozoite-stage parasites (2N), schizont-stage parasites (> 2N) as described [57, 151]. Fluorescence was collected in the FL-1 channel (FITC signal) on a Becton Dickenson Accuri™ C6 Plus cytometer. A total of 100 000 events were captured and analysed using FlowJo version 10.1 software. Bar graphs were generated using GraphPad Prism version 6.01 software. Data are representative of one biological replicate (n=1± SD), performed in technical triplicates. Error bars represent standard deviation. Morphology of representative parasite population was confirmed through SYBR Green I confocal fluorescence microscopy using a Zeiss LSM 880 Confocal Laser Scanning Microscope (LSM).

The experiment was initiated on 5% sorbitol synchronised early ring-stage *P. falciparum* 3D7 parasites (0 – 10 hpi). Untreated parasites developed from a majority 1N (60.4%) ring-stage population (0 h after treatment; ≤10 hpi) to >2N schizont-stage population (36 h after treatment; ≤46 hpi) with 1N parasites decreasing (36.7%). DFMO treatment (2xIC_{50}) arrested parasites in early trophozoite-stage (18 – 22 hpi) of parasite development and ≥60% of the parasites remained predominantly in a 1N nuclear state throughout DFMO exposure time (Fig. 3.6). Approximately 20% of parasites were not affected by the DFMO block because they already progressed to 2N (>12 hpi) and therefore already synthesised AdoMetDC/ODC together with polyamines [142]. Flow cytometric quantification of nuclear content was confirmed through fluorescent imaging in all cases. Collectively, normal cell cycle progression occurred in untreated parasites and DFMO treatment arrested parasites at G_1/S transition, as expected [142]. This validated the requirement of polyamines for parasite life cycle progression and DFMO treatment as an effective synchronisation tool, as previously indicated [142].

3.1.2.4 Life cycle progression of DFMO-arrested parasite reversal through putrescine supplementation

To validate life cycle arrest as cell cycle arrest, re-entry into the correct cell cycle phase from an arrested state is required, without compromising cell viability and ensuring proper ploidy [58, 144, 154]. DFMO treatment of *P. falciparum* parasites produce metabolically and structurally uncompromised arrested parasites [138, 155] and the arrested parasites are fully reversable upon putrescine supplementation at non-toxic levels (2 mM) [145]. Arrested *P. falciparum* 3D7 parasites were reversed after 24 h of DFMO treatment through putrescine supplementation (in the presence of DFMO), or through DFMO washout and cultivation in normal media (Fig. 3.7A). Culture media normally contains high levels of polyamines [156], which are sufficient to restore proliferation in the absence of continuous DFMO pressure.

A significant difference ($P<0.05$) in parasitaemia between untreated *P. falciparum* 3D7 parasites and putrescine-rescued parasites was detected 36 h up to 48 h; however, no significant difference ($P>0.05$) in parasitaemia between untreated *P. falciparum* 3D7 parasites and putrescine-rescued parasites (9.97% and 9.31%, respectively) was detected at 72 h after treatment (Fig. 3.7A). Significant differences were calculated using a paired two-tailed equal variance students t-test. This suggest life cycle, and implied cell cycle, progression of reversed parasites was not compromised during schizogony.

A constant parasitaemia (~2-3%) was maintained in DFMO-arrested parasites (Fig. 3.7A), as DFMO induces cytostasis [112]. These parasites were arrested in early trophozoite-stages (Fig. 3.7B). However, a significant ($P<0.05$) increase in parasitaemia was detected 18 h after putrescine supplementation (from 42 h onward) (Fig. 3.7A) or when DFMO was washed out with no additional putrescine added. These parasites progressed to mature schizonts and subsequently released merozoites that could re-invade erythrocytes, as confirmed through SYBR Green I fluorescence microscopy (Fig. 3.7B) [102]. No difference was observed in the DFMO-washout parasites compared to the putrescine-rescued parasites, confirming the reversible nature of DFMO-treatment.

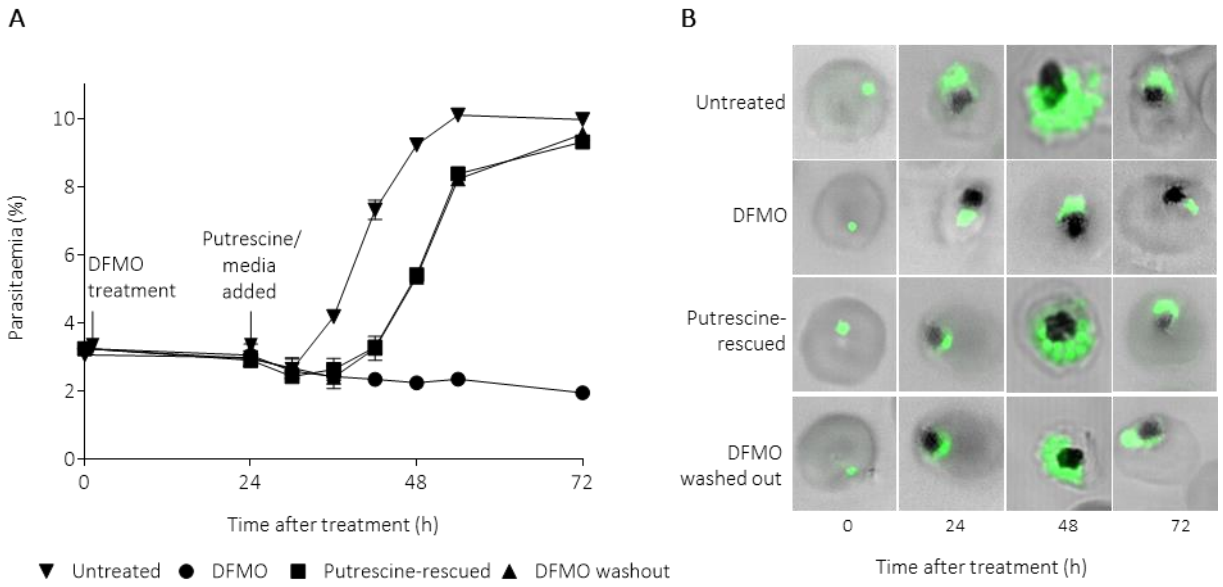

Figure 3.7: DFMO arrest and reversal associated to G_1/S cell cycle control in intraerythrocytic *P. falciparum* parasites.
DFMO-synchronised intraerythrocytic *P. falciparum* 3D7 parasites (3% parasitaemia, 5% haematocrit) were reversed after 24 h (~18 hpi) of DFMO treatment through 2 mM putrescine supplementation, or through DFMO-washout **(A)** Proliferation of untreated (▼) *P. falciparum* 3D7 parasites and parasites treated with DFMO (2xIC_{50}) (●), reversal with putrescine supplementation (■) and without putrescine supplementation (▲) was evaluated using flow cytometry. Fluorescence was collected in the FL-1 channel (FITC signal) on a Becton Dickenson Accuri™ C6 Plus cytometer. A total of 100 000 events were captured and analysed using FlowJo version 10.1 software. Line graph was generated using GraphPad Prism version 6.01 software. Data are representative of one biological replicate (n=1± SD), performed in technical triplicates. Error bars represent standard deviation. **(B)** Parasite life cycle progression monitored through SYBR Green I fluorescence microscopy using a Zeiss LSM 880 Confocal Laser Scanning Microscope (LSM).

3.2 DFMO synchronisation system applicable to study M-phase of the cell cycle

In previous reports, 33-37 hpi has been marked as the commencement of the M-phase in *P. falciparum* parasites [84]. For cell cycle studies, a minimal age range within parasites is required, and parasites must be synchronised to a specific cell cycle phase [58]. Here, DFMO synchronisation was assessed as an applicable system to synchronise parasites to study M-phase events (Fig. 3.8).

3.2.1 Validate the developmental stage of putrescine-rescued parasites

Following DFMO arrest and putrescine rescue, the parasite DNA copy number was measured to validate nuclear development during the M-phase of untreated and putrescine-rescued *P. falciparum* 3D7 parasites. Untreated and putrescine-rescued parasites differed in nuclear development at corresponding, time-matched hours after treatment (Appendix I: Fig. A1). The most observable difference in nuclear development was seen at 72 h after treatment in untreated >2N parasites (>56% of parasite population) and putrescine-rescued >2N parasites (<29% of

parasite population). While dissonance between untreated and putrescine-rescued parasites occurred, similar trends in nuclear development throughout parasite life cycle progression suggest a delay in putrescine-rescued parasites. Therefore, untreated and putrescine-rescued parasites were corrected regarding parasite age (Fig. 3.8A). Untreated and putrescine-rescued parasites had an approximate 6 h age difference. By contrast, age corrected parasites showed no observed differences in nuclear development between untreated and putrescine-rescued parasites.

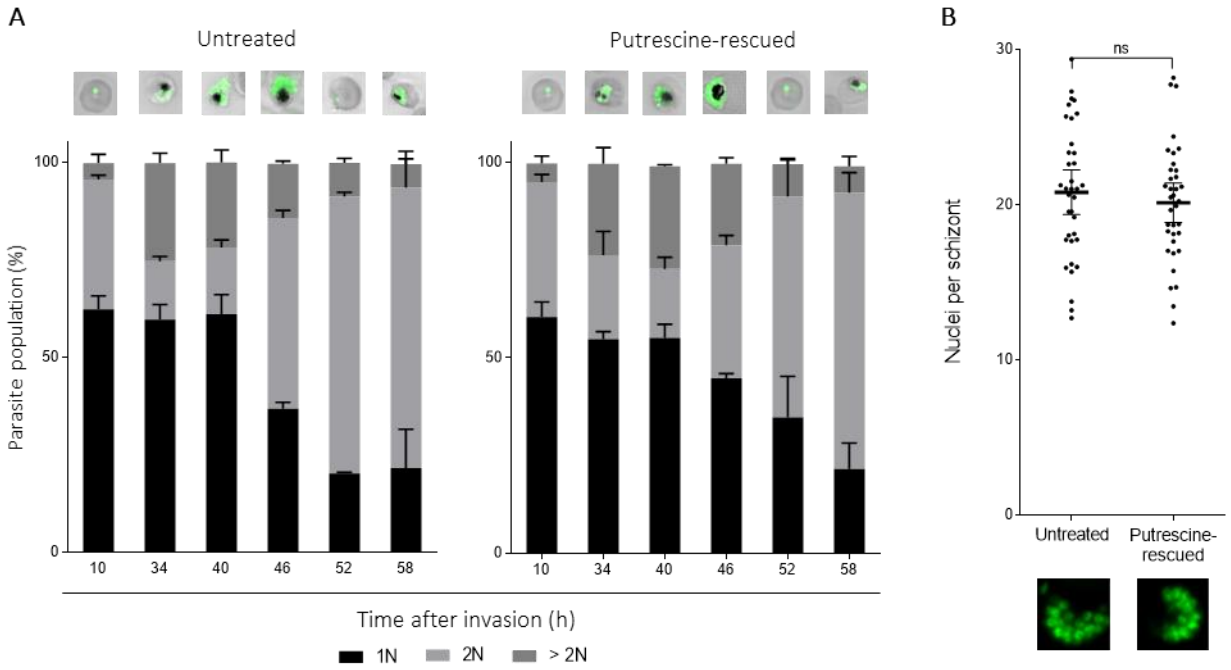

Figure 3.8: *P. falciparum* parasite cell cycle progression to M-phase of putrescine-rescued parasites.
DFMO-synchronised intraerythrocytic *P. falciparum* 3D7 parasites (3% parasitaemia, 5% haematocrit, ~18 hpi) were reversed with 2 mM putrescine supplementation and correlated to untreated parasites. Parasite samples were stained with SYBR Green I for flow cytometry and fluorescence microscopy analysis. **(A)** Parasite DNA copy number (N) was measured by flow cytometry as described [57, 151]. Untreated and putrescine-rescued parasites have been corrected regarding to parasite age (hpi). Fluorescence was collected in the FL-1 channel (FITC signal) on a Becton Dickenson Accuri™ C6 Plus cytometer. A total of 100 000 events were captured and analysed using FlowJo version 10.1 software. Data are representative of one biological replicate (n=1± SD), performed in technical triplicates. Error bars represent standard deviation. Morphology of representative parasite population was confirmed through SYBR Green I confocal fluorescence microscopy using a Zeiss LSM 880 Confocal Laser Scanning Microscope (LSM). **(B)** Untreated and putrescine-rescued parasite nuclei development was quantitatively assessed through SYBR Green I fluorescence microscopy. Significant differences were calculated using two-tailed equal variance students t-test, ns=P>0.05. Error bars represent 95% CI of the mean (n=36). Al graphs were generated using GraphPad Prism version 6.01 software.

To confirm that putrescine-rescued parasites progress normally through schizogony, nuclei were microscopically evaluated. Previous microscopic reports indicate that *P. falciparum* nuclei counts ranges from 16 to 32 distinct nuclei per schizont [34, 35]. These parasites completed mitosis with sharply defined nuclei commencing cytodifferentiation prior to merozoite formation [34, 35, 84]. Confocal fluorescence microscopy was used to compare nuclei counts of untreated

and putrescine-rescued *P. falciparum* 3D7 parasites during late stage schizogony in M-phase prior to cytodifferentiation (Fig. 3.8B). In both untreated and putrescine-rescued parasites, the number of nuclei of a minimum of 30 mature schizonts (42-48 hpi) was counted (Appendix I: Fig. A2-3).

An average of 21 and 20 nuclei per schizont was counted for untreated and putrescine-rescued *P. falciparum* 3D7 parasites, respectively with no significant difference ($P>0.05$) indicated. Significant difference was calculated using a paired two-tailed equal variance students t-test. The M-phase progression to cytodifferentiation in mature schizonts was confirmed in putrescine-rescued parasites. Therefore, DFMO synchronisation as can be used to study the cell cycle M-phase, using control parasites that were synchronised by DFMO treatment followed by putrescine rescue.

3.3 *P. falciparum* ARK function is required for cell cycle M-phase progression

Human Aurora kinase inhibition is known to lead to G_2/M cell cycle arrest, abnormal mitotic spindle formation and development of polyploid cells, without necessarily affecting cell viability [157]. The role of *P. falciparum* ARK in cell cycle regulation is poorly understood. Here, *P. falciparum* ARK inhibition through hesperadin drug treatment was monitored throughout the parasite IDC. The control parasites that are used for PfARK inhibition are therefore cell cycle compartmentalised parasites (DFMO-synchronised parasites reversed with putrescine supplementation) and hesperadin treatment was initiated (0 h) on these cell cycle compartmentalised parasites (Fig. 3.9).

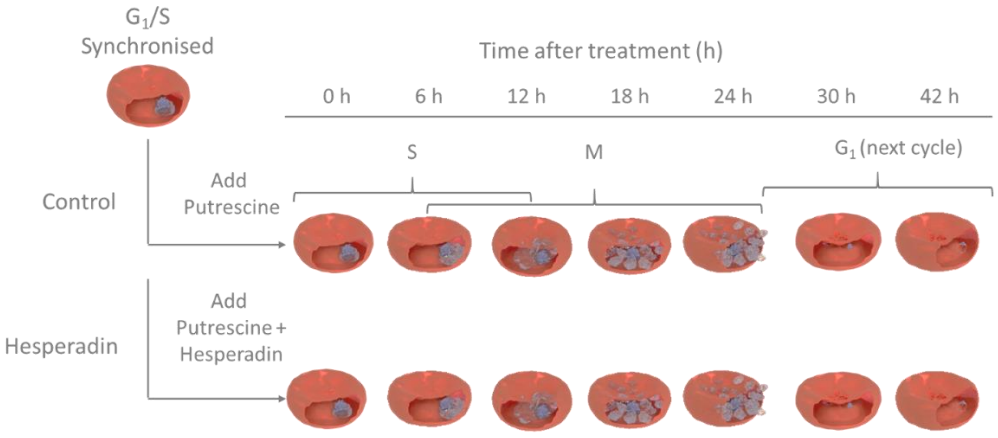

Figure 3.9: Experimental setup for *P. falciparum* ARK interrogation in M-phase cell cycle regulation,
DFMO treatment was initiated on 0-12 hpi, ring-stage (G_1) *P. falciparum* 3D7 parasites, resulting in G_1/S (18-22 hpi) cell cycle compartmentalised parasites, which was reversed upon 2 mM putrescine addition (control). Subsequently, PfARK inhibition was assessed through 10xIC_{50} hesperadin treatment on putrescine-rescued parasites (0 h) and sampled every 6 h onwards to the following cell cycle (42 h). Images were created using Blender software (www.blender.org).

3.3.1 Hesperadin have antiproliferative properties against *P. falciparum* parasites

Antiproliferative properties of hesperadin, an Aurora kinase specific indolinone (Fig. 3.10A), on *P. falciparum* parasites in the low nanomolar range (10 – 50 nM) have been established in previous reports [133, 158]. Here, the antiproliferative effects of hesperadin on *P. falciparum* NF54^{PfS16} parasites were confirmed through *in vitro* SYBR Green I-based fluorescence assay for 96 h (Fig. 3.10B). The IC_{50} of hesperidin treatment on *P. falciparum* NF54$^{PfS16\text{-}GFP\text{-}Luc}$ parasites was determined to be 2.07 ± 0.08 nM SD (n=1). Further PfARK inhibition studies were performed at 10×IC_{50} (500 nM) hesperadin as previously reported [158]. To assess the effect of PfARK inhibition on parasite life cycle progression and proliferation, cell cycle compartmentalised *P. falciparum* 3D7 parasites were treated with 10xIC_{50} hesperadin.

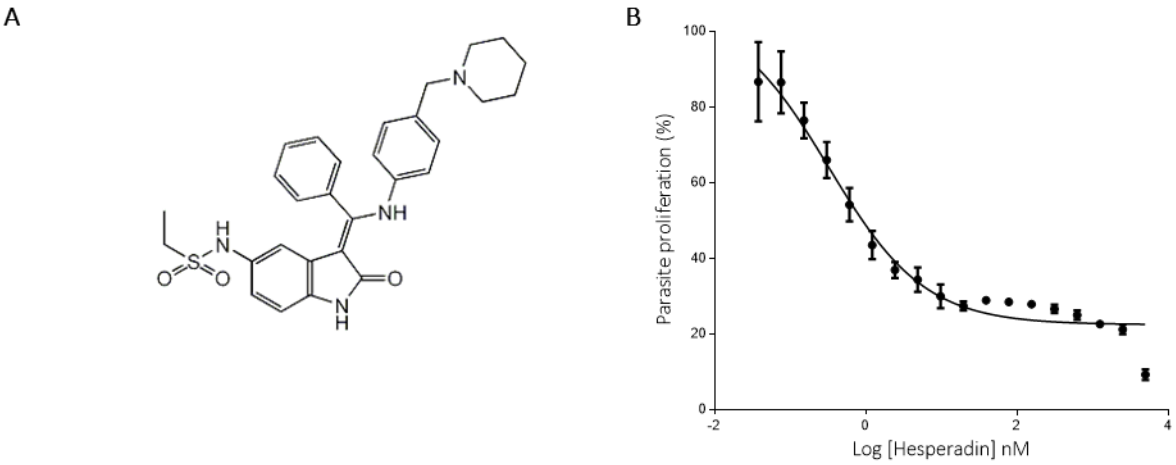

Figure 3.10: Dose-response evaluation of hesperadin inhibition of intraerythrocytic *P. falciparum* NF54$^{PfS16\text{-}GFP\text{-}Luc}$ parasites.
(A) Hesperadin chemical structure. **(B)** Hesperadin dose-response was determined using SYBR Green I-based assay for 96 h drug pressure initiated on ring-stage *P. falciparum* NF54$^{PfS16\text{-}GFP\text{-}Luc}$ parasite culture (1% parasitaemia, 1% haematocrit). Results are representative of one biological replicate (n=1± SD), performed in technical triplicate. Non-linear regression curves were generated using GraphPad Prism version 6.01 software. Error bars represent standard deviation. For some points, error bars fall within the symbols.

3.3.2 Parasite life cycle progression and proliferation

The growth inhibitory effects of 500 nM hesperadin on synchronised *P. falciparum* 3D7 parasite was assessed with regards to life cycle progression (Fig. 3.11). The parasitaemia of hesperadin-treated parasites was significantly lower (P<0.05) compared to the control parasites (Fig. 3.11A). Furthermore, to understand the ability of parasite cell cycle recovery during the M-phase, PfARK inhibition was released through removal of hesperadin after 18 h (Fig. 3.11A). Parasites released from hesperadin pressure through drug washout during schizogony progressed in a comparable manner to hesperadin-treated parasites, with no significant difference (P>0.05) (Fig. 3.11A).

SYBR Green I fluorescence microscopy was used to assess parasite life cycle progression and showed morphologically normal trophozoites but abnormal schizont-stage parasites after hesperadin treatment (Fig. 3.11B). This suggest that parasites cannot reverse PfARK inhibition after 24 h hesperadin treatment, indicating the essential role of PfARK in cell cycle regulation.

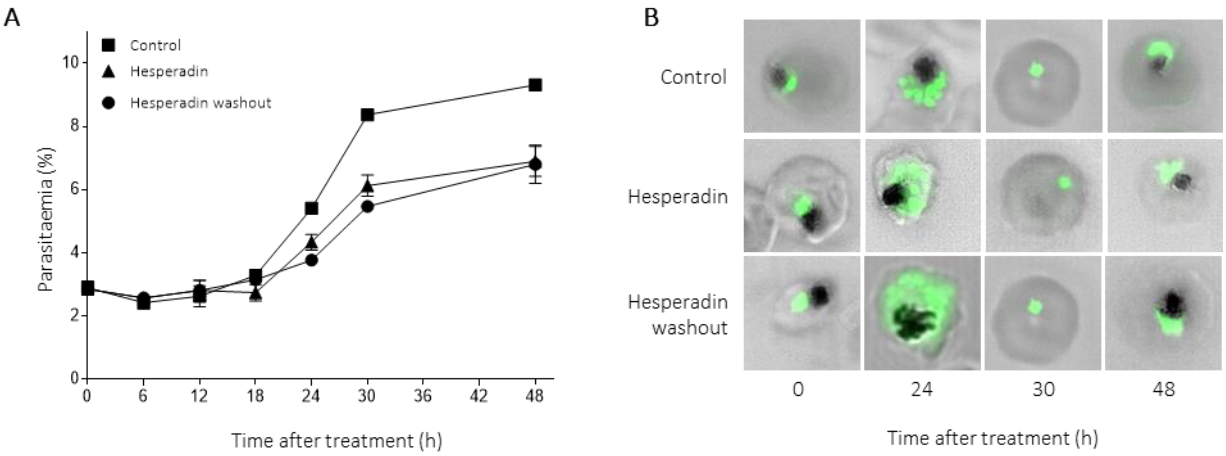

Figure 3.11: Life cycle progression and proliferation of PfARK-inhibited *P. falciparum* 3D7 parasites.
Intraerythrocytic *P. falciparum* 3D7 control parasites (3% parasitaemia, 5% haematocrit) were treated with 500 nM hesperadin and sampled every 6 h after hesperadin treatment. Samples were stained with SYBR Green I for flow cytometry and fluorescence microscopy analysis. **(A)** Proliferation of *P. falciparum* 3D7 control parasites (■), hesperadin-treated parasites (▲) and hesperadin washed out parasites (●) was evaluated using flow cytometry. Fluorescence was collected in the FL-1 channel (FITC signal) on a Becton Dickenson Accuri™ C6 Plus cytometer. A total of 100 000 events were captured and analysed using FlowJo version 10.1 software. Line graph was generated using GraphPad Prism version 6.01 software. Results are representative of one biological replicate (n=1± SD), performed in triplicates. Error bars represent standard deviation. For some points, error bars fall within the symbols. **(B)** Parasite life cycle progression monitored through SYBR Green I fluorescence microscopy using a Zeiss LSM 880 Confocal Laser Scanning Microscope (LSM).

3.3.3 Parasites remain viable at nanomolar range PfARK inhibition

Hesperadin-treated parasite viability was assessed to eliminate the possibility of reduction in parasitaemia and abnormal nuclear development due to non-viability (Fig. 3.12A). Hoechst nuclear staining was used as a positive control for parasite nuclear content in both viable and non-viable (methanol-fixed) parasites. Propidium iodide (PI) fluorochrome is a DNA intercalating agent commonly used to detect non-viable cells as it does not readily permeate live cell walls. Hesperadin-treated *P. falciparum* 3D7 parasites did not show significant PI fluorescence intensity (FI) (0.161 ± 0.916) compared to viable parasite cells (0.275 ± 0.887 SD). The FI of non-viable parasites (4.529 ± 10.226) (Fig. 3.12B), significantly differed from both viable and hesperadin-treated parasites ($P<0.0001$, students' using t-test). Therefore, the reduction in parasitaemia and ambiguous nuclear development were not due to a decrease in viability following hesperadin treatment.

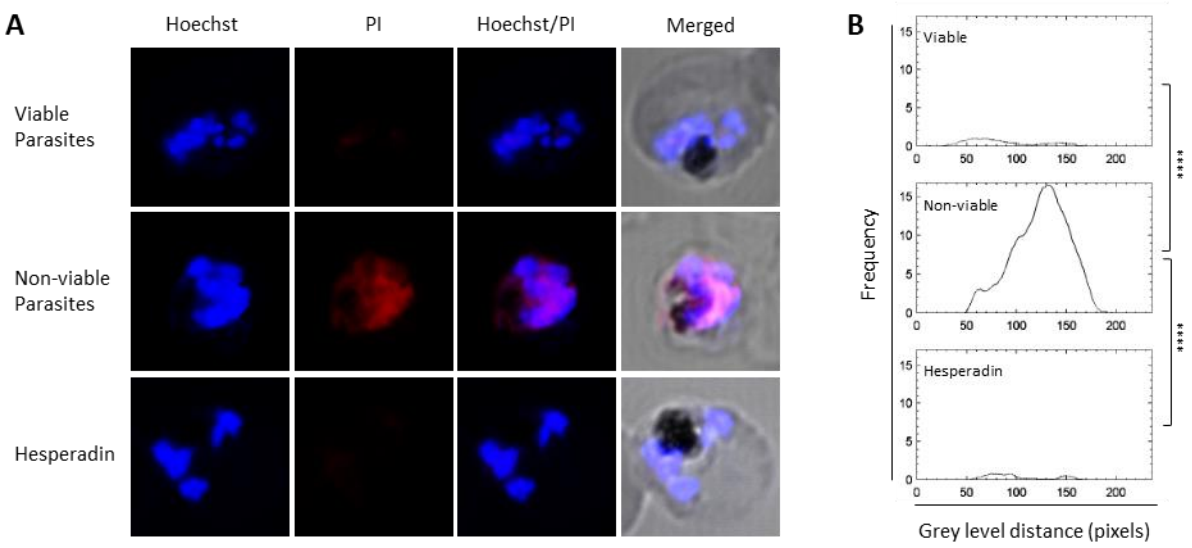

Figure 3.12: *P. falciparum* parasite life cycle progression of hesperadin parasites.
Intraerythrocytic *P. falciparum* 3D7 parasites were stained with Hoechst (blue) nuclear stain in combination with Propidium iodide (red) to monitor parasite viability after 24 h hesperadin treatment. **(A)** Parasite viability was monitored through fluorescence microscopy using a Zeiss LSM 880 Confocal Laser Scanning Microscope (LSM). **(B)** Histograms represent propidium iodide fluorescence intensity as a frequency of image grey level distance in pixels, generated using ImageJ software. Significant differences were calculated using two-tailed equal variance students t-test, ****= $P<0.0001$.

3.3.4 PfARK inhibition causes polyploidy in *P. falciparum* parasites

Previous reports concluded that in other protozoan organisms, hesperadin induced Aurora kinase inhibition is associated with blocked nuclear division and cytokinesis, while remaining viable [132]. Phenotypic differences in nuclei development of hesperadin-treated *P. falciparum* 3D7 parasites was studied using SYBR Green I staining in confocal fluorescence microscopy (Fig. 3.13A, Appendix: Fig. A5).

Hesperadin-treated *P. falciparum* parasites showed compromised morphology and nuclei development *in vitro*. Hesperadin-treated *P. falciparum* parasites had multi-lobed nuclear morphology with no clear nuclei edges observed but rather diffuse nuclei present, especially evident at 24 h after hesperadin treatment (Fig. 3.13B). Hesperadin-treated parasites displayed abnormally large inter-nuclei distances (≥500 nm) in schizonts compared to control parasites with adjacent nuclei (Fig. 3.13B). A concentration dependent effect was seen with 500 nM hesperadin treatment, which leads to more severe defects in parasite nuclei morphology compared to 100 nM hesperadin treatment (Fig. 3.13B). A significant reduction ($P<0.0001$, n=36, students' t-test) in the number of nuclei per schizont was detected after hesperidin treatment, with the latter on average having 10 nuclei per schizont compared to control parasites (20 nuclei per schizont) (Fig. 3.13C, Appendix I, Fig. A3-4).

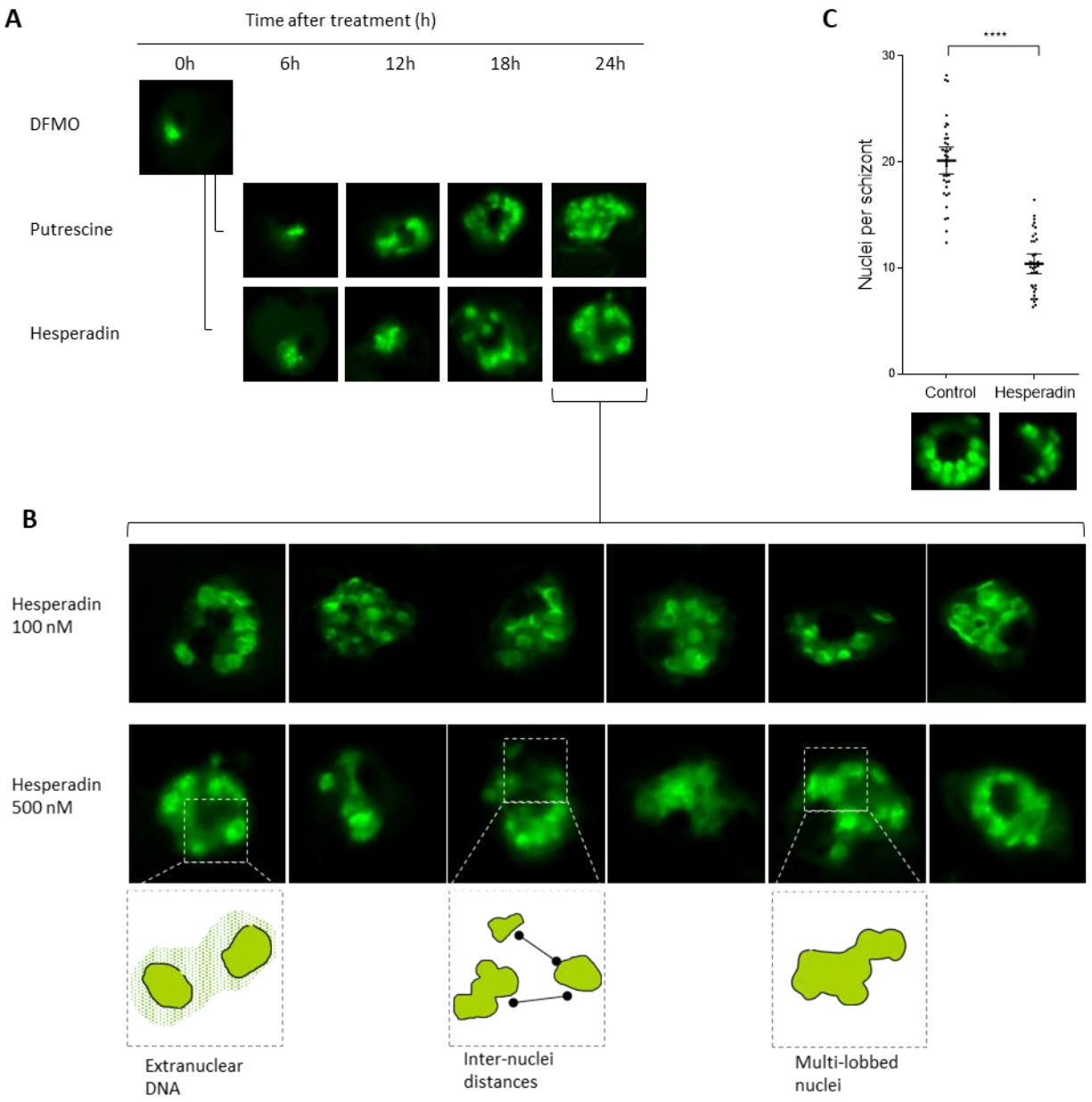

Figure 3.13: PfARK inhibition causes polyploidy in *P. falciparum* parasites.
Intraerythrocytic *P. falciparum* 3D7 control parasites were treated with hesperadin and sampled every 6 h after hesperadin treatment. **(A)** Parasite life cycle progression monitored through SYBR Green I fluorescence microscopy using a Zeiss LSM 880 Confocal Laser Scanning Microscope (LSM). **(B)** Parasite morphology assessed through SYBR Green I fluorescence microscopy after hesperidin treatment at 100 nM and 500 nM, respectively. Schematic diagrams were drawn to illustrate morphological observations. **(C)** Control and hesperadin-treated parasite nuclei development was quantitatively assessed through SYBR Green I fluorescence microscopy. Inter-nculei distances were determined for a minimum of 10 nuclei. Significant difference was calculated using two-tailed equal variance students t-test, ****= P<0.0001, n=36. Error bars represent 95% CI of the mean. Scatter plot were generated using GraphPad Prism version 6.01 software.

Collectively with the data presented in Fig. 3.11A, the re-invasion rate of intraerythrocytic *P. falciparum* ARK-inhibited parasites was determined by the number of nuclei formed per schizont (Fig. 3.13C) after hesperadin treatment and correlating it to the number of merozoites that successfully re-invaded erythrocytes in the following life cycle. Compared to control parasites, hesperadin-treated parasites showed 25% lower merozoite re-invasion in the following life cycle.

To calculate the number of merozoites that successfully re-invaded, the parasitaemia (%) ratio ($x_{second\ cycle}$: $x_{first\ cycle}$) over two consecutive life cycles was determined. For the control parasites, the parasitaemia ratio was 9.3%: 2.9% (3:1) and therefore, 3 merozoites re-invaded in the following life cycle. The parasitaemia ratio of the hesperadin-treated parasites was 6.9%: 2.9% (2:1) and therefore, 2 merozoites re-invaded in the following life cycle. This strongly suggest the decrease in parasitaemia of hesperadin-treated parasites is associated with multi-lobed nuclei formation and the significant reduction in the number of nuclei formed per schizont after hesperadin treatment.

3.3.5 The coordination between DNA replication and nuclear division is lost in PfARK-inhibited parasites

To determine cell cycle progression of *P. falciparum* ARK inhibited parasites, parasite DNA copy number after hesperadin treatment was measured and correlated to control parasites (Fig. 3.14).

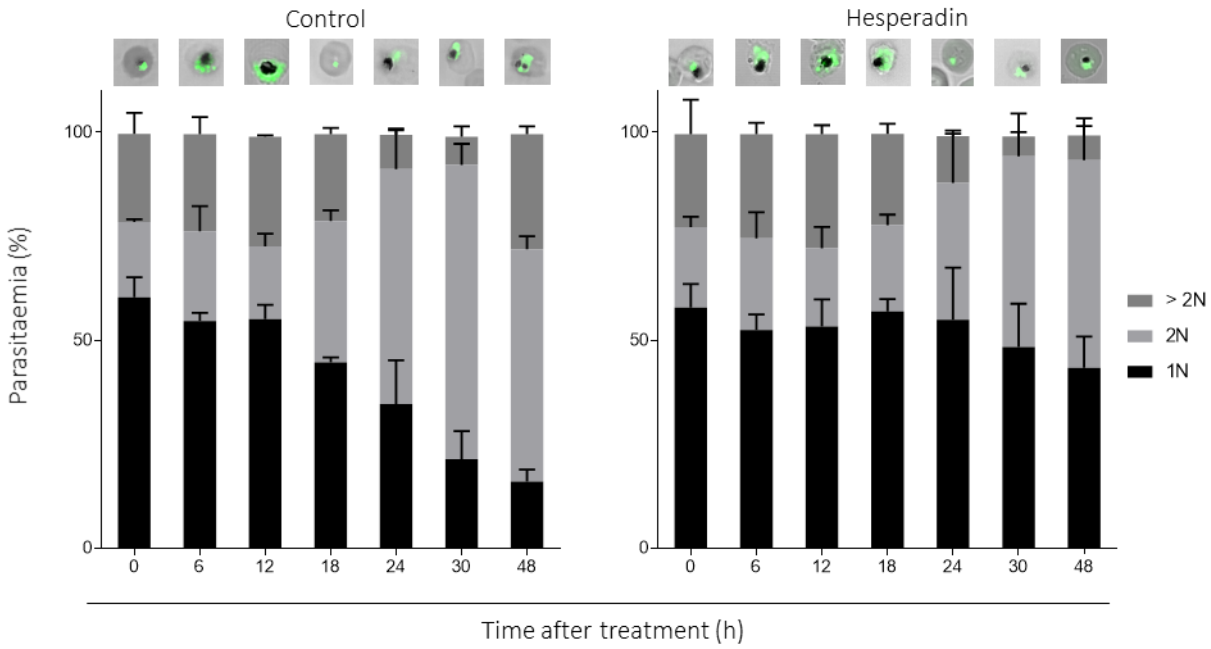

Figure 3.14: The effect of hesperadin on parasite cell cycle progression.
Intraerythrocytic *P. falciparum* 3D7 control parasites (3% parasitaemia, 5% haematocrit, ~18 hpi) was treated with hesperadin and samples were stained with SYBR Green I for flow cytometry and fluorescence microscopy analysis. Control and hesperadin-treated parasite DNA copy number (N) was measured by flow cytometry as described [57, 151]. Fluorescence was collected in the FL-1 channel (FITC signal) on a Becton Dickenson Accuri™ C6 Plus cytometer. A total of 100 000 events were captured and analysed using FlowJo version 10.1 software. Data are representative of one biological replicate (n=1± SD), performed in technical triplicates. Error bars represent standard deviation. Morphology of representative parasite population was confirmed through SYBR Green I confocal fluorescence microscopy using a Zeiss LSM 880 Confocal Laser Scanning Microscope (LSM). Bar graphs were generated using GraphPad Prism version 6.01 software.

No difference in DNA copy number was observed during the initial phases of the life cycle (0 h to 12 h) between control parasites and hesperadin-treated parasites (Fig. 3.14). However, a

difference was detected in parasite population DNA copy number at 18 h onwards between control parasites and hesperadin-treated parasites. A substantial (≥40%) percentage of the population of hesperadin-treated parasites remained at 1N DNA copy number up to 42 h after hesperadin treatment (Fig. 3.14). Hesperadin-treated parasites showed no decrease in 1N parasite population through life cycle progression as seen in control parasites.

To confirm the effect of hesperadin on parasite cell cycle progression, flow cytometry analysis using both SYBR Green I and Pyronin Y fluorescence signal allowed for sorting of parasite populations into specific cell cycle compartments: G_1 and S/M-phase parasites (Fig. 3.15).

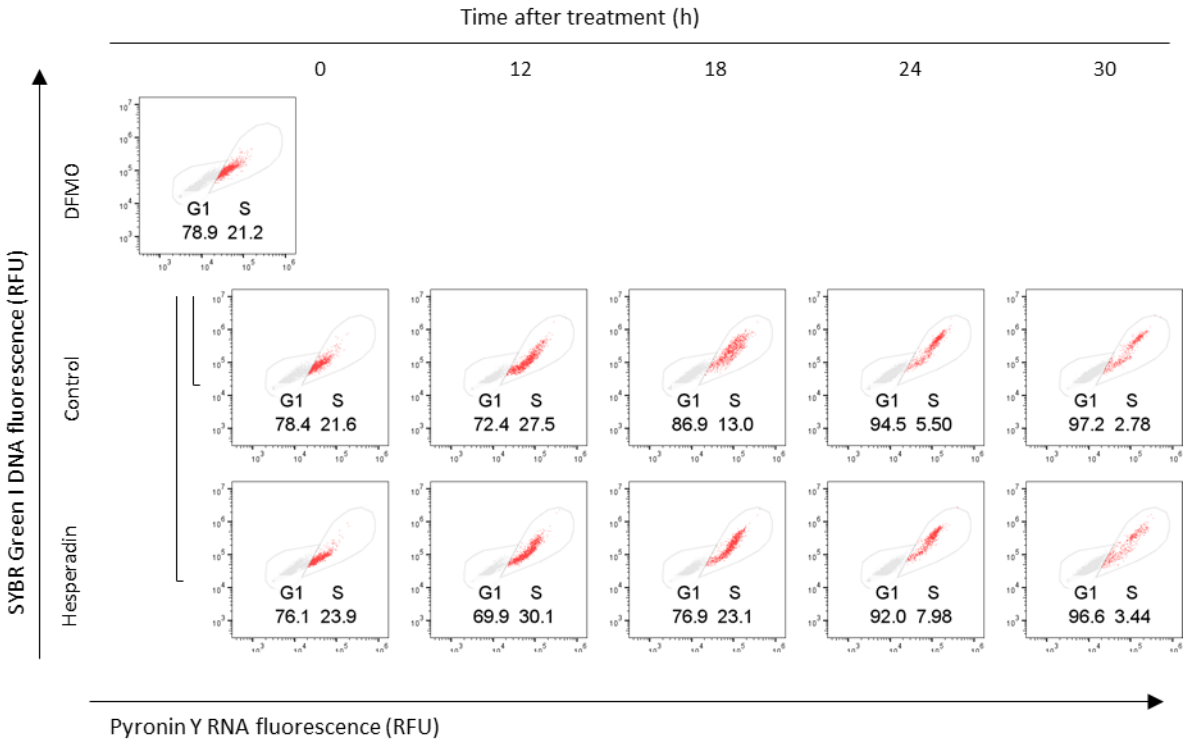

Figure 3.15: The effect of PfARK inhibition on *P. falciparum* parasite cell cycle profile.
Intraerythrocytic *P. falciparum* 3D7 control parasites (3% parasitaemia, 5% haematocrit, ~18 hpi) was treated with hesperadin and sampled every 6 h up to 30 h after hesperadin treatment. Samples were stained with SYBR Green I and Pyronin Y for flow cytometry analysis. SYBR Green I fluorescence against Pyronin Y fluorescence scatter plots are representative of parasite cell cycle profiles at specific timepoints. Parasite population (%) in G_1 (grey)and S-phase (red) are indicated in scatter plots. Fluorescence was collected for SYBR Green I in the FL-1 channel (FITC signal) and Pyronin Y in the FL-2 channel (PE signal) on a Becton Dickenson Accuri™ C6 Plus cytometer. A total of 100 000 events were captured and analysed using FlowJo version 10.1 software. Data are representative of one biological replicate (n=1± SD), performed in a single technical repeat.

G_1-phase parasites remain present at any given time of the parasite cell cycle, representative of not only ring-stage parasites, but also non-dividing nuclei. S-phase parasites, however, increase during parasite cell cycle progression and are representative of actively dividing schizonts. Control parasites resumed parasite cell cycle progression to S-phase and subsequent G_1-phase of the following IDC (Appendix: Fig. A7). However, hesperadin-treated parasites progressed to

S-phase and remained in S-phase for an extended period (up to 42 h after treatment), compared control parasites.

3.3.6 PfARK ensures correct spindle formation initiation during early mitosis

PfARK-1 is known to be associated with the SPB, in pairs, during mitosis in *P. falciparum* parasites [119]. Also, previous reports have shown that the parasite microtubule spindles are anchored to the nuclear face of the SPB during mitosis [14]. Therefore, to confirm whether the multi-lobed nuclear morphology and extended S-phase of PfARK-inhibited parasites are due to compromised nuclei segregation, α-tubulin formation was monitored after hesperadin treatment (Fig 3.16).

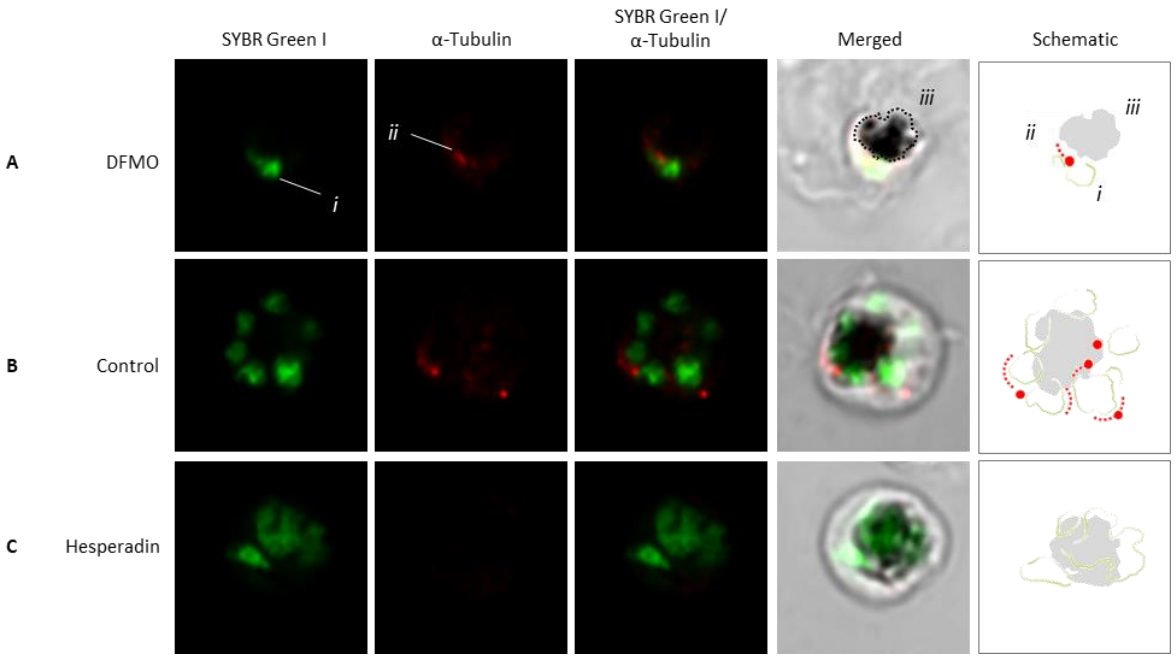

Figure 3.16: Spindle formation initiation during early mitosis in *P. falciparum* 3D7 parasites.
Fluorescence microscopy of spindle formation during mitosis of *P. falciparum* 3D7 parasites. SYBR Green I (green) nuclear control staining was used in combination with anti-α-tubulin antibody (red) to monitor parasite spindle formation using a Zeiss LSM 880 Confocal Laser Scanning Microscope (LSM). Panel A is representative of DFMO-arrested parasites. Panel B represents uncompromised control parasites. Hesperadin-treated parasites are represented in panel C. For each example, a schematic diagram illustrates; (i) nuclei (green structures), (ii) spindle formation (red dots), (iii) hemozoin crystal (grey structures). Images was prepared using ZEN Blue software. Gain were set to 600 (gamma: 2) and 900 (gamma: 4) for SYBR Green I and anti-α-tubulin AlexaFluor 647, respectively. Images are representative of 7 parasites evaluated per sample (Appendix: Fig. A8).

In both, DFMO-arrested and control parasites, anti-α-tubulin (red) were detected in close proximity of nuclei (green) similar to what has been previously reported [57, 119]. However, no distinct foci of anti-α-tubulin AlexaFluor 647 fluorescence was detected for hesperadin-treated parasites (Fig. 3.16). Collectively, these data indicate no spindle formation in hesperadin-treated parasites.

4 Chapter 4: Discussion

The multistage *P. falciparum* parasite life cycle, and implied cell cycle, is strictly controlled and rather unique compared to the classic eukaryotic cell cycle model. This allows the parasite to rapidly develop during the IDC associated with pathogenicity. An unusual occurrence is seen of alternating DNA synthesis and mitosis during parasite endocyclic schizogony [57], contrasting to classic eukaryotic cell cycle progression, which is regulated by an interplay of protein kinases and the degradation thereof. Aroura kinases have been previously identified as potential mitotic cell cycle regulators in *P. falciparum* parasites [90, 98], however, the exact role of the PfARKs during mitosis have not yet been clarified. This study aimed to define the role of PfARK during M-phase cell cycle regulation in IDC of *P. falciparum* parasites. The study relied on the ability to evaluate only the M-phase of the cell cycle due to prior tight cell cycle compartmentalisation using mitogen depletion through DFMO treatment as a synchronisation tool.

The novelty of the dissertation is therefore embedded in using an innovative approach for cell cycle phase-specific synchronisation of malaria parasites as a tool to provide an environment in which specific molecular processes embedded in a single cell cycle compartment can be investigated. In this project, this was used to gain extensive insights in the importance of PfARKs in M-phase regulation during the intraerythrocytic stages of the parasite.

The regulation and control mechanisms of asynchronous nuclear division in *P. falciparum* parasites is poorly understood mainly due to the difficulty of interrogating alternating S- and M-phase parasites. To aid in cell cycle studies, a minimal age range within parasites is required and achieved through parasite synchronisation to a specific cell cycle phase [58]. DFMO-induced parasite cell cycle arrest revealed *P. falciparum* parasites enforce cell cycle control at mitogen-dependent R-point prior to the G_1/S transition through quiescence-proliferating decision-making abilities [142]. At 33-37 hpi, the M-phase of *P. falciparum* parasites commence [84]. Through DFMO-induced cell cycle arrest highly synchronised G_1/S-phase specific parasites allowed subsequent M-phase cell cycle studies, overcoming a barrier in *P. falciparum* parasite cell cycle studies [58].

The study strategy was based on drug-induced PfARK inhibition of highly synchronised parasites, to interrogate the involvement of PfARKs in *P. falciparum* cell cycle. The PfARKs are essential for intraerythrocytic stages of the *Plasmodium* parasite of which some members, especially PfARK-1, are highly conserved and associated with SPB during schizogony [119]. Human Aurora kinase

inhibition is known to lead to G_2/M cell cycle arrest, abnormal mitotic spindle formation and development of polyploid cells, without necessarily affecting cell viability [157]. Similar phenotypes were previously observed in other protozoans [132]. Interestingly, drug-induced PfARK inhibition, at nanomolar range, does not affect parasite viability despite being essential for the IDC of the parasite. Using this strategy, rather than forward genetics, allowed interrogation of a highly conserved kinase. Through strict evaluation, it was possible to determine key functions of PfARK in *P. falciparum* parasite cell cycle regulation during a kinase control point during the M-phase of the parasite cell cycle.

In *P. falciparum* parasites PfARK inhibition compromise parasite proliferation during schizogony, despite normal parasite progression from ring to trophozoite-stages. *P. falciparum* parasites form up to 32 distinct nuclei per schizont with sharply defined nuclei commencing cytodifferentiation prior to merozoite formation [34, 35, 84]. However, PfARK inhibition reduces merozoite formation significantly, releasing less merozoites for re-invasion in the following cell cycle. In attempt to recover the compromised parasite state, the effect of PfARK inhibition was shown to be irreversible after mature schizont formation. This supports the indispensable role of PfARKs in parasite proliferation during mitosis [94, 98, 119] and the short active window of PfARKs.

Furthermore, PfARK inhibition resulted in multi-lobed parasite nuclei with no discernible edges, suggestive of incomplete nuclear segregation. Also, PfARK resulted in nuclei developing abnormally far apart with what seems like extranuclear DNA content. Classic eukaryotic chromosomal DNA segregation depends on correct attachment at kinetochores through microtubules from both spindle poles during metaphase, reminiscent of *P. falciparum* parasites [65]. The human Aurora B kinase revises kinetochore-microtubule attachment with implied spindle assembly checkpoint maintenance as a response to unattached kinetochore signalling [130]. It is still unclear whether the timing of mitosis in *P. falciparum* parasites is controlled by a spindle assembly checkpoint as in a classic eukaryotic cell cycle, however, improper chromosomal segregation in PfARK-inhibited parasites suggests impaired spindle assembly and the presence of a spindle assembly control or checkpoint.

A decrease in the number of distinct nuclei formed during parasite schizogony was associated with PfARK inhibition. However, despite compromised nuclei formation, parasite DNA copy number increased in abundance during parasite life cycle progression. This strongly suggest the coordination between DNA replication and nuclear division is lost in PfARK-inhibited parasites, emphasising the crucial role of PfARKs in nuclear division. This phenomenon is indicative of a

control point during the M-phase. PfARK-inhibited parasites extend the S-phase confirming the role of PfARK in nuclei division rather than DNA replication. However, nuclei segregation cannot be inferred from nucleic acid staining only, but rather through detection of M-phase markers such as α-tubulin assembly during spindle formation.

Impaired spindle formation is characteristic of Aurora kinase inhibition in other organisms [132], however, for the first time, we show here that this is also true for *P. falciparum* parasites. An early hallmark of cell division is SPB duplication as the S-phase of the parasite's cell cycle commences [57]. PfARK-1 has been previously shown to be associated with the SPB during mitosis [94] and homologues of PfARK-1 have been described in various organisms with a close link to the interplay of centrosomes and bipolar microtubules, chromosomal DNA segregation and ensuing cytokinesis [130, 132].Through strict evaluation of α-tubulin assembly during schizogony, the data suggest that PfARK is responsible for the initiation of correct spindle formation during early onset of mitosis, corresponding to previous studies. In this study, PfARK-inhibited parasites had impaired spindle initiation and formation, reminiscent to phenotypes previously reported in *T. brucei* parasites [132]. The data are suggestive of nuclei division occurring without functional spindle supports the phenomenon of extranuclear DNA during schizogony.

The *Plasmodium* parasite is highly complex and remains poorly understood. For future studies, exploring mitotic kinases more in depth may advance our knowledge in the parasite cell cycle regulation. Besides ARKs, NEK kinases have recently received much attention as centrosomal cycle regulators [91, 92]. Previous reports have indicated that numerous cellular functions, particularly involving MTOCs, are controlled by NEK kinases [159]. Also, the BUB1 and BUBR1 kinases in mammalian cells are mitotic checkpoint kinases responsible for kinetochore attachment status signalling, which in turn directs other mitotic and centrosomal kinases [130]. However, the interplay of these centrosomal kinases in regulating the cell cycle of *Plasmodium* parasites remain unclear. Understanding the dynamic network of kinase regulators will give insights as to how these kinases regulate the parasite cell cycle and how it implicates the parasite development. Furthermore, live cell fluorescence imaging could greatly advance our understanding of the progression and the sequential order of events during parasite schizogony. This strategy was recently used, with great success, for monitoring male gamete formation in *P. falciparum* parasites [160]. Multi-immunofluorescence strategies are rapidly advancing, allowing interrogation of multiple structures simultaneously. Whether spindle formation is directly or indirectly controlled by PfARKs in *P. falciparum* parasites, remains unclear. Therefore, it would

be preferable to investigate SPB development and functioning in conjunction with hallmark mitotic biomarkers, specifically in PfARK-inhibited parasites, to determine whether spindle formation is a direct or indirect effect.

In conclusion, a comprehensive qualitative and quantitative evaluation of PfARK in *P. falciparum* parasites revealed several central features of its importance in the parasite's cell cycle regulation. Firstly, the data suggest that S/M-phase transition is controlled by PfARK in *P. falciparum* parasites. The data suggest S-phase re-initiation in PfARK-inhibited parasites, therefore, continuing DNA synthesis in the absence of nuclei segregation. Furthermore, PfARK facilitates proper chromosomal segregation during mitosis. PfARK inhibition result in multi-lobed polyploidy nuclei with no discernible edges and extranuclear DNA content, suggestive of poorly segregated nuclei. Also, PfARK ensures correct spindle formation initiation during early mitosis, either directly or indirectly. In the absence of functional PfARK in *P. falciparum* parasites, spindle formation is not initiated during mitosis.

5 Chapter 5: Conclusion

The vector borne protozoan disease, malaria, remains responsible for nearly half a million deaths annually and in many second and third world countries the serious health burden limits social and economic progress [5]. The development of strains of the *P. falciparum* parasite resistant to current antimalarial drugs, is responsible for the difficulty of controlling malaria. Protein phosphorylation has been studied extensively as potential drug targets in several human diseases, but to a lesser extend in *Plasmodium* parasites. *P. falciparum* parasites have a relatively small kinome of <100 kinases, of which several kinases have been identified as essential for the parasite's life cycle progression. However, the *Plasmodium* kinome has not been exploited fully with respect to its involvement in cell cycle regulation in *P. falciparum*.

The difficulty of cell cycle studies of the malaria parasite has been overcome through DFMO mitogen depletion that can be used as a tool to compartmentalise parasites into a particular cell cycle phase. In this study, drug-induced PfARK inhibition of cell cycle compartmentalised parasites, was used to interrogate the involvement of ARKs in *P. falciparum* cell cycle, as it is poorly understood. In *P. falciparum* parasites, PfARK inhibition irreversibly compromise parasite proliferation during schizogony resulting in significant reduction of merozoite formation due to the development of multi-lobed parasite nuclei with no discernible edges, suggestive of incomplete nuclear segregation. However, despite compromised nuclei formation, parasite DNA copy number increased in abundance during parasite life cycle progression through extending the S-phase, confirming the role of PfARK in nuclei division rather than DNA replication. The data suggest that PfARK is responsible for the initiation of correct spindle formation during early onset of mitosis, reminiscent of other organisms [132].

In totality, a comprehensive qualitative and quantitative evaluation of PfARK in *P. falciparum* parasites revealed several central features of its importance in the parasite cell cycle regulation; 1) S/M-phase transition is controlled by PfARKs, 2) PfARKs facilitates proper chromosomal segregation during mitosis and 3) PfARK ensures correct spindle formation initiation during early mitosis, either directly or indirectly. Therefore, the data revealed key functions of PfARKs in *P. falciparum* parasite cell cycle regulation during a kinase control point present in the M-phase of the parasite cell cycle.

The complexity of the *Plasmodium* parasite's cell cycle regulation and the underlying mechanisms remain poorly understood. Therefore, it is critical to functionally validate essential

Plasmodium cell cycle regulators and understand their dynamic interplay. These essential cell cycle regulators and their involved pathways serve as attractive targets for future antimalarial drug discovery and development in *Plasmodium* parasites.

6 References

1. World Malaria Report 2017. Geneva: WHO; 2017. 2018.
2. Gatton, M.L., Chitnis, N., Churcher, T., Donnelly, M.J., Ghani, A.C., Godfray, H.C.J., Gould, F., Hastings, I., Marshall, J., and Ranson, H., The importance of mosquito behavioural adaptations to malaria control in Africa. Evolution: international journal of organic evolution, 2013. 67(4): p. 1218-1230.
3. Ranson H, N'guessan R, Lines J, Moiroux N, Nkuni Z, and V., C., Pyrethroid resistance in African anopheline mosquitoes: what are the implications for malaria control? Trends Parasitol. , 2011 27(2): p. 91-98.
4. Bhatt, S., Weiss, D., Cameron, E., Bisanzio, D., Mappin, B., Dalrymple, U., Battle, K., Moyes, C., Henry, A., and Eckhoff, P., The effect of malaria control on *Plasmodium falciparum* in Africa between 2000 and 2015. Nature, 2015. 526(7572): p. 207-211.
5. Béguin, A., Hales, S., Rocklöv, J., Åström, C., Louis, V.R., and Sauerborn, R., The opposing effects of climate change and socio-economic development on the global distribution of malaria. Global Environmental Change, 2011. 21(4): p. 1209-1214.
6. Hemingway, J., Shretta, R., Wells, T.N., Bell, D., Djimdé, A.A., Achee, N., and Qi, G., Tools and strategies for malaria control and elimination: what do we need to achieve a grand convergence in malaria? PLoS biology, 2016. 14(3): p. e1002380.
7. Lengeler, C., Insecticide treated bednets and curtains for malaria control. Cochrane database of systematic reviews, 1998(2).
8. Edi CV, K.B., Jones CM, Weetman D, Ranson H., Multiple-insecticide resistance in *Anopheles gambiae* mosquitoes, Southern Côte d'Ivoire. Emerg Infect Dis., 2012. 18(9): p. 1508-1511.
9. Hemingway J and H., R., Insecticide resistance in insect vectors of human disease. Annu Rev Entomol. , 2000. 45: p. 371-391.
10. Zofou D, N.R., Nsagha DS, Ntie-Kang F, Meriki HD, Assob JC, Kuete V., Control of malaria and other vector-borne protozoan diseases in the tropics: enduring challenges despite considerable progress and achievements. Infect Dis Poverty, 2014. 3(1): p. 1-14.
11. Moiroux N, G.M., Pennetier C, Elanga E, Djènontin A, Chandre F, Djègbé I, Guis H, Corbel V., Changes in Anopheles funestus biting behavior following universal coverage of long-lasting insecticidal nets in Benin. J Infect Dis., 2012 206(10): p. 1622-1629.
12. Majori G, Short history of malaria and its eradication in Italy with short notes on the fight against the infection in the mediterranean basin. Mediterr J Hematol Infect Dis., 2012. 4(1).
13. Cox FE, History of the discovery of the malaria parasites and their vectors. Parasit Vectors. , 2010. 3 (1): p. 1-9.
14. Girard MP, Reed ZH, Friede M, and MP., K., A review of human vaccine research and development: malaria. Vaccine., 2007. 25: p. 1567-1580.
15. Hill AV, Vaccines against malaria. Philos Trans R Soc Lond B Biol Sci., 2011. 366(1579): p. 2806-2814.
16. O'Meara WP, Hall BF, and FE., M., Malaria vaccine efficacy: the difficulty of detecting and diagnosing malaria. Malar J., 2007. 6(36).
17. Hill, A.V., Pre-erythrocytic malaria vaccines: towards greater efficacy. Nature Reviews Immunology, 2006. 6(1): p. 21.
18. Graves P and Gelband H, Vaccines for preventing malaria (pre-erythrocytic). Cochrane Database Syst Rev. , 2006(4).
19. Cohen J, N.V., Nussenzweig R, Vekemans J, Leach A., From the circumsporozoite protein to the RTS, S/AS candidate vaccine. Hum Vaccin. , 2010. 6(1): p. 90-96.
20. Targett GA, Moorthy VS, and Brown GV, Malaria vaccine research and development: the role of the WHO MALVAC committee. Malar J., 2013. 12(362).
21. RTSS Clinical Trials Partnership et al, A phase 3 trial of RTS,S/AS01 malaria vaccine in African infants. N Engl J Med. , 2012 367(24): p. 2284-2295.
22. Foquet L, H.C., van Gemert GJ, Van Braeckel E, Weening KE, Sauerwein R, Meuleman P, Leroux-Roels G., Vaccine-induced monoclonal antibodies targeting circumsporozoite protein prevent *Plasmodium falciparum* infection. J Clin Invest. , 2014. 124(1): p. 140-144.
23. Wells, T.N. and Poll, E.M., When is enough enough? The need for a robust pipeline of high-quality antimalarials. Discovery medicine, 2010. 9(48): p. 389-398.
24. Hott, A., Casandra, D., Sparks, K.N., Morton, L.C., Castanares, G.-G., Rutter, A., and Kyle, D.E., Artemisinin-resistant *Plasmodium falciparum* exhibit altered patterns of development in infected erythrocytes. Antimicrobial agents and chemotherapy, 2015: p. AAC. 00197-15.
25. Alonso, P.L., Brown, G., Arevalo-Herrera, M., Binka, F., Chitnis, C., Collins, F., Doumbo, O.K., Greenwood, B., Hall, B.F., and Levine, M.M., A research agenda to underpin malaria eradication. PLoS medicine, 2011. 8(1): p. e1000406.

26. Rabinovich, R.N., Drakeley, C., Djimde, A.A., Hall, B.F., Hay, S.I., Hemingway, J., Kaslow, D.C., Noor, A., Okumu, F., and Steketee, R., malERA: An updated research agenda for malaria elimination and eradication. PLoS medicine, 2017. 14(11): p. e1002456.
27. Levine, N.D., Progress in taxonomy of the Apicomplexan protozoa. The Journal of protozoology, 1988. 35(4): p. 518-520.
28. Yamauchi, L.M., Coppi, A., Snounou, G., and Sinnis, P., *Plasmodium* sporozoites trickle out of the injection site. Cellular microbiology, 2007. 9(5): p. 1215-1222.
29. Girard, M.P., Reed, Z.H., Friede, M., and Kieny, M.P., A review of human vaccine research and development: malaria. Vaccine, 2007. 25(9): p. 1567-80.
30. Biamonte, M.A., Wanner, J., and Le Roch, K.G., Recent advances in malaria drug discovery. Bioorganic & Medicinal Chemistry Letters, 2013. 23(10): p. 2829-2843.
31. Dvorak, J.A., Miller, L.H., Whitehouse, W.C., and Shiroishi, T., Invasion of erythrocytes by malaria merozoites. Science, 1975. 187(4178): p. 748-50.
32. Bannister, L., Hopkins, J., Fowler, R., Krishna, S., and Mitchell, G., A brief illustrated guide to the ultrastructure of *Plasmodium falciparum* asexual blood stages. Parasitology Today, 2000. 16(10): p. 427-433.
33. Bannister, L. and Mitchell, G., The ins, outs and roundabouts of malaria. Trends in parasitology, 2003. 19(5): p. 209-213.
34. Cowman, A.F. and Crabb, B.S., Invasion of red blood cells by malaria parasites. Cell, 2006. 124(4): p. 755-766.
35. Garg, S., Agarwal, S., Dabral, S., Kumar, N., Sehrawat, S., and Singh, S., Visualization and quantification of *Plasmodium falciparum* intraerythrocytic merozoites. Systems and synthetic biology, 2015. 9(1): p. 23-26.
36. White, N.J., Pukrittayakamee, S., Hien, T.T., Faiz, M.A., Mokuolu, O.A., and Dondorp, A.M., Malaria. Lancet, 2014. 383(9918): p. 723-35.
37. Bruce, M., Alano, P., Duthie, S., and Carter, R., Commitment of the malaria parasite *Plasmodium falciparum* to sexual and asexual development. Parasitology, 1990. 100(2): p. 191-200.
38. Alano, P. and Carter, R., Sexual differentiation in malaria parasites. Annual Reviews in Microbiology, 1990. 44(1): p. 429-449.
39. Silvestrini, F., Alano, P., and Williams, J., Commitment to the production of male and female gametocytes in the human malaria parasite Plasmodium falciparum. Parasitology, 2000. 121(05): p. 465-471.
40. Smith, T., Lourenco, P., Carter, R., Walliker, D., and Ranford-Cartwright, L., Commitment to sexual differentiation in the human malaria parasite, Plasmodium falciparum. Parasitology, 2000. 121(02): p. 127-133.
41. Read, A., Narara, A., Nee, S., Keymer, A., and Day, K., Gametocyte sex ratios as indirect measures of outcrossing rates in malaria. Parasitology, 1992. 104(3): p. 387-395.
42. Kuehn, A. and Pradel, G., The coming-out of malaria gametocytes. BioMed Research International, 2010. 2010.
43. Baker, D.A., Malaria gametocytogenesis. Molecular and biochemical parasitology, 2010. 172(2): p. 57-65.
44. Smalley, M., Abdalla, S., and Brown, J., The distribution of Plasmodium falciparum in the peripheral blood and bone marrow of Gambian children. Transactions of the Royal Society of Tropical Medicine and Hygiene, 1981. 75(1): p. 103-105.
45. Rogers, N.J., Hall, B.S., Obiero, J., Targett, G.A., and Sutherland, C.J., A model for sequestration of the transmission stages of Plasmodium falciparum: adhesion of gametocyte-infected erythrocytes to human bone marrow cells. Infection and immunity, 2000. 68(6): p. 3455-3462.
46. Smalley, M. and Sinden, R., Plasmodium falciparum gametocytes: their longevity and infectivity. Parasitology, 1977. 74(01): p. 1-8.
47. Billker, O., Dechamps, S., Tewari, R., Wenig, G., Franke-Fayard, B., and Brinkmann, V., Calcium and a calcium-dependent protein kinase regulate gamete formation and mosquito transmission in a malaria parasite. Cell, 2004. 117(4): p. 503-514.
48. Guinet, F., Dvorak, J.A., Fujioka, H., Keister, D.B., Muratova, O., Kaslow, D.C., Aikawa, M., Vaidya, A.B., and Wellems, T.E., A developmental defect in *Plasmodium falciparum* male gametogenesis. The Journal of cell biology, 1996. 135(1): p. 269-278.
49. Billker, O., Shaw, M., Margos, G., and Sinden, R., The roles of temperature, pH and mosquito factors as triggers of male and female gametogenesis of *Plasmodium berghei* in vitro. Parasitology, 1997. 115(01): p. 1-7.
50. Janse, C.J., van der Klooster, P.F., van der Kaay, H.J., van der Ploeg, M., and Overdulve, J.P., DNA synthesis in *Plasmodium berghei* during asexual and sexual development. Molecular and biochemical parasitology, 1986. 20(2): p. 173-182.

51. Cox, F.E., History of the discovery of the malaria parasites and their vectors. Parasit Vectors, 2010. 3(1): p. 5.
52. Bousema, T. and Drakeley, C., Epidemiology and infectivity of *Plasmodium falciparum* and *Plasmodium vivax* gametocytes in relation to malaria control and elimination. Clinical microbiology reviews, 2011. 24(2): p. 377-410.
53. Sinden, R., Plasmodium differentiation in the mosquito. Parassitologia, 1999. 41(1-3): p. 139-148.
54. Haase, S.B. and Wittenberg, C., Topology and control of the cell-cycle-regulated transcriptional circuitry. Genetics, 2014. 196(1): p. 65-90.
55. Csikász-Nagy, A., Battogtokh, D., Chen, K.C., Novák, B., and Tyson, J.J., Analysis of a generic model of eukaryotic cell-cycle regulation. Biophysical journal, 2006. 90(12): p. 4361-4379.
56. Doerig, C., Chakrabarti, D., Kappes, B., and Matthews, K., The cell cycle in protozoan parasites, in Progress in cell cycle research. 2000, Springer. p. 163-183.
57. Arnot, D.E., Ronander, E., and Bengtsson, D.C., The progression of the intra-erythrocytic cell cycle of *Plasmodium falciparum* and the role of the centriolar plaques in asynchronous mitotic division during schizogony. International journal for parasitology, 2011. 41(1): p. 71-80.
58. Naughton, J. and Bell, A., Studies on cell-cycle synchronization in the asexual erythrocytic stages of Plasmodium falciparum. Parasitology, 2007. 134(3): p. 331.
59. Rao, P.N. and Johnson, R.T., Cell Fusion and Its Application to Studies on the Regulation of the Cell Cycle1, in Methods in Cell Biology. 1972, Elsevier. p. 75-126.
60. Jacobberger, J., Horan, P., and Hare, J., Cell cycle analysis of asexual stages of erythrocytic malaria parasites. Cell proliferation, 1992. 25(5): p. 431-445.
61. Alm, K. and Oredsson, S., Cells and polyamines do it cyclically. Essays in biochemistry, 2009. 46: p. 63-76.
62. Hartwell, L.H. and Kastan, M.B., Cell cycle control and cancer. Science, 1994. 266(5192): p. 1821-1828.
63. Hartwell, L.H. and Weinert, T.A., Checkpoints: controls that ensure the order of cell cycle events. Science, 1989. 246(4930): p. 629.
64. Bertoli, C., Skotheim, J.M., and De Bruin, R.A., Control of cell cycle transcription during G1 and S phases. Nature reviews Molecular cell biology, 2013. 14(8): p. 518.
65. Gerald, N., Mahajan, B., and Kumar, S., Mitosis in the human malaria parasite *Plasmodium falciparum*. Eukaryotic cell, 2011.
66. Reece, J.B., Urry, L.A., Cain, M.L., Wasserman, S.A., Minorsky, P.V., and Jackson, R.B., Campbell biology. 2011: Pearson Boston.
67. Gritzmacher, C.A. and Reese, R.T., Protein and nucleic acid synthesis during synchronized growth of *Plasmodium falciparum*. Journal of bacteriology, 1984. 160(3): p. 1165-1167.
68. Newlon, C.S., Yeast chromosome replication and segregation. Microbiological reviews, 1988. 52(4): p. 568.
69. Azimzadeh, J. and Bornens, M., Structure and duplication of the centrosome. Journal of cell science, 2007. 120(13): p. 2139-2142.
70. De Souza, C.P. and Osmani, S.A., Mitosis, not just open or closed. Eukaryotic cell, 2007. 6(9): p. 1521-1527.
71. Rieder, C.L., Formation of the astral mitotic spindle: ultrastructural basis for the centrosome-kinetochore interaction. Electron microscopy reviews, 1990. 3(2): p. 269-300.
72. Cao, L.-g. and Wang, Y., Mechanism of the formation of contractile ring in dividing cultured animal cells. I. Recruitment of preexisting actin filaments into the cleavage furrow. The Journal of Cell Biology, 1990. 110(4): p. 1089-1095.
73. Perry, M., John, H., and Thomas, N., Actin-like filaments in the cleavage furrow of newt egg. Experimental cell research, 1971. 65(1): p. 249-253.
74. Spencer, S.L., Cappell, S.D., Tsai, F.-C., Overton, K.W., Wang, C.L., and Meyer, T., The proliferation-quiescence decision is controlled by a bifurcation in CDK2 activity at mitotic exit. Cell, 2013. 155(2): p. 369-383.
75. Elledge, S.J., Cell cycle checkpoints: preventing an identity crisis. Science, 1996. 274(5293): p. 1664.
76. Shaltiel, I.A., Krenning, L., Bruinsma, W., and Medema, R.H., The same, only different–DNA damage checkpoints and their reversal throughout the cell cycle. J Cell Sci, 2015: p. jcs. 163766.
77. Bohórquez, E.B., Juliano, J.J., Kim, H.-S., and Meshnick, S.R., Mefloquine exposure induces cell cycle delay and reveals stage-specific expression of the pfmdr1 gene. Antimicrobial agents and chemotherapy, 2013. 57(2): p. 833-839.
78. Gray, A.M., Arguin, P.M., and Hamed, K., Surveillance for the safety and effectiveness of artemether-lumefantrine in patients with uncomplicated *Plasmodium falciparum* malaria in the USA: a descriptive analysis. Malaria journal, 2015. 14(1): p. 349.

79. Babbitt, S.E., Altenhofen, L., Cobbold, S.A., Istvan, E.S., Fennell, C., Doerig, C., Llinás, M., and Goldberg, D.E., *Plasmodium falciparum* responds to amino acid starvation by entering into a hibernatory state. Proceedings of the National Academy of Sciences, 2012: p. 201209823.
80. Arnot, D. and Gull, K., The *Plasmodium* cell cycle: facts and questions. Annals of tropical medicine and parasitology, 1998. 92(4): p. 361-365.
81. Gray, K.-A., Gresty, K.J., Chen, N., Zhang, V., Gutteridge, C.E., Peatey, C.L., Chavchich, M., Waters, N.C., and Cheng, Q., Correlation between cyclin dependent kinases and artemisinin-induced dormancy in *Plasmodium falciparum in vitro.* PLoS One, 2016. 11(6): p. e0157906.
82. Gupta, D.K., Patra, A.T., Zhu, L., Gupta, A.P., and Bozdech, Z., DNA damage regulation and its role in drug-related phenotypes in the malaria parasites. Scientific reports, 2016. 6: p. 23603.
83. Francia, M.E. and Striepen, B., Cell division in apicomplexan parasites. Nature Reviews Microbiology, 2014. 12(2): p. 125.
84. Read, M., Sherwin, T., Holloway, S., Gull, K., and Hyde, J., Microtubular organization visualized by immunofluorescence microscopy during erythrocytic schizogony in Plasmodium falciparum and investigation of post-translational modifications of parasite tubulin. Parasitology, 1993. 106(3): p. 223-232.
85. Murray, A.W., Recycling the cell cycle: cyclins revisited. Cell, 2004. 116(2): p. 221-234.
86. Roques, M., Wall, R.J., Douglass, A.P., Ramaprasad, A., Ferguson, D.J., Kaindama, M.L., Brusini, L., Joshi, N., Rchiad, Z., and Brady, D., Plasmodium P-type cyclin CYC3 modulates endomitotic growth during oocyst development in mosquitoes. PLoS pathogens, 2015. 11(11): p. e1005273.
87. Ganter, M., Goldberg, J.M., Dvorin, J.D., Paulo, J.A., King, J.G., Tripathi, A.K., Paul, A.S., Yang, J., Coppens, I., and Jiang, R.H., *Plasmodium falciparum* CRK4 directs continuous rounds of DNA replication during schizogony. Nature microbiology, 2017. 2(5): p. 17017.
88. Deshmukh, A.S., Agarwal, M., and Dhar, S.K., Regulation of DNA replication proteins in parasitic protozoans: possible role of CDK-like kinases. Current genetics, 2016. 62(3): p. 481-486.
89. Merckx, A., Le Roch, K., Nivez, M.-P., Dorin, D., Alano, P., Gutierrez, G.J., Nebreda, A.R., Goldring, D., Whittle, C., and Patterson, S., Identification and initial characterization of three novel cyclin-related proteins of the human malaria parasite Plasmodium falciparum. Journal of Biological Chemistry, 2003. 278(41): p. 39839-39850.
90. Carvalho, T.G., Doerig, C., and Reininger, L., Nima-and Aurora-related kinases of malaria parasites. Biochimica et Biophysica Acta (BBA)-Proteins and Proteomics, 2013. 1834(7): p. 1336-1345.
91. Dorin, D., Le Roch, K., Sallicandro, P., Alano, P., Parzy, D., Poullet, P., Meijer, L., and Doerig, C., Pfnek-1, a NIMA-related kinase from the human malaria parasite *Plasmodium falciparum.* European journal of Biochemistry, 2001. 268(9): p. 2600-2608.
92. Dorin-Semblat, D., Schmitt, S., Semblat, J.-P., Sicard, A., Reininger, L., Goldring, D., Patterson, S., Quashie, N., Chakrabarti, D., and Meijer, L., *Plasmodium falciparum* NIMA-related kinase Pfnek-1: sex specificity and assessment of essentiality for the erythrocytic asexual cycle. Microbiology, 2011. 157(10): p. 2785-2794.
93. O'regan, L., Blot, J., and Fry, A.M., Mitotic regulation by NIMA-related kinases. Cell division, 2007. 2(1): p. 25.
94. Reininger, L., Billker, O., Tewari, R., Mukhopadhyay, A., Fennell, C., Dorin-Semblat, D., Doerig, C., Goldring, D., Harmse, L., and Ranford-Cartwright, L., A NIMA-related protein kinase is essential for completion of the sexual cycle of malaria parasites. Journal of Biological Chemistry, 2005. 280(36): p. 31957-31964.
95. Reininger, L., Tewari, R., Fennell, C., Holland, Z., Goldring, D., Ranford-Cartwright, L., Billker, O., and Doerig, C., An essential role for the Plasmodium Nek-2 Nima-related protein kinase in the sexual development of malaria parasites. Journal of Biological Chemistry, 2009. 284(31): p. 20858-20868.
96. English, D., Phosphatidic acid: a lipid messenger involved in intracellular and extracellular signalling. Cellular signalling, 1996. 8(5): p. 341-347.
97. Ardito, F., Giuliani, M., Perrone, D., Troiano, G., and Lo Muzio, L., The crucial role of protein phosphorylation in cell signaling and its use as targeted therapy. International journal of molecular medicine, 2017. 40(2): p. 271-280.
98. Solyakov, L., Halbert, J., Alam, M.M., Semblat, J.-P., Dorin-Semblat, D., Reininger, L., Bottrill, A.R., Mistry, S., Abdi, A., and Fennell, C., Global kinomic and phospho-proteomic analyses of the human malaria parasite Plasmodium falciparum. Nature communications, 2011. 2: p. 565.
99. Krebs, E.G. and Fischer, E.H., The phosphorylase b to a converting enzyme of rabbit skeletal muscle. Biochimica et biophysica acta, 1956. 20: p. 150-157.
100. Srinivasan, N. and Krupa, A., A genomic perspective of protein kinases in Plasmodium falciparum. Proteins: Structure, Function, and Bioinformatics, 2005. 58(1): p. 180-189.
101. Talevich, E., Mirza, A., and Kannan, N., Structural and evolutionary divergence of eukaryotic protein kinases in Apicomplexa. BMC evolutionary biology, 2011. 11(1): p. 321.

102. Ward, P., Equinet, L., Packer, J., and Doerig, C., Protein kinases of the human malaria parasite *Plasmodium falciparum*: the kinome of a divergent eukaryote. BMC genomics, 2004. 5(1): p. 79.
103. Talevich, E., Tobin, A.B., Kannan, N., and Doerig, C., An evolutionary perspective on the kinome of malaria parasites. Phil. Trans. R. Soc. B, 2012. 367(1602): p. 2607-2618.
104. Hanks, S.K., Genomic analysis of the eukaryotic protein kinase superfamily: a perspective. Genome biology, 2003. 4(5): p. 111.
105. Schneider, A.G. and Mercereau-Puijalon, O., A new Apicomplexa-specific protein kinase family: multiple members in Plasmodium falciparum, all with an export signature. BMC genomics, 2005. 6(1): p. 30.
106. Nunes, M.C., Goldring, J., Doerig, C., and Scherf, A., A novel protein kinase family in Plasmodium falciparum is differentially transcribed and secreted to various cellular compartments of the host cell. Molecular microbiology, 2007. 63(2): p. 391-403.
107. Zhao, Y., Kappes, B., and Franklin, R., Gene structure and expression of an unusual protein kinase from *Plasmodium falciparum* homologous at its carboxyl terminus with the EF hand calcium-binding proteins. Journal of Biological Chemistry, 1993. 268(6): p. 4347-4354.
108. Harmon, A.C., Gribskov, M., and Harper, J.F., CDPKs–a kinase for every Ca 2+ signal? Trends in plant science, 2000. 5(4): p. 154-159.
109. Parker, P. and Parkinson, S., AGC protein kinase phosphorylation and protein kinase C. 2001, Portland Press Limited.
110. Haste, N.M., Talabani, H., Doo, A., Merckx, A., Langsley, G., and Taylor, S.S., Exploring the Plasmodium falciparum cyclic-adenosine monophosphate (cAMP)-dependent protein kinase (PfPKA) as a therapeutic target. Microbes and infection, 2012. 14(10): p. 838-850.
111. Tewari, R., Straschil, U., Bateman, A., Böhme, U., Cherevach, I., Gong, P., Pain, A., and Billker, O., The systematic functional analysis of Plasmodium protein kinases identifies essential regulators of mosquito transmission. Cell host & microbe, 2010. 8(4): p. 377-387.
112. Deng, W. and Baker, D.A., A novel cyclic GMP-dependent protein kinase is expressed in the ring stage of the *Plasmodium falciparum* life cycle. Molecular microbiology, 2002. 44(5): p. 1141-1151.
113. Taylor, H.M., McRobert, L., Grainger, M., Sicard, A., Dluzewski, A.R., Hopp, C.S., Holder, A.A., and Baker, D.A., The malaria parasite cyclic GMP-dependent protein kinase plays a central role in blood-stage schizogony. Eukaryotic cell, 2010. 9(1): p. 37-45.
114. Vaid, A., Thomas, D.C., and Sharma, P., Role of Ca2+/calmodulin-PfPKB signaling pathway in erythrocyte invasion by Plasmodium falciparum. Journal of Biological Chemistry, 2008. 283(9): p. 5589-5597.
115. Abdi, A., Eschenlauer, S., Reininger, L., and Doerig, C., SAM domain-dependent activity of PfTKL3, an essential tyrosine kinase-like kinase of the human malaria parasite *Plasmodium falciparum*, in Cellular and molecular life sciences. 2010. p. 3355-3369.
116. Billker, O., Lourido, S., and Sibley, L.D., Calcium-dependent signaling and kinases in apicomplexan parasites. Cell host & microbe, 2009. 5(6): p. 612-622.
117. Dorin-Semblat, D., Quashie, N., Halbert, J., Sicard, A., Doerig, C., Peat, E., Ranford-Cartwright, L., and Doerig, C., Functional characterization of both MAP kinases of the human malaria parasite *Plasmodium falciparum* by reverse genetics. Molecular microbiology, 2007. 65(5): p. 1170-1180.
118. Lye, Y.M., Chan, M., and Sim, T.-S., Pfnek3: an atypical activator of a MAP kinase in *Plasmodium falciparum*. FEBS letters, 2006. 580(26): p. 6083-6092.
119. Reininger, L., Wilkes, J.M., Bourgade, H., Miranda-Saavedra, D., and Doerig, C., An essential Aurora-related kinase transiently associates with spindle pole bodies during Plasmodium falciparum erythrocytic schizogony. Molecular microbiology, 2011. 79(1): p. 205-221.
120. Doerig, C., Meijer, L., and Mottram, J.C., Protein kinases as drug targets in parasitic protozoa. Trends in parasitology, 2002. 18(8): p. 366-371.
121. Jirage, D., Chen, Y., Caridha, D., O'Neil, M.T., Eyase, F., Witola, W.H., Mamoun, C.B., and Waters, N.C., The malarial CDK Pfmrk and its effector PfMAT1 phosphorylate DNA replication proteins and co-localize in the nucleus. Molecular and biochemical parasitology, 2010. 172(1): p. 9-18.
122. Droucheau, E., Primot, A., Thomas, V., Mattei, D., Knockaert, M., Richardson, C., Sallicandro, P., Alano, P., Jafarshad, A., and Baratte, B., *Plasmodium falciparum* glycogen synthase kinase-3: molecular model, expression, intracellular localisation and selective inhibitors. Biochimica et Biophysica Acta (BBA)-Proteins and Proteomics, 2004. 1697(1): p. 181-196.
123. Agarwal, S., Kern, S., Halbert, J., Przyborski, J.M., Baumeister, S., Dandekar, T., Doerig, C., and Pradel, G., Two nucleus-localized CDK-like kinases with crucial roles for malaria parasite erythrocytic replication are involved in phosphorylation of splicing factor. Journal of cellular biochemistry, 2011. 112(5): p. 1295-1310.
124. Wang, G., Jiang, Q., and Zhang, C., The role of mitotic kinases in coupling the centrosome cycle with the assembly of the mitotic spindle. J Cell Sci, 2014: p. jcs. 151753.

125. Schrevel, J., Asfaux-Foucher, G., and Bafort, J., Ultrastructural study of multiple mitosis during sporogony of Plasmodium b. berghei. Journal of ultrastructure research, 1977. 59(3): p. 332-350.
126. Vader, G. and Lens, S.M., The Aurora kinase family in cell division and cancer. Biochimica et Biophysica Acta (BBA)-Reviews on Cancer, 2008. 1786(1): p. 60-72.
127. Dar, A.A., Goff, L.W., Majid, S., Berlin, J., and El-Rifai, W., Aurora kinase inhibitors-rising stars in cancer therapeutics? Molecular cancer therapeutics, 2010: p. 1535-7163. MCT-09-0765.
128. Boss, D.S., Beijnen, J.H., and Schellens, J.H., Clinical experience with aurora kinase inhibitors: a review. The oncologist, 2009. 14(8): p. 780-793.
129. Keen, N. and Taylor, S., Aurora-kinase inhibitors as anticancer agents. Nature Reviews Cancer, 2004. 4(12): p. 927.
130. Hauf, S., Cole, R.W., LaTerra, S., Zimmer, C., Schnapp, G., Walter, R., Heckel, A., Van Meel, J., Rieder, C.L., and Peters, J.-M., The small molecule Hesperadin reveals a role for Aurora B in correcting kinetochore–microtubule attachment and in maintaining the spindle assembly checkpoint. J Cell Biol, 2003. 161(2): p. 281-294.
131. Ladygina, N., Latsis, R., and Yen, T., Effect of the pharmacological agent hesperadin on breast and prostate tumor cultured cells. Biomeditsinskaia khimiia, 2005. 51(2): p. 170-176.
132. Jetton, N., Rothberg, K.G., Hubbard, J.G., Wise, J., Li, Y., Ball, H.L., and Ruben, L., The cell cycle as a therapeutic target against *Trypanosoma brucei*: Hesperadin inhibits Aurora kinase-1 and blocks mitotic progression in bloodstream forms. Molecular microbiology, 2009. 72(2): p. 442-458.
133. Patel, G., Roncal, N.E., Lee, P.J., Leed, S.E., Erath, J., Rodriguez, A., Sciotti, R.J., and Pollastri, M.P., Repurposing human Aurora kinase inhibitors as leads for anti-protozoan drug discovery. MedChemComm, 2014. 5(5): p. 655-658.
134. Li, Z., Gourguechon, S., and Wang, C.C., Tousled-like kinase in a microbial eukaryote regulates spindle assembly and S-phase progression by interacting with Aurora kinase and chromatin assembly factors. Journal of cell science, 2007. 120(21): p. 3883-3894.
135. Glover, D.M., Leibowitz, M.H., McLean, D.A., and Parry, H., Mutations in aurora prevent centrosome separation leading to the formation of monopolar spindles. Cell, 1995. 81(1): p. 95-105.
136. Clark, K., Niemand, J., Reeksting, S., Smit, S., Van Brummelen, A., Williams, M., Louw, A., and Birkholtz, L., Functional consequences of perturbing polyamine metabolism in the malaria parasite, *Plasmodium falciparum.* Amino acids, 2010. 38(2): p. 633-644.
137. Fukumoto, G.H. and Byus, C.V., A kinetic characterization of putrescine and spermidine uptake and export in human erythrocytes. Biochimica et Biophysica Acta (BBA)-Biomembranes, 1996. 1282(1): p. 48-56.
138. Assaraf, Y., Golenser, J., Spira, D., and Bachrach, U., Polyamine levels and the activity of their biosynthetic enzymes in human erythrocytes infected with the malarial parasite, *Plasmodium falciparum.* Biochemical Journal, 1984. 222(3): p. 815-819.
139. Wallace, H.M., Fraser, A.V., and Hughes, A., A perspective of polyamine metabolism. Biochem J, 2003. 376(Pt 1): p. 1-14.
140. Assaraf, Y., Abu-Elheiga, L., Spira, D., Desser, H., and Bachrach, U., Effect of polyamine depletion on macromolecular synthesis of the malarial parasite, *Plasmodium falciparum*, cultured in human erythrocytes. Biochemical Journal, 1987. 242(1): p. 221-226.
141. Wright, P.S., Byers, T.L., Cross-Doersen, D.E., McCann, P.P., and Bitonti, A.J., Irreversible inhibition of *S*-adenosylmethionine decarboxylase in *Plasmodium falciparum*-infected erythrocytes: growth inhibition *in vitro.* Biochemical pharmacology, 1991. 41(11): p. 1713-1718.
142. van Biljon, R., Niemand, J., van Wyk, R., Clark, K., Verlinden, B., Abrie, C., von Grüning, H., Smidt, W., Smit, A., Reader, J., Painter, H., Llinás, M., Doerig, C., and Birkholtz, L.-M., Inducing controlled cell cycle arrest and re-entry during asexual proliferation of *Plasmodium falciparum* malaria parasites. Scientific Reports, 2018. 8(1): p. 16581.
143. Landau, G., Ran, A., Bercovich, Z., Feldmesser, E., Horn-Saban, S., Korkotian, E., Jacob-Hirsh, J., Rechavi, G., Ron, D., and Kahana, C., Expression profiling and biochemical analysis suggest stress response as a potential mechanism inhibiting proliferation of polyamine-depleted cells. Journal of Biological Chemistry, 2012. 287(43): p. 35825-35837.
144. Toettcher, J.E., Loewer, A., Ostheimer, G.J., Yaffe, M.B., Tidor, B., and Lahav, G., Distinct mechanisms act in concert to mediate cell cycle arrest. Proceedings of the National Academy of Sciences, 2009. 106(3): p. 785-790.
145. Niemand, J., Louw, A., Birkholtz, L., and Kirk, K., Polyamine uptake by the intraerythrocytic malaria parasite, Plasmodium falciparum. International journal for parasitology, 2012. 42(10): p. 921-929.
146. Hoppe, H., Verschoor, J., and Louw, A., *Plasmodium falciparum*: a comparison of synchronisation methods for *in vitro* cultures. Experimental parasitology, 1991. 72(4): p. 464-467.
147. Trager, W. and Jensen, J.B., Human malaria parasites in continuous culture. Science, 1976. 193(4254): p. 673-675.

148. Lambros, C. and Vanderberg, J.P., Synchronization of *Plasmodium falciparum* erythrocytic stages in culture. The Journal of parasitology, 1979: p. 418-420.
149. Rengarajan, K., Cristol, S.M., Mehta, M., and Nickerson, J.M., Quantifying DNA concentrations using fluorometry: a comparison of fluorophores. Mol Vis, 2002. 8: p. 416-421.
150. Verlinden, B.K., De Beer, M., Pachaiyappan, B., Besaans, E., Andayi, W.A., Reader, J., Niemand, J., Van Biljon, R., Guy, K., and Egan, T., Interrogating alkyl and arylalkylpolyamino (bis) urea and (bis) thiourea isosteres as potent antimalarial chemotypes against multiple lifecycle forms of Plasmodium falciparum parasites. Bioorganic & medicinal chemistry, 2015. 23(16): p. 5131-5143.
151. Grimberg, B.T., Erickson, J.J., Sramkoski, R.M., Jacobberger, J.W., and Zimmerman, P.A., Monitoring *Plasmodium falciparum* growth and development by UV flow cytometry using an optimized Hoechst-thiazole orange staining strategy. Cytometry Part A: The Journal of the International Society for Analytical Cytology, 2008. 73(6): p. 546-554.
152. Gupta, R.D., Krause-Ihle, T., Bergmann, B., Müller, I.B., Khomutov, A.R., Müller, S., Walter, R.D., and Lüersen, K., 3-Aminooxy-1-aminopropane and derivatives have an antiproliferative effect on cultured *Plasmodium falciparum* by decreasing intracellular polyamine concentrations. Antimicrobial agents and chemotherapy, 2005. 49(7): p. 2857-2864.
153. Grimberg, B.T., Methodology and application of flow cytometry for investigation of human malaria parasites. Journal of immunological methods, 2011. 367(1-2): p. 1-16.
154. Harper, J.V., Synchronization of Cell Populations in G1/S and G 2/M Phases of the Cell Cycle, in Cell Cycle Control. 2005, Springer. p. 157-166.
155. Khan, T., van Brummelen, A.C., Parkinson, C.J., and Hoppe, H.C., ATP and luciferase assays to determine the rate of drug action in in vitro cultures of *Plasmodium falciparum.* Malaria journal, 2012. 11(1): p. 369.
156. Chulay, J.D., Haynes, J.D., and Diggs, C.L., *Plasmodium falciparum*: assessment of in vitro growth by [3H] hypoxanthine incorporation. Experimental parasitology, 1983. 55(1): p. 138-146.
157. Kitzen, J., de Jonge, M., and Verweij, J., Aurora kinase inhibitors. Critical reviews in oncology/hematology, 2010. 73(2): p. 99-110.
158. Gamo, F.-J., Sanz, L.M., Vidal, J., de Cozar, C., Alvarez, E., Lavandera, J.-L., Vanderwall, D.E., Green, D.V., Kumar, V., and Hasan, S., Thousands of chemical starting points for antimalarial lead identification. Nature, 2010. 465(7296): p. 305.
159. Kim, S., Lee, K., Choi, J.-H., Ringstad, N., and Dynlacht, B.D., Nek2 activation of Kif24 ensures cilium disassembly during the cell cycle. Nature communications, 2015. 6: p. 8087.
160. Delves, M.J., Miguel-Blanco, C., Matthews, H., Molina, I., Ruecker, A., Yahiya, S., Straschil, U., Abraham, M., León, M.L., and Fischer, O.J., A high throughput screen for next-generation leads targeting malaria parasite transmission. Nature communications, 2018. 9(1): p. 3805.

7 Appendices

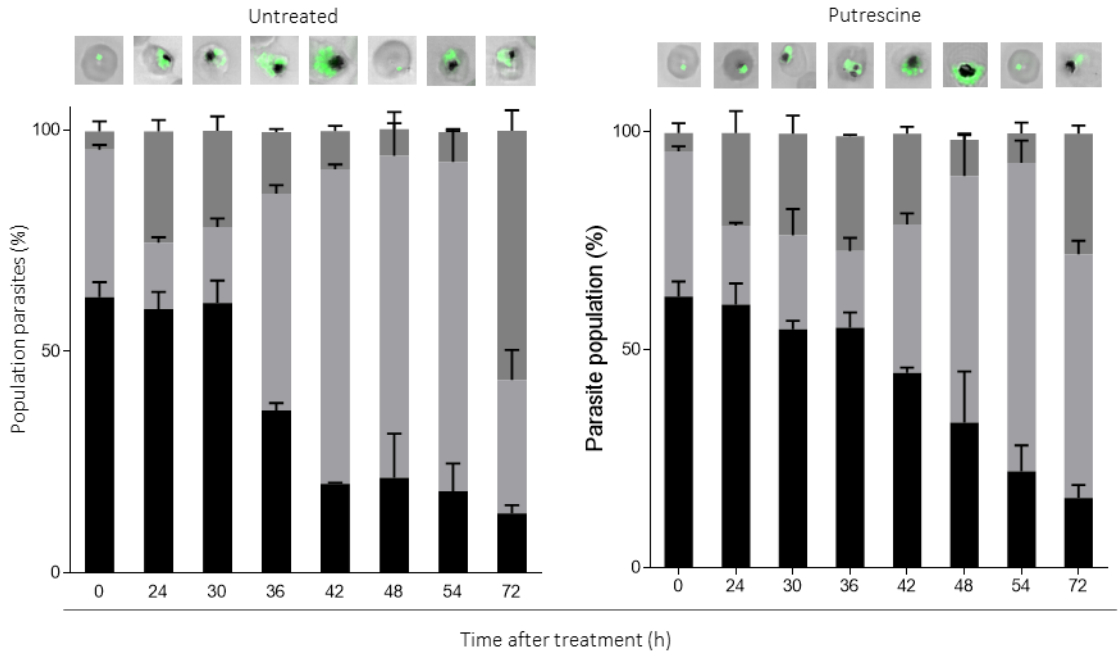

Figure A.1: *P. falciparum* parasite cell cycle progression to M-phase of putrescine-rescued parasites.
DFMO-synchronised intraerythrocytic *P. falciparum* 3D7 parasites (3% parasitaemia, 5% haematocrit, ~18 hpi) was reversed with 2 mM putrescine supplementation and correlated to untreated parasites. Parasites samples was stained with SYBR Green I for flow cytometry and fluorescence microscopy analysis. Parasite DNA copy number (N) was measured by flow cytometry as described [57, 151]. Fluorescence was collected in the FL-1 channel (FITC signal) on a Becton Dickenson Accuri™ C6 Plus cytometer. A total of 100 000 events were captured and analysed using FlowJo version 10.1 software. Data are representative of one biological replicate (n=1± SD), performed in technical triplicates. Error bars represent standard deviation. Morphology of representative parasite population was confirmed through SYBR Green I confocal fluorescence microscopy using a Zeiss LSM 880 Confocal Laser Scanning Microscope (LSM).

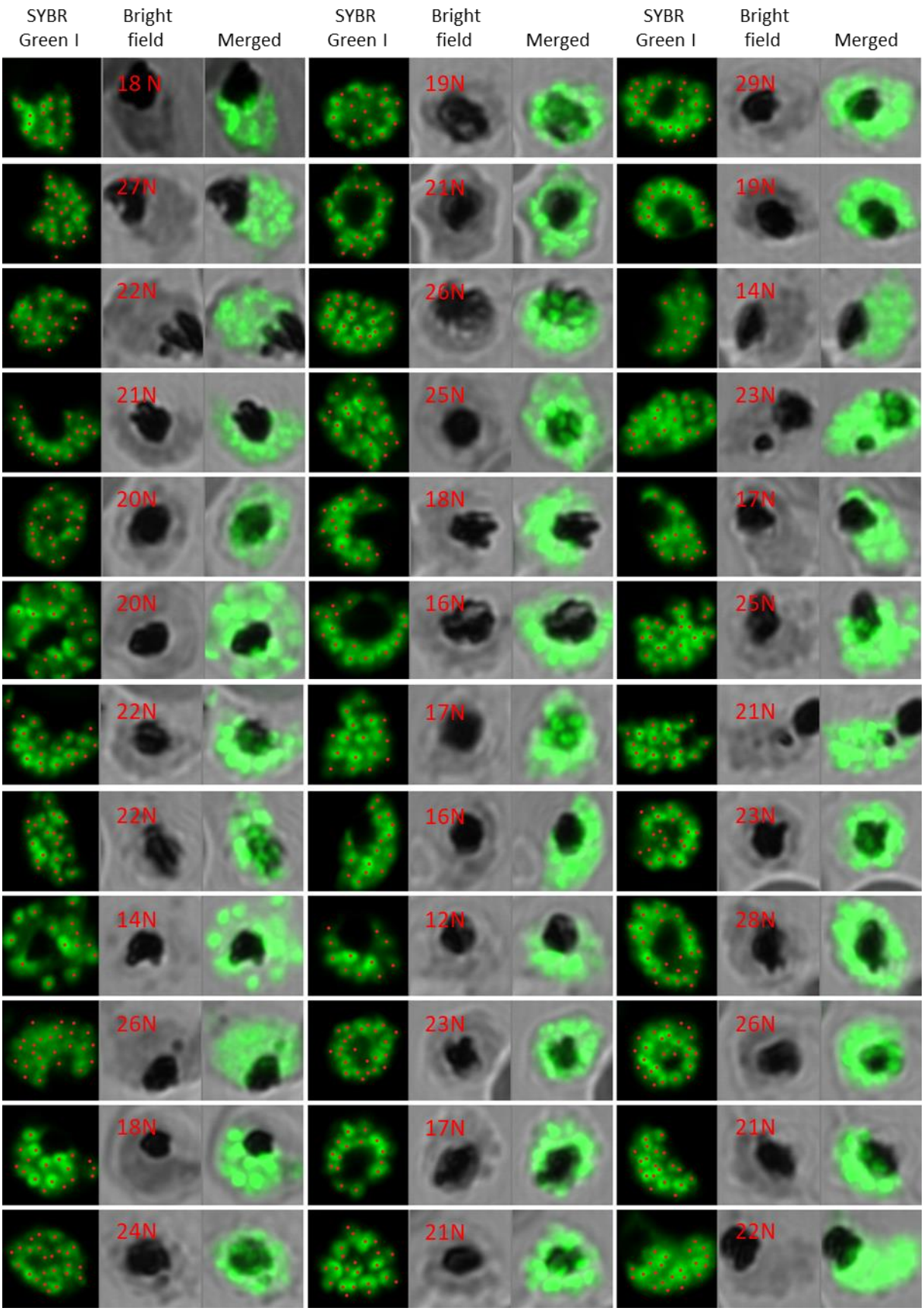

Figure A.2: Untreated *P. falciparum* parasite nuclei counts
Untreated parasite nuclei development (~48 hpi) was quantitatively assessed through SYBR Green I fluorescence microscopy using a Zeiss LSM 880 Confocal Laser Scanning Microscope (LSM). n = 36.

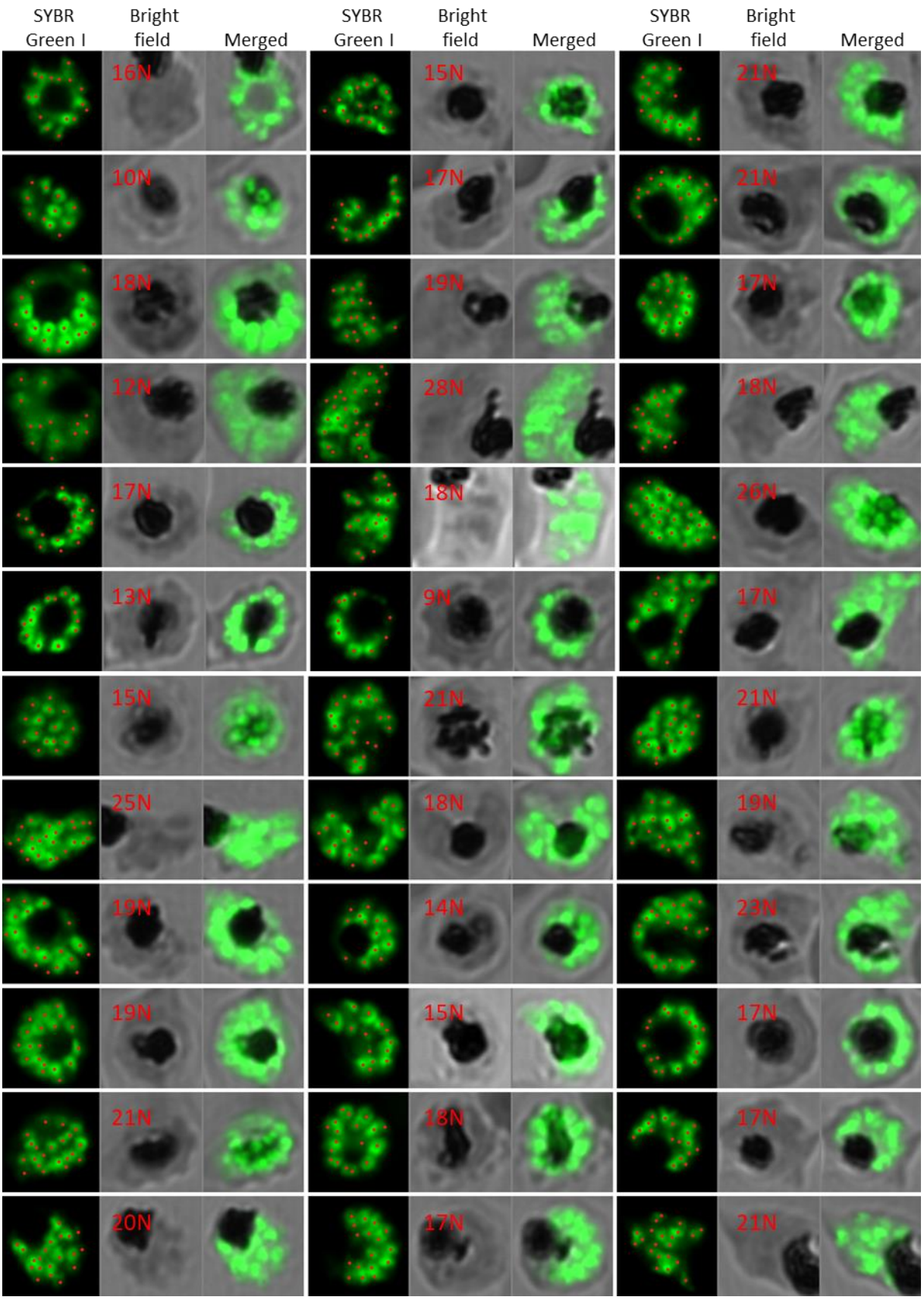

Figure A.3: Putrescine-rescued *P. falciparum* parasite nuclei counts

Putrescine-rescued parasite nuclei development (48 hpi) was quantitatively assessed through SYBR Green I fluorescence microscopy using a Zeiss LSM 880 Confocal Laser Scanning Microscope (LSM). n = 36.

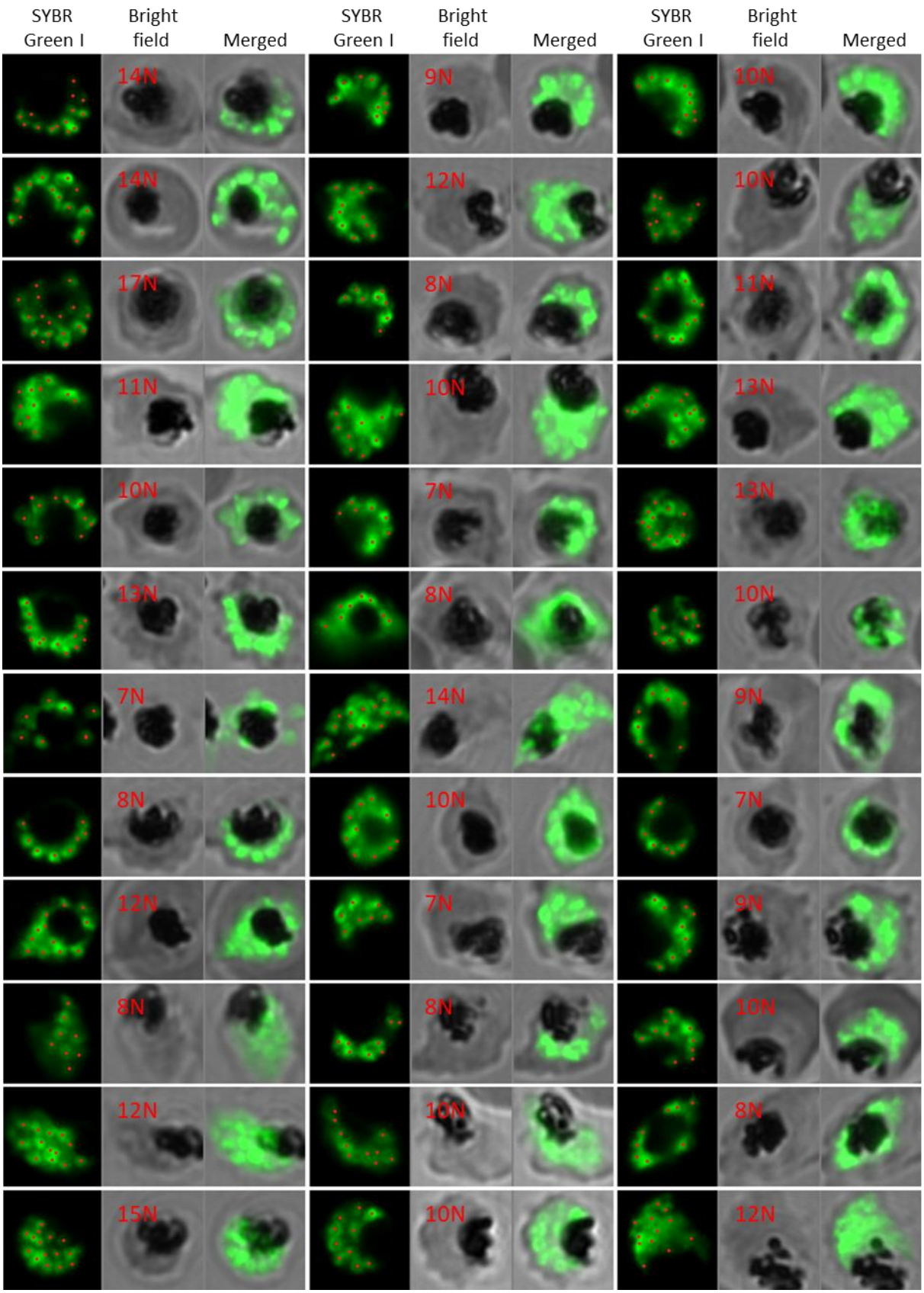

Figure A.4: Hesperadin-treated *P. falciparum* parasite nuclei counts

Hesperadin-treated parasite nuclei development (~48 hpi) was quantitatively assessed through SYBR Green I fluorescence microscopy using a Zeiss LSM 880 Confocal Laser Scanning Microscope (LSM). n = 36.

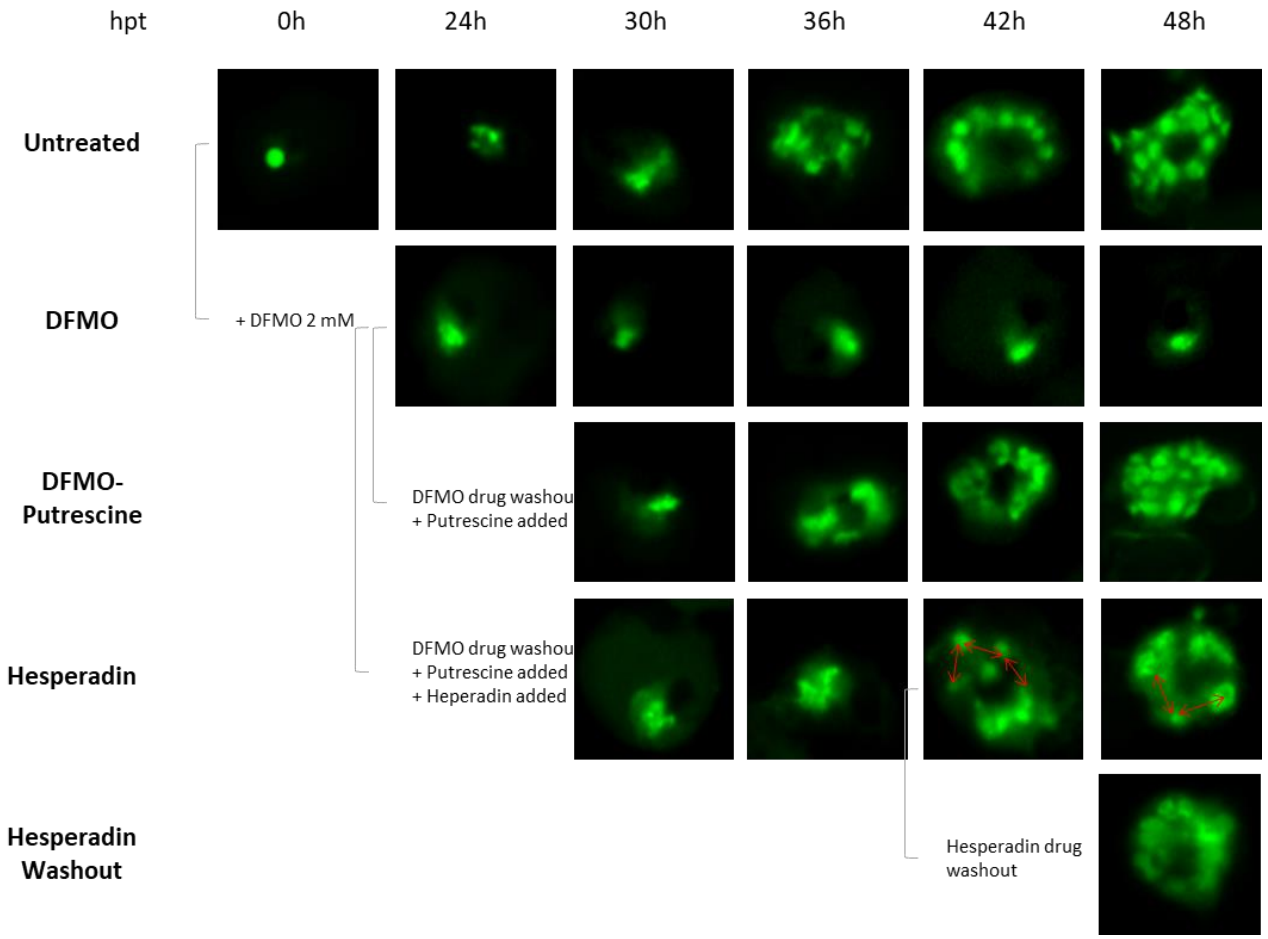

Figure A.5: Hesperadin causes polyploidy in *P. falciparum* parasites
Parasite life cycle progression monitored through SYBR Green I fluorescence microscopy. DFMO treatment was initiated on early ring-stage *P. falciparum* 3D7 parasites (0 – 10 hpi, 3% parasitaemia, 5% haematocrit) at 2xIC_{50}. Untreated, DFMO-arrested, putrescine-rescued and hesperadin-treated parasites were sampled after 24 h then every 6 h onwards. Samples were staine with SYBR Green I and parasites were assessed using a Zeiss LSM 880 Confocal Laser Scanning Microscope (LSM).

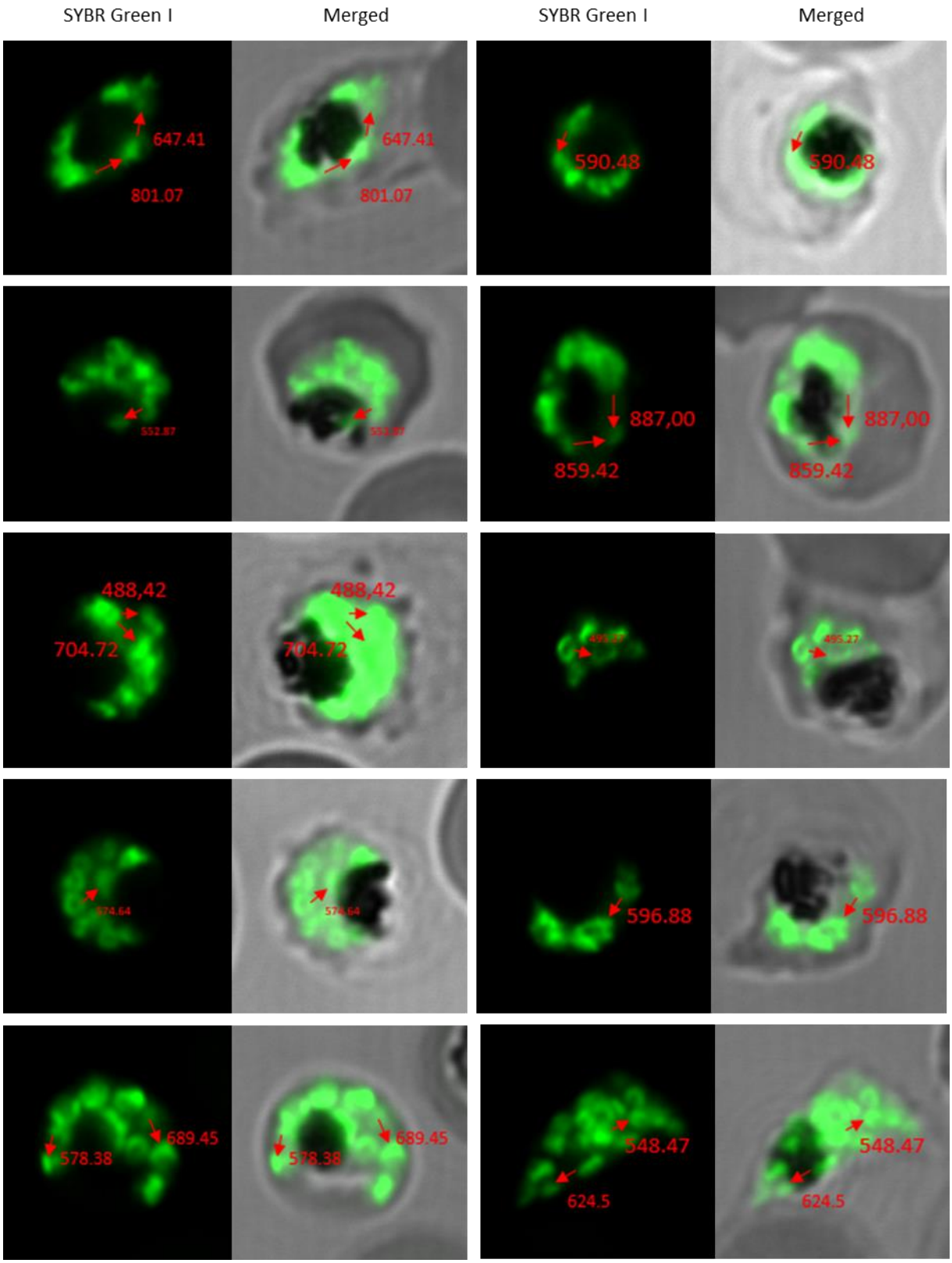

Figure A.6: Inter-nuclear distances measured in hesperadin-treated *P. falciparum* parasites.
Intraerythrocytic *P. falciparum* 3D7 control parasites (3% parasitaemia, 5% haematocrit, ~18 hpi) was treated with hesperadin and sampled at ~48 hpi for fluorescence microscopy. SYBR Green I nuclear staining was used to monitor parasite nuclei formation using a Zeiss LSM 880 Confocal Laser Scanning Microscope (LSM). Inter-nuclear distances were measured in nm (red text and arrows). 10 representative images were prepared using ZEN Blue software.

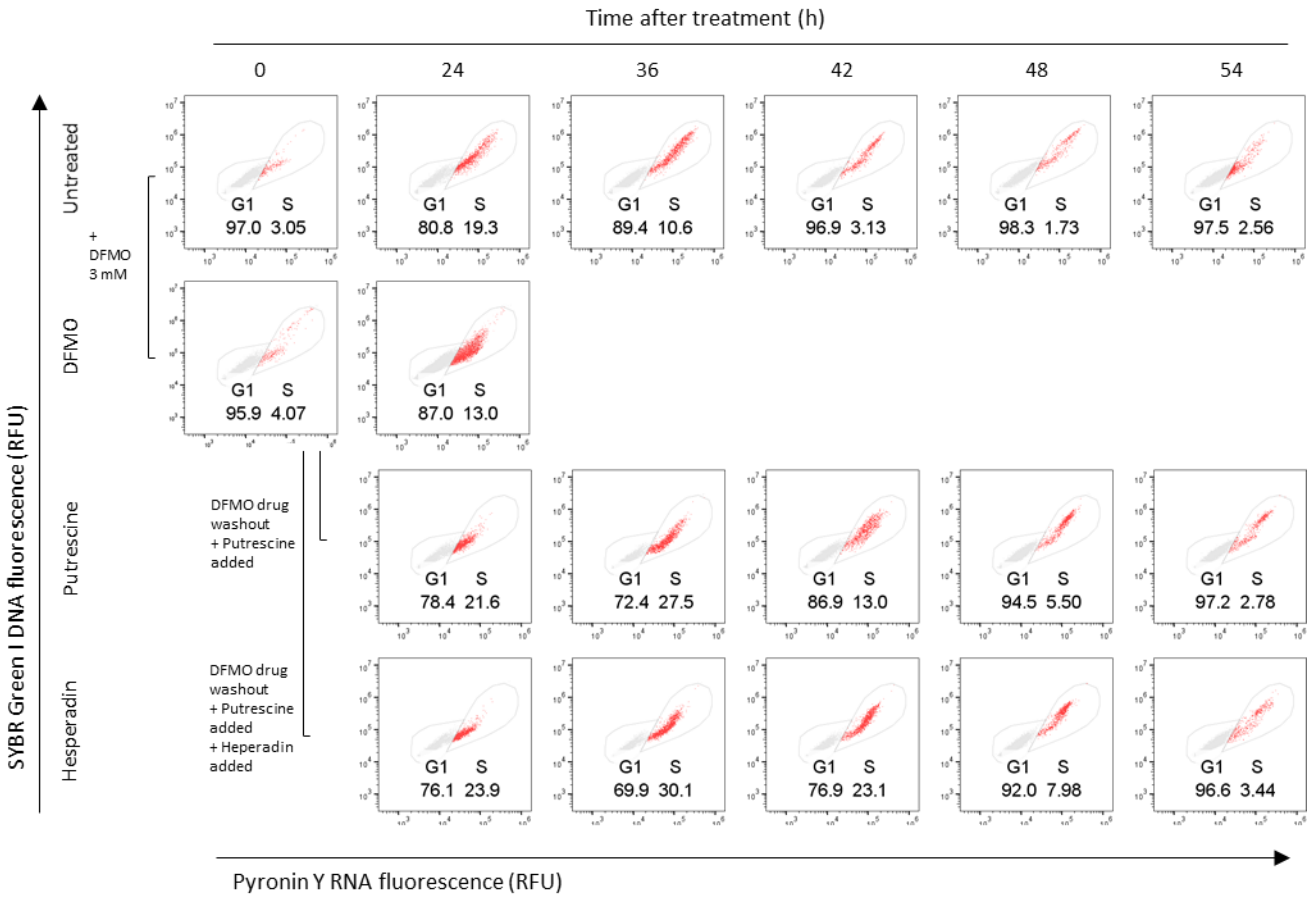

Figure A.7: The effect of PfARK inhibition on *P. falciparum* parasite cell cycle profile.
Intraerythrocytic *P. falciparum* 3D7 control parasites (3% parasitaemia, 5% haematocrit, ~18 hpi) was treated with hesperadin and sampled every 6 h up to 30 h after hesperadin treatment. Samples were stained with SYBR Green I and Pyronin Y for flow cytometry analysis. SYBR Green I fluorescence against Pyronin Y fluorescence scatter plots are representative of parasite cell cycle profiles at specific timepoints. Parasite population (%) in G_1 (grey)and S-phase (red) are indicated in scatter plots. Fluorescence was collected for SYBR Green I in the FL-1 channel (FITC signal) and Pyronin Y in the FL-2 channel (PE signal) on a Becton Dickenson Accuri™ C6 Plus cytometer. A total of 100 000 events were captured and analysed using FlowJo version 10.1 software. Data are representative of one biological replicate (n=1± SD), performed in a single technical repeat.

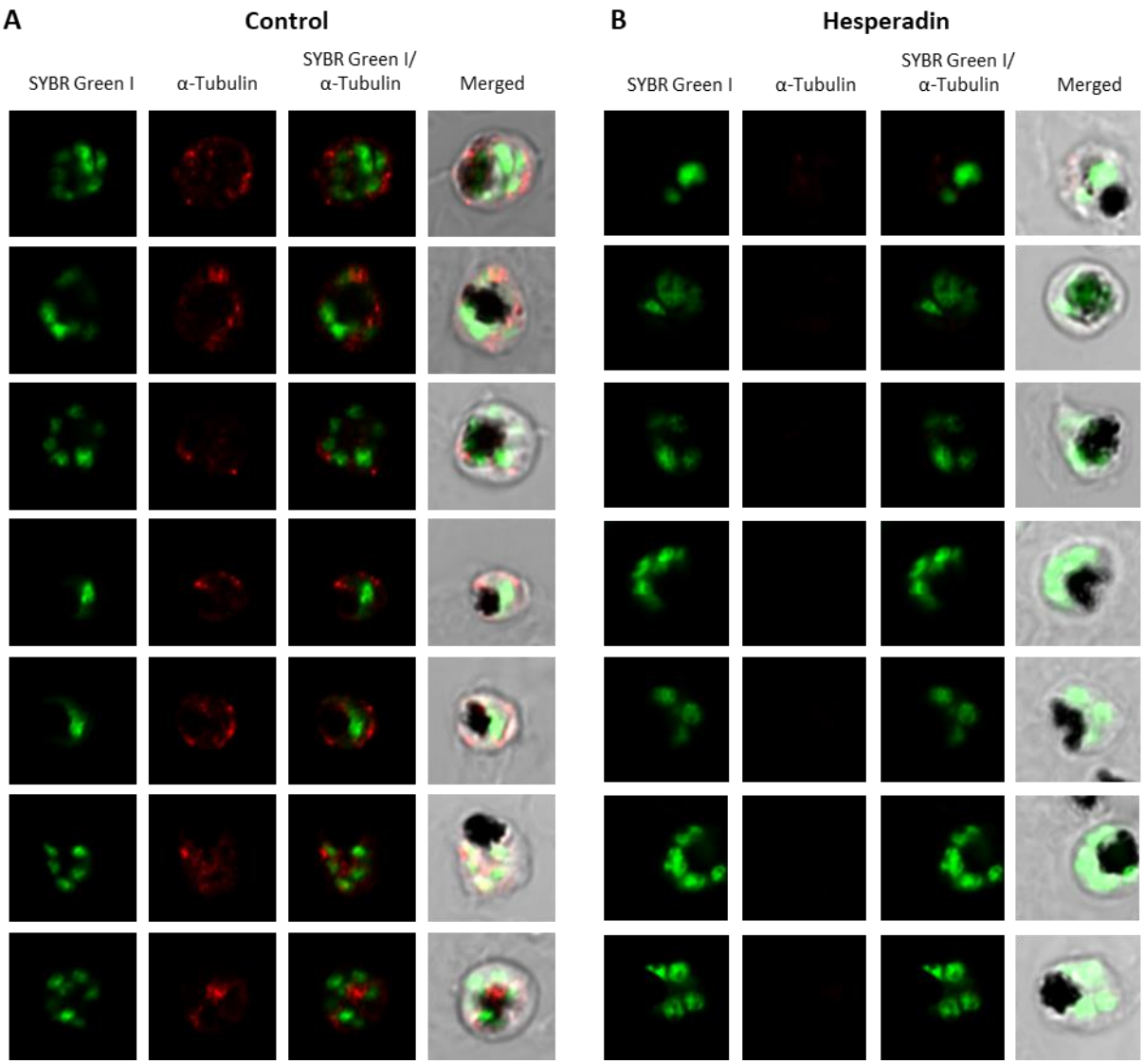

Figure A.8: Spindle formation initiation during early mitosis in *P. falciparum* 3D7 parasites.
Fluorescence microscopy of spindle formation during mitosis of *P. falciparum* 3D7 parasites. SYBR Green I (green) nuclear control staining was used in combination with anti-α-tubulin antibody (red) to monitor parasite spindle formation using a Zeiss LSM 880 Confocal Laser Scanning Microscope (LSM). Images was prepared using ZEN Blue software. Gain were set to 600 (gamma: 2) and 900 (gamma: 4) for SYBR Green I and Anti-α-tubulin AlexaFluor 647, respectively.